AD NUMBER
AD393249
CLASSIFICATION CHANGES
TO: **UNCLASSIFIED**
FROM: **CONFIDENTIAL**
LIMITATION CHANGES
TO: **Approved for public release; distribution is unlimited.**
FROM: **Distribution authorized to U.S. Gov't. agencies only; Administrative/Operational Use; 31 JUL 1968. Other requests shall be referred to Office of Naval Research, Arlington, VA 22203.**
AUTHORITY
ONR ltr 15 Jun 1977 ; ONR ltr 15 Jun 1977

SECURITY MARKING

The classified or limited status of this report applies to each page, unless otherwise marked.
Separate page printouts MUST be marked accordingly.

THIS DOCUMENT CONTAINS INFORMATION AFFECTING THE NATIONAL DEFENSE OF THE UNITED STATES WITHIN THE MEANING OF THE ESPIONAGE LAWS, TITLE 18, U.S.C., SECTIONS 793 AND 794. THE TRANSMISSION OR THE REVELATION OF ITS CONTENTS IN ANY MANNER TO AN UNAUTHORIZED PERSON IS PROHIBITED BY LAW.

NOTICE: When government or other drawings, specifications or other data are used for any purpose other than in connection with a definitely related government procurement operation, the U. S. Government thereby incurs no responsibility, nor any obligation whatsoever; and the fact that the Government may have formulated, furnished, or in any way supplied the said drawings, specifications, or other data is not to be regarded by implication or otherwise as in any manner licensing the holder or any other person or corporation, or conveying any rights or permission to manufacture, use or sell any patented invention that may in any way be related thereto.

CONFIDENTIAL

122354

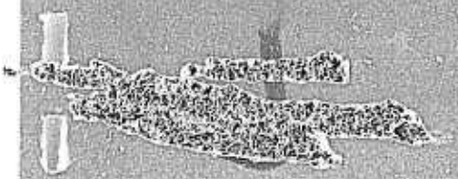

SUBIC

[redacted]

Submarine Integrated Control

OFFICE OF NAVAL RESEARCH

GENERAL DYNAMICS CORPORATION
ELECTRIC BOAT DIVISION
GROTON, CONNECTICUT

CONFIDENTIAL

CONFIDENTIAL

GENERAL DYNAMICS CORPORATION
Electric Boat division
Groton, Connecticut

PROCESSING OF DATA FROM SONAR SYSTEMS (U)

VOLUME V

by

John H. Chang
Verne H. McDonald
Peter M. Schultheiss
Franz B. Tuteur
Yale University

Examined: J. W. Herring
J. W. Herring
SUBIC Project Manager

Approved: Dr. A. J. van Woerkom
Dr. A. J. van Woerkom
Chief Scientist

C417-68-078
July 31, 1968

CONFIDENTIAL

ABSTRACT

Volume V deals with the following topics:

1) Passive detection in an anisotropic noise field

Earlier studies of passive detection in an anisotropic noise environment were only concerned with the anisotropy caused by a single plane wave interference (Volumes III and IV). The present volume presents analyses of detection in a noise field dominated by several plane wave interferences or by a single spatially distributed interference. Conventional as well as optimal detectors are considered.

2) Passive tracker accuracy

a) One study examines the effect of a plane wave interference on the performance of a split beam tracker. Conventional as well as null steering types of beam-formers are analyzed. The contribution of the interference to the measured bearing error is decomposed into a systematic and a random component. Factors which affect the relative magnitude of these components are discussed.

b) A second study initiates an effort to set absolute lower bounds on the bearing accuracy attainable with a given array in a given noise environment. Only the simplest case (two element array, independent noise) is discussed here.

3) Active receivers using replica correlation

The performance of a simple replica correlator is compared with that of a similar instrumentation using clipped (binary) hydrophone outputs. Detection as well as range and Doppler measurement are

examined. One finds that large clipping losses can occur when the target is moving rapidly. In most other situations the clipping loss is small.

4) Adaptive Signal Processing

In situations where processor design is hampered by lack of adequate knowledge concerning signal or noise statistics one can employ stochastic approximation techniques to cause the processor to approach an optimum configuration. This procedure is used to adjust a tapped delay line filter for operation in a noise environment with unknown spectral properties. Conditions of convergence and rates of convergence are examined.

TABLE OF CONTENTS

Report No.	Title	Page
	Abstract	iii
	Foreword	v
	Introduction	1
29	Tracking in the Presence of Interference	A-1
30	The Effect of Multiple or Distributed Interferences on the Performance of a Conventional Passive Sonar Detector	B-1
*31	The Effect of Clipping on the Performance of Replica Correlators	A-1
*32	Some Comments on Optimum Bearing Estimation	B-1
*33	The Effect of Noise Anisotropy on Detectability in an Optimum Array Processor	C-1
*34	Methods of Stochastic Approximation Applied to the Analysis of Adaptive Tapped Delay Line Filters	D-1

*These reports are unclassified and are issued as a Supplement to Volume V.

FOREWORD

This report is the fifth in a series describing work performed by Yale University under subcontract to Electric Boat division of General Dynamics Corporation. The report covers the period from 1 July 1966 to 1 July 1967. An unclassified supplement to this volume has been bound as a separate document (U417-68-079). Electric Boat is prime contractor of the SUBIC (Submarine Integrated Control) Program under Office of Naval Research contract NOnr 2512(00). LCDR. E.W. Lull, USN, is Project Officer for ONR; J W. Herring is Project Manager for Electric Boat division under the direction of Dr. A.J. vanWoerkom.

I. Introduction

The following is a summary of work performed under contract 8050-31-55001 between Yale University and the Electric Boat Company during the period, 1 July 1966 to 30 September 1967. More detailed discussions of the results as well as their derivations are contained in a series of six progress reports which are appended.

Several studies reported in earlier volumes of this series were concerned with passive detection in the presence of strong interference from a point source. The general subject of passive sonars operating in an anisotropic noise environment is pursued further in the present volume. The effort reported here has taken two new directions:

1) Anisotropies are no longer attributed to a single interfering plane wave. Environments containing several point sources of interference or a spatially distributed interference are studied. Conventional as well as optimal detectors are analyzed.
2) The effect of a single plane wave interference on tracking accuracy is examined.

The problem of tracking accuracy is also considered in another context. An attempt is made to divorce the accuracy problem from particular instrumentations and to set absolute bounds on the bearing accuracy attainable by processing the outputs of a set of hydrophones operating in a specified noise environment. Only the simplest possible case (two hydrophones, noise independent from phone to phone) is presented here.

In addition, this volume continues the study of active sonar systems initiated in Volume IV. The specific problem considered here is the effect of clipping on the performance of replica correlators. Results are obtained for a wide class of signal waveshapes and for environments dominated either by reverberation or by ambient noise.

Finally, an effort is initiated to deal with the signal detection and extraction problem in a noise environment whose statistical properties are largely or wholly unknown. This leads to the study of adaptive processing procedures. Only preliminary results, based on the method of stochastic approximation, are presented in this volume.

II. Detection in an Anisotropic Noise Environment

Report No. 30 deals with the performance of a conventional detector operating in a noise environment dominated by several point sources of interference or, as a limiting case, by an interference source spatially distributed over some finite angle. The results indicate that the performance degradation due to such complex interference sources is less serious than that caused by a single point source of interference with the same total power. For a linear array of M equally spaced hydrophones the maximum differential amounts to $10.\log_{10}\sqrt{2M/3}$ db of equivalent input signal-to-noise ratio. This is precisely the performance differential between a conventional array operating in a noise environment independent from hydrophone to hydrophone and a similar array operating in a noise environment of equal power but originating largely from a point source of interference. One therefore suspects that a smooth transition will take place from the case of a single point source of interference to that of isotropic noise as the number of interferences increases and their locations become more uniformly distributed in space. Numerical computations generally confirm this inference. For several closely spaced interferences all relatively remote from the target in bearing one finds, not surprisingly, that the configuration is equivalent to a single interference. As the spacing between interferences increases the performance index rises quickly to its asymptotic value. For the situations considered in the computations the asymptotic improvement is somewhat less than the figure of $10.\log_{10}\sqrt{2M/3}$ db quoted above. One major reason for this discrepancy is the fact that the postulated spectra (falloff with second power of frequency above 5000 cps) are not sufficiently broad to yield noise independent from hydrophone to hydrophone in the isotropic limit.

Qualitatively similar results are obtained for the case of a distributed interference. Again one finds that the performance index quickly approaches its asymptotic maximum as the interference spread grows. This approach becomes more rapid as the number of hydrophones increases (and hence the beam-width decreases, since fixed spacing between hydrophones is assumed).

Report No. 33 studies a likelihood ratio detector operating in an anisotropic environment similar to the one just discussed. It had been shown in earlier work (Volume III) that interference from a single plane wave resulted in a performance degradation not exceeding the degradation caused by the loss of one hydrophone in the absence of the interference. A similar statement remains true in the presence of several interferences, i.e., the effect of R interferences can be eliminated at a cost not exceeding R hydrophones. However, it appears that this bound on performance degradation is often quite pessimistic. Thus interferences in close angular proximity of each other have the effect of a single interference and can be dealt with at a sacrifice of only one hydrophone. Only when all interferences are widely separated from each other and from the target can the loss figure approach R hydrophones (and then only in a strongly interference dominated environment). A spatially distributed interference may again be interpreted as the limiting version of a large number of closely spaced individual interferences. These may then be grouped into clusters more or less equivalent to single point sources of interference so that serious losses occur only if the number of clusters, i.e., the total angular spread of the interference, is large. Since analytical evaluation of the likelihood ratio detector leads to expressions that are formally simple but practically difficult to evaluate and interpret, many of the conclusions are based on numerical computations. Arrays of different geometries (circular and linear) and a variety of interference configurations are considered.

III. Tracking Accuracy

Report No. 29 analyzes the performance of a split beam tracker operating in an environment consisting of ambient noise (assumed independent from hydrophone to hydrophone) and a plane wave interference. Signal, noise and interference are assumed to be stationary Gaussian processes with similar power spectra. Two types of beam-formers are considered:

1) Conventional beam-formers (in each array half: delay for alignment with target, then add).
2) Null steering (in each array half: steer on interference, subtract hydrophone outputs pairwise, then beam-form on target and add).

In each case one of the beams is shifted 90° in phase relative to the other, after which multiplication and smoothing completes the tracking procedure.

In the conventional tracker plane wave interferences (or other spatial asymmetries in the noise field) contribute to the tracking error through two distinct mechanisms.

a) The null of the <u>average</u> tracker output is shifted away from its nominal location by an amount depending on the proximity, strength and spectral properties of the interference (systematic error).
b) The output fluctuation is increased by an amount depending primarily (except for interferences close to the target in bearing) on the interference power (random error).

The null steering tracker eliminates the complete time function of interference (at least ideally) and therefore removes both sources of error.

Whether tracking problems caused by noise field asymmetry warrant the use of instrumentations more complex than the conventional split beam tracker clearly depends on the total additional error [a) plus b)]. However, the choice of remedial measures (spectrum shaping, null steering, more

powerful adaptive procedures, etc.) might depend to a considerable extent on the relative magnitude of errors a) and b) . The following considerations appear relevant:

1) Only when the noise field is interference dominated does the interference contribute significantly to the random error. (With a linear array of 2M equally spaced hydrophones the environment is interference dominated when the interference to ambient noise ratio exceeds $\sqrt{(4/3)M}$).

2) Even when the noise field is interference dominated the systematic error tends to exceed the random error in many practically interesting situations.

3) A certain amount of control can be exerted over the systematic error by shaping the spectrum of each channel prior to multiplication.

If the primary source of difficulty is systematic error, only statistical properties of the asymmetrical noise component are required for correction. These may not be known a priori so that measurement and at least a primitive form of adaptation may be indicated. However, if one wishes to deal with the random component of error, one must obtain an estimate of the actual interference time function and the need for adaptation becomes more fundamental. Even in that case one should, of course, still use all available a priori information. Thus, if one knows that the noise field asymmetry is caused by an interfering plane wave, one need only measure the interference bearing. Then the relatively simple null steering procedure solves the problem. In the absence of such strong information concerning the cause of noise field asymmetry one may be forced into more elaborate adaptive techniques.

Report No. 32 considers the tracking problem from a much more general point of view. The basic aim is to determine the best passive bearing accuracy attainable with a given array in a given noise environment, without making any prior assumptions about data processing procedures. Report No. 32 deals only with the simplest possible case, that of a two element array with noise independent from hydrophone to hydrophone. In that situation a simple crosscorrelator attains the Cramér-Rao lower bound of bearing error and is therefore an optimal bearing estimator. A two element split beam tracker using differentiation to achieve the 90° phase shift between channels is equivalent in performance to the autocorrelator. If a pure 90° phase shift is used in place of the differentiation there is a slight degradation of performance. The rms bearing error of the optimal instrumentations varies as $(S/N)^{-1}$ for $S/N << 1$ [$S/N \equiv$ input signal-to-noise ratio] and as $(S/N)^{-\frac{1}{2}}$ for $S/N >> 1$.

IV. Clipped Replica Correlators

Report No. 31 examines the performance of an active sonar receiver using replica correlation. Detection as well as range and Doppler measurement are considered. The output of each array element is clipped prior to conventional beamforming and the subject of primary interest is the performance degradation due to clipping. Ambient noise as well as reverberation limited environments are studied, with primary emphasis on the latter. The reverberation model is the one developed in Volume IV (stationary, independent, Poisson distributed point scatterers).

The general conclusions may be summarized as follows: Serious clipping losses can arise in a reverberation limited environment when the target is moving rapidly enough to shift the target return almost entirely out of the reverberation band. In such cases the unclipped detector has an output essentially free from reverberation in the signal band, whereas the clipping operation transfers part of the reverberation power into the signal band. In other words, clipping destroys much of the potential signal-to-noise advantage of a rapidly moving target. With this exception the clipping loss appears to be quite small in most practically interesting situations. If one defines the clipping loss R as the ratio of the output signal-to-noise ratios with and without clipping, one can show under fairly general conditions that $R > 0.89$ (equivalent to a loss of about 1 db of input signal-to-noise ratio). The primary requirement for this statement to be true is that the transmitted signal be narrowband in some meaningful sense (in a reverberation limited environment it is sufficient - but by no means necessary - that the wavelength of the highest modulation frequency be large compared with the array dimensions). In the absence of such minimal requirements one can construct pathological examples which yield values of R arbitrarily close to zero.

V. Adaptive Signal Processing

The structure and performance of the optimum detectors discussed in earlier volumes of this series depends critically on prior knowledge of signal and noise statistics. It has been pointed out that such knowledge is likely to be incomplete at best. Several reports have postulated that certain noise parameters (e.g. total noise power) were unknown and have studied the resulting detection problem, arriving at primitive forms of adaptation to the noise field.

Report No. 34 represents the first attempt in this series to deal with a truly adaptive situation, one in which there is an absolute minimum of available a priori information. The report is of an introductory nature. It seeks to define the problems and create the mathematical framework for later studies. Specific results are obtained only for a signal processor using a single hydrophone, but the procedures discussed generalize without difficulty to array processing problems.

In the situation analized here the output of the single hydrophone is passed through a tapped delay line filter whose tap weights are adaptively adjusted to minimize the mean square error between the filter output and the signal component of the input. Stochastic approximation is used as the basic technique of adjustment.

It is clear that detection is impossible in the total absence of any information concerning signal or noise. Three cases short of such total ignorance are considered: 1) The signal waveshape is known, the noise is a stationary stochastic process with unknown statistical properties 2) Signal and noise are stationary stochastic processes, the signal spectrum is known, the noise spectrum is not 3) Signal and noise are stationary stochastic processes, the noise spectrum is known, the signal spectrum is not.

In each case one finds that proper use of the stochastic approximation technique generates a filter which converges to the optimum Wiener filter. Conditions of convergence and rates of convergence are similar for the three cases. A convenient choice of the gain parameter in the stochastic approximation algorithm causes the mean square error to converge to its minimum with the approximate first power of time. Certain preliminary results dealing with the application of stochastic approximation techniques to non-stationary noise fields are also presented.

CONFIDENTIAL

TRACKING IN THE PRESENCE OF INTERFERENCE

by

Peter M. Schultheiss

Progress Report No. 29

General Dynamics/Electric Boat Research

(8050-31-55001)

November 1966

DEPARTMENT OF ENGINEERING

AND APPLIED SCIENCE

YALE UNIVERSITY

CONFIDENTIAL

Summary

The report analyzes the effect of a plane wave interference on the performance of a split beam tracker. The performance of a conventional tracker is compared with that of a tracker designed to null the interference prior to beam forming on the target. The receiving array is assumed to be linear with equally spaced hydrophones. Signal, ambient noise and interference are assumed to be statistically independent Gaussian random processes with power spectra of the same form. The observation time T is assumed to be large compared with the correlation time of signal, ambient noise and interference, but short enough so that target and interference bearings do not change significantly in T seconds. For computational simplicity the ambient noise is assumed to be statistically independent from hydrophone to hydrophone. The following results are obtained

1) The tracking error consists, in general, of two parts:
   a) Systematic error is measured by the displacement of the target null of the average tracker output from the true target bearing. It is due to asymmetry in the noise field, caused here by the interference.
   b) Random error is the fluctuation of the tracker output about its average value. It is due to the finite smoothing time T .
2) The nulling tracker completely eliminates the interference. With the spatially symmetrical ambient noise postulated in the analysis, its output is therefore free from systematic error and exhibits a random error depending only on the ambient noise.

3) The conventional tracker has both systematic and random error components. The ratio of systematic to random error is greatest for spectra whose Fourier transforms decay slowly (e.g., white spectra) and smallest for spectra with rapidly decaying Fourier transforms. However, even in the latter case the systematic error tends to exceed the random error (often by a large factor) under most reasonable operating conditions, as long as the environment is interference dominated. For interferences well separated from the target the borderline between interference dominated and ambient noise dominated operation is reached at an ambient noise to interference ratio of $\sqrt{(4/3)M}$. M is the number of hydrophones in each half of the array.

4) At low interference to signal ratios the systematic error of the conventional tracker rises linearly with the interference to signal ratio. The slope of this rise depends strongly on the spectral shape, being largest for spectra with slowly decaying Fourier transforms. Spectrum shaping can be accomplished by insertion of appropriate filters into each channel of the tracker. When the interference to signal ratio increases beyond a certain point the systematic error increases rapidly. Soon thereafter the target null disappears entirely and tracking becomes impossible. This may happen at interference levels at which the random error is not at all excessive. Even at interference to signal ratios as low as 5 the systematic error can easily amount to a major fraction of a degree.

5) With fixed hydrophone spacing the rms random error of the conventional tracker varies as $T^{-\frac{1}{2}}\ \omega_o^{-3/2}\ M^{-3/2}\ I$ in an interference

dominated environment and as $T^{-\frac{1}{2}} \omega_o^{-3/2} M^{-2} N$ in an ambient noise dominated environment. ω_o is the bandwidth of the spectrum, I the average interference power and N the average noise power. For fixed array length (hydrophone spacing inversely proportional to M) the M dependence is $M^{-\frac{1}{2}}$ (interference dominant) and M^{-1} (ambient noise dominant) respectively.

6) The rms error of the nulling tracker is approximately the same as that of the conventional tracker in an ambient noise dominated environment. In an interference dominated environment the rms error of the conventional tracker is larger by the factor $\sqrt{8/9}\ \sqrt{M}\ (I/N)$.

7) It is apparent from 2) and 6) that one might employ interference nulling for two reasons

   a) To eliminate systematic error

   b) To reduce random error

Since nulling achieves significant random error reduction only in a strongly interference dominated environment, one must inquire whether such an environment occurs sufficiently often to justify the added complexity of instrumentation. If it does not, one must further inquire whether one cannot eliminate systematic error by procedures much simpler to implement than nulling. This appears distinctly possible because systematic error depends only on average parameters of the interference (bearing, power, etc.), not on details of the interference time function.

1. Introduction

This report is concerned with the effect of interference from a point source on the performance of split beam trackers. Instrumentations with and without provisions for null steering on the interference are analyzed. Because interest centers on the interference problem, the simplest possible assumptions are made concerning all other aspects of the system. Thus interference, ambient noise, and signal are assumed to be independent Gaussian random processes with spectra identical over the processed frequency band. The ambient noise is regarded as statistically independent from hydrophone to hydrophone. The processing array is linear and consists of equally spaced elements.

Various possible instrumentations differ considerably in their detailed characteristics, but each exhibits an average output $\bar{z}$ which varies with steering angle θ roughly in the manner outlined in Figure 1, at least for values of θ close to the target bearing θ_o and reasonably remote from the interference bearing θ_I. In the absence of systematic error, $\bar{z}$ passes through zero at $\theta = \theta_o$ The instantaneous tracker output is the value of θ near θ_o at which the random variable $z(t;\theta)$ (whose mean value is $\bar{z}$) passes through zero. The rms tracking error is therefore the standard

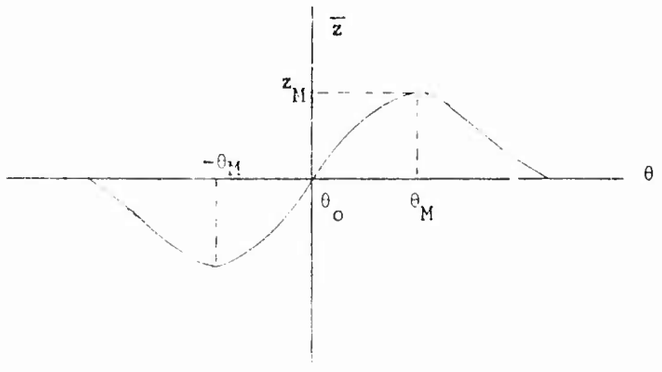

Figure 1

deviation of this zero location. As long as this standard deviation is small compared with θ_M there is no serious danger that the target will be lost. On the other hand, if the rms error becomes comparable to θ_M (i.e., if z(t) can exceed z_M with a probability that is not negligible), sustained tracking is no longer practical.

Formal computation of the zero distribution of a random process such as $z(t;\theta)$ (considered as a function of θ) is an extremely difficult problem. However, a simple approximation can be obtained for the situation of primary interest here, the case of trackers employing smoothing times large compared with the correlation time of the tracker input. The assumption of large smoothing times has two important consequences:

1) The tracker output $z(t;\theta)$, considered as a function of t, is an approximately Gaussian random process.[1] Furthermore, $\left\{ z(t_1;\theta_1), z(t_1;\theta_2) \right\}$ may be regarded as Gaussian in two dimensions.

2) Smoothing over a long period of time results in relatively small scattering in both amplitude and slope of $z(t;\theta)$--considered as a function of θ--about the averages specified by $\bar{z}$. Sensitivity considerations require the slope $\frac{\partial \bar{z}}{\partial \theta}$ to be reasonably large near $\theta = \theta_o$. But if $\frac{\partial \bar{z}}{\partial \theta}$ is a sizable positive number (as suggested by Figure 1) and the scattering in slope is small, the probability of $\frac{\partial z}{\partial \theta}$ assuming a negative value near θ_o is extremely small. In other words, with a probability close to unity, $z(t;\theta)$--considered as a function of θ--has one and only one zero in the neighborhood of θ_o.

---

[1] For a detailed statement of the required conditions, see M. Rosenblatt, "Some Comments on Narrow Band-Pass Filters," Quarterly of Applied Math., 15, No. 4, January 1961.

As soon as the possibility of multiple zeros in the θ range of interest can be ruled out, it becomes a relatively simple matter to calculate the zero distribution by computing the closely related probability that $z(t;\theta)$ has a zero in $(\theta,\theta+d\theta)$. Designating the latter probability by $P(\theta)\,d\theta$ one obtains

$$P(\theta)\,d\theta = \Pr\{z(t;\theta+d\theta) > 0\} - \Pr\{z(t;\theta) > 0\} \tag{1}$$

Hence

$$P(\theta) = \frac{\partial}{\partial\theta}\left[\Pr\{z(t;\theta) > 0\}\right] \tag{2}$$

In view of the Gaussian nature of $z(t;\theta)$

$$\Pr\{z(t;\theta) > 0\} = \int_0^\infty \frac{1}{\sqrt{2\pi}\,\sigma_z}\, e^{-\frac{(z-\bar{z})^2}{2\sigma_z^2}}\, dz \tag{3}$$

where σ_z is the standard deviation of z. Both $\bar{z}$ and σ_z are, in general, functions of θ. Substituting into (2) one obtains

$$P(\theta) = \frac{\partial}{\partial\theta}\int_0^\infty \frac{1}{\sqrt{2\pi}\,\sigma_z}\, e^{-\frac{(z-\bar{z})^2}{2\sigma_z^2}}\, dz$$

$$= \frac{1}{\sqrt{2\pi}\,\sigma_z}\int_0^\infty dz\, e^{-\frac{(z-\bar{z})^2}{2\sigma_z^2}}\left\{\frac{z-\bar{z}}{\sigma_z^2}\frac{\partial\bar{z}}{\partial\theta} + \frac{(z-\bar{z})^2}{\sigma_z^3}\frac{\partial\sigma_z}{\partial\theta}\right\} \tag{4}$$

Straightforward evaluation of the integral leads to the result

$$P(\theta) = \frac{1}{\sqrt{2\pi}\sigma_z}\, e^{-\frac{\bar{z}^2}{2\sigma_z^2}}\left(\frac{\partial\bar{z}}{\partial\theta} - \frac{\bar{z}}{\sigma_z}\frac{\partial\sigma_z}{\partial\theta}\right) - \frac{1}{2\sigma_z}\left[1 + \operatorname{erf}\left(\frac{\bar{z}}{\sqrt{2}\,\sigma_z}\right)\right]\frac{\partial\sigma_z}{\partial\theta} \tag{5}$$

where

$$\text{erf } x \equiv \frac{2}{\sqrt{\pi}} \int_0^x e^{-y^2}\, dy \tag{6}$$

If the standard deviation of z is constant over the θ range of interest, $\frac{\partial \sigma_z}{\partial \theta} = 0$ and Eq. (5) reduces to

$$P(\theta) = \frac{1}{\sqrt{2\pi}\,\sigma_z}\, e^{-\frac{\bar{z}^2}{2\sigma_z^2}}\, \frac{\partial \bar{z}}{\partial \theta} \tag{7}$$

Sustained tracking is clearly feasible only if the typical fluctuation in indicated θ is small compared with $|\theta_M - \theta_o|$ (see Figure 1). In that case σ_z must be small compared with $z_{..}$ and one can approximate

$$\bar{z} \approx \bar{z}_o + \left.\frac{\partial \bar{z}}{\partial \theta}\right|_0 (\theta - \theta_o) \tag{8}$$

$\bar{z}_o$ and $\left.\frac{\partial \bar{z}}{\partial \theta}\right|_0$ are the values of $\bar{z}$ and its derivative at $\theta = \theta_o$.

Substituting into Eq. (7) one then obtains

$$P(\theta) = \frac{1}{\sqrt{2\pi}\,\sigma_z} \exp\left\{ - \frac{\left[\bar{z}_o + \left.\frac{\partial \bar{z}}{\partial \theta}\right|_0 (\theta - \theta_o) \right]^2}{2\sigma_z^2} \right\} \left.\frac{\partial \bar{z}}{\partial \theta}\right|_0$$

$$= \frac{1}{\sqrt{2\pi}\left(\dfrac{\sigma_z}{\left.\frac{\partial \bar{z}}{\partial \theta}\right|_0} \right)} \exp\left\{ - \frac{\left[\theta - \theta_o + \dfrac{\bar{z}_o}{\left.\frac{\partial \bar{z}}{\partial \theta}\right|_0} \right]^2}{2 \left[\dfrac{\sigma_z}{\left.\frac{\partial \bar{z}}{\partial \theta}\right|_0} \right]^2} \right\} \tag{9}$$

Thus the zero location (the indicated bearing) has an approximately normal distribution with mean $\theta_o - \frac{\bar{z}_o}{\left.\frac{\partial \bar{z}}{\partial \theta}\right|_0}$ and standard deviation $\left|\frac{\sigma_z}{\left.\frac{\partial \bar{z}}{\partial \theta}\right|_0}\right|$. The latter is, of course, the ratio of fluctuation to sensitivity at the null, the figure of merit frequently used to measure the accuracy of null seeking devices. $\frac{\bar{z}_o}{\left.\frac{\partial \bar{z}}{\partial \theta}\right|_0}$ is a systematic error in indicated bearing due to such factors as asymmetry in the noise field or imperfections in the instrumentation.

If the standard deviation of z varies with θ one must revert to Eq. (5). However, for most cases of interest in the present study it will be found that the contribution to Eq. (5) of terms involving $\frac{\partial \sigma_z}{\partial \theta}$ is small, so that Eq. (9) gives a reasonable approximation. This is almost evident by inspection of Eq. (5), for if one multiplies this equation by $\partial\theta$ it reads

$$P(\theta)\,\partial\theta = \frac{1}{\sqrt{2\pi}\,\sigma_z} e^{-\frac{\bar{z}^2}{2\sigma_z^2}} \left(\partial\bar{z} - \frac{\bar{z}}{\sigma_z}\partial\sigma_z\right) - \frac{1}{2\sigma_z}\left[1 + \operatorname{erf}\frac{\bar{z}}{\sqrt{2}\,\sigma_z}\right]\partial\sigma_z \qquad (5a)$$

Consider values of $\bar{z}$ satisfying $|\bar{z}| \leq \sigma_z$, the range in which the exponential function has a value significantly different from zero. Omission of the term $\left(\frac{\bar{z}}{\sigma_z}\right)\partial\sigma_z$ requires that the change of σ_z be much smaller than the change of $\bar{z}$. But since $\bar{z} = 0$ at some point near θ_o it follows that $\partial\bar{z} = \bar{z}$. The maximum $\bar{z}$ being considered is σ_z. Hence the term $\left(\frac{\bar{z}}{\sigma_z}\right)\partial\sigma_z$ can certainly be ignored if the variation $\partial\sigma_z$ of the standard deviation is a small fraction of σ_z over the θ interval corresponding to $0 \leq \bar{z} \leq \sigma_z$.[1] To eliminate the last term of Eq. (5a)

---

[1] The argument has been conducted for the finite interval $0 \leq z \leq \sigma_z$. To derive from it the point-wise condition required for the simplification of Eq. (5a) one need only postulate linearity of $\bar{z}(\theta)$ and $\sigma_z(\theta)$ in the neighborhood of θ_o.

one need only recognize that the error function has a maximum value of unity. Hence variation of σ_z by only a small percentage over the θ range of interest makes the term negligible compared with the term in $\partial\bar{z}$ for $|\bar{z}| \leq \sigma_z$.

It appears reasonable--and numerical examples worked out confirm this by an ample margin--that the variation of σ_z over the operating θ range of a functioning tracker should indeed be a small fraction of σ_z. Hence Eq. (9) is a good approximation to Eq. (5) for all θ such that the condition $|z| \leq \sigma_z$ is not violated drastically. Under these conditions the θ range for which Eq. (9) is satisfactory has a cumulative probability very close to unity.

II. Conventional Trackers

A. General Relations

An elementary version of the conventional split beam (phase) tracker is shown in Figure 2. Suppose that the delay of the signal from hydrophone to hydrophone is t_o while the delay of the interference from hydrophone to hydrophone is Δ. Then

$$\text{signal} \qquad s_j(t) = s_1\left[t+(j-1)t_o\right] \tag{10}$$

and

$$\text{interference} \qquad i_j(t) = i_1\left[t+(j-1)\Delta\right] \tag{11}$$

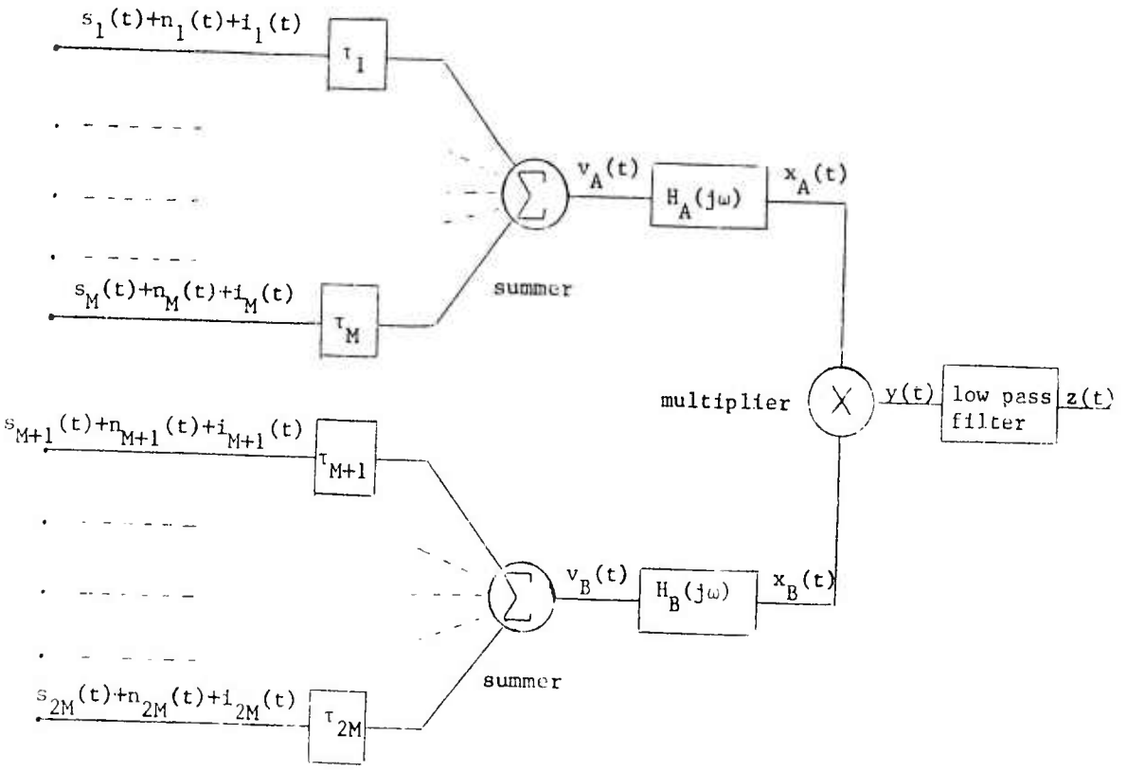

Figure 2

If the delays τ_j are adjusted so that

$$\tau_j = (j-1)t_1 \tag{12}$$

then the summer outputs are

$$v_A(t) = \sum_{j=1}^{M} \left\{ s_1\left[t+(j-1)(t_o-t_1)\right] + i_1\left[t+(j-1)(\Delta-t_1)\right] + n_j\left[t-(j-1)t_1\right] \right\} \tag{13}$$

and

$$v_B(t) = \sum_{j=1}^{M} \left\{ s_1\left[t+(j+M-1)(t_o-t_1)\right] + i_1\left[t+(j+M-1)(\Delta-t_1)\right] + n_{M+j}\left[t-(j+M-1)t_1\right] \right\} \tag{14}$$

If $t_1 = t_o$ the array is steered on target. The time delay t_1 is related to steering angle θ ($\theta = 0$ corresponds to broadside) through the equation

$$t_1 = \frac{d}{c} \sin \theta$$

d is the spacing between hydrophones and c is the velocity of sound in water.

$H_A(j\omega)$ and $H_B(j\omega)$ in Figure 2 are linear filters whose transfer functions remain unspecified for the moment. For proper functioning of the tracker they should, of course, differ in phase shift by 90^o over the entire frequency band processed. The symbols $h_A(t)$ and $h_B(t)$ will be used to designate the weighting functions (impulse responses) corresponding to the transfer functions $H_A(j\omega)$ and $H_B(j\omega)$ respectively. In terms of this nomenclature the output y(t) of the multiplier is

$$y(t) = \int_0^\infty d\sigma\ h_A(\sigma)\ v_A(t-\sigma) \int_0^\infty d\rho\ h_B(\rho)\ v_B(t-\rho) \tag{15}$$

Assuming, without loss of generality, that the low pass filter has a transfer function with unity gain at zero frequency, the average tracker output $\bar{z}$ is given by

$$\bar{z} = \overline{y(t)} = \int_0^\infty d\sigma\, h_A(\sigma) \int_0^\infty d\rho\, h_B(\rho)\, R_{v_A v_B}(\sigma-\rho) \tag{16}$$

where $R_{v_A v_B}(\tau) = \overline{v_A(t)\, v_A(t+\tau)}$, the crosscorrelation between v_A and v_B.

If one defines the cross-spectral density by

$$G_{v_A v_B}(\omega) = \frac{1}{2\pi} \int_{-\infty}^{\infty} R_{v_A v_B}(\tau)\, e^{-j\omega\tau}\, d\tau \tag{17}$$

then

$$R_{v_A v_B}(\tau) = \int_{-\infty}^{\infty} G_{v_A v_B}(\omega)\, e^{j\omega\tau}\, d\omega \tag{18}$$

and Eq. (16) becomes

$$\bar{z} = \int_{-\infty}^{\infty} d\omega\, H_A^*(j\omega)\, H_B(j\omega)\, G_{v_A v_B}(\omega) \tag{19}$$

The fluctuation of the tracker output is characterized by the variance σ_z^2. Postulating a low pass filter with the weighting function

$$h(t) = \begin{cases} \frac{1}{T} & 0 \leq t \leq T \\ 0 & t > T \end{cases} \tag{20}$$

and assuming T large compared with the correlation time of y(t), one obtains[1]

$$\sigma_z^2 = \frac{1}{T} \int_{-\infty}^{\infty} \left[R_y(\tau) - R_y(\infty) \right] d\tau \tag{21}$$

$R_y(\tau)$, the autocorrelation of y(t), is given by

$$R_y(\tau) = \overline{y(t)\, y(t+\tau)} = \overline{x_A(t)\, x_A(t+\tau)\, x_B(t)\, x_B(t+\tau)} \tag{22}$$

---

[1] Report No. 10, Eq. (9).

Since $x_A(t)$ and $x_B(t)$ are Gaussian random processes, this fourfold average can be expressed in terms of correlation functions.

$$R_y(\tau) = R^2_{x_A x_B}(0) + R_{x_A}(\tau)\, R_{x_B}(\tau) + R_{x_A x_B}(\tau)\, R_{x_A x_B}(-\tau) \tag{23}$$[1]

Recognizing that

$$R_{x_A x_B}(0) = R_y(\infty) \tag{24}$$

one obtains from Eq. (21)

$$\sigma_z^2 = \frac{1}{T}\int_{-\infty}^{\infty} d\tau\, R_{x_A}(\tau)\, R_{x_B}(\tau) + \frac{1}{T}\int_{-\infty}^{\infty} d\tau\, R_{x_A x_B}(\tau)\, R_{x_A x_B}(-\tau) \tag{25}$$

Now invoking Parseval's theorem

$$\sigma_z^2 = \frac{2\pi}{T}\int_{-\infty}^{\infty} d\omega\, G_{x_A}(\omega)\, G_{x_B}(\omega) + \frac{2\pi}{T}\int_{-\infty}^{\infty} d\omega \left| G_{x_A x_B}(\omega) \right|^2 \tag{26}$$

Finally, expressing the result in terms of the auto- and crosscorrelation functions of $v_A(t)$ and $v_B(t)$,

$$\sigma_z^2 = \frac{2\pi}{T}\int_{-\infty}^{\infty} d\omega \left\{ |H_A(j\omega)|^2\, |H_B(j\omega)|^2\, G_{v_A}(\omega)\, G_{v_B}(\omega) + \left[H_A^*(j\omega)\, H_B(j\omega) \right]^2 \left[G_{v_A v_B}(\omega) \right]^2 \right\} \tag{27}$$

Equations (19) and (27) are the fundamental relations describing the operation of the tracker. Note that they depend only on the spectral properties of the summer outputs. They will therefore hold equally well when the beam-forming system contains provisions for nulling an interference or for discriminating against an anisotropic noise. The effect of such

---

[1] R with a single subscript denotes the autocorrelation of the subscripted variable. A double subscript indicates the crosscorrelation between the two subscripted variables.

provisions on tracker performance is completely described by their influence on the spectral properties of (v_A, v_B).

The simplest possible choice of $H_A(j\omega)$ and $H_B(j\omega)$, retaining only the feature essential for tracking, (the 90° relative phase shift) is

$$H_A(j\omega) = \frac{j\omega}{|\omega|} \tag{28}$$

$$H_B(j\omega) = 1 \tag{29}$$

It will shortly become apparent that changes in the filter functions can be treated as equivalent changes in the input spectra (see p. 15), so that Eqs. (28) and (29) are not restrictive in any important sense.

Using Eqs. (28) and (29), Eq (19) becomes

$$\bar{z} = 2 \int_0^\infty d\omega \, \mathfrak{J}\left\{G_{v_A v_B}(\omega)\right\} \tag{30}$$[1]

while Eq. (27) reduces to

$$\sigma_z^2 = \frac{2\pi}{T} \int_{-\infty}^{\infty} d\omega \left[G_{v_A}(\omega) \, G_{v_B}(\omega) - \left\{ G_{v_A v_B}(\omega) \right\}^2 \right] \tag{31}$$

Equations (30) and (31) will form the basis for most computations in this report.

B. Average Tracker Output

According to Eq. (30) the average tracker output depends only on the cross-spectral density of $v_A(t)$ and $v_B(t)$. This quantity is easily computed from the corresponding autocorrelation function. Using Eqs. (13) and (14) and assuming independence of the ambient noise from hydrophone to hydrophone (as well as the independence of signal, interference, and ambient noise from each other)

---

[1] $\mathfrak{J}(\ )$ stands for the imaginary part of the bracketed quantity.

$$R_{v_A v_B}(\tau) = E\left[\left[\sum_{\ell=1}^{M}\sum_{k=1}^{M}\left\{s_1\left[t+(\ell-1)(t_o-t_1)\right] + i_1\left[t+(\ell-1)(\Delta-t_1)\right] + n_\ell\left[t-(\ell-1)t_1\right]\right\}\right.\right.$$
$$\left.\left.\times\left\{s_1\left[t+\tau+(k-M-1)(t_o-t_1)\right] + i_1\left[t+\tau+(k+M-1)(\Delta-t_1)\right] + n_{M+k}\left[t+\tau-(k+M-1)t_1\right]\right\}\right]$$
$$= S\sum_{\ell=1}^{M}\sum_{k=1}^{M}\rho_S\left[\tau+(k-\ell+M)(t_o-t_1)\right] + I\sum_{\ell=1}^{M}\sum_{k=1}^{M}\rho_I\left[\tau+(k-\ell+M)(\Delta-t_1)\right] \qquad (32)^1$$

$\rho_S(\tau)$ and $\rho_I(\tau)$ are the normalized autocorrelation functions of signal and interference respectively. S is the average signal power and I the average interference power.

Applying Eq. (17) to Eq. (32) one obtains

$$G_{v_A v_B}(\omega) = S\sum_{\ell=1}^{M}\sum_{k=1}^{M} g_S(\omega)\, e^{j\omega(k-\ell+M)(t_o-t_1)} + I\sum_{\ell=1}^{M}\sum_{k=1}^{M} g_I(\omega)\, e^{j\omega(k-\ell+M)(\Delta-t_1)} \qquad (33)$$

$g_S(\omega)$ and $g_I(\omega)$ are the normalized spectral densities of signal and interference respectively, i.e.

$$\int_{-\infty}^{\infty} g_S(\omega)\, d\omega = \int_{-\infty}^{\infty} g_I(\omega)\, d\omega = 1$$

It is clear from Eqs. (19) and (33) that modification of $H_A(j\omega)$ and $H_B(j\omega)$ by the same factor $H(j\omega)$ is equivalent to modification of $g_S(\omega)$ and $g_I(\omega)$ by the factor $|H(j\omega)|^2$. As anticipated on p.14 one can therefore study the effect of filtering operations, such as prewhitening, simply by considering appropriate modifications in the input spectra.[2]

---

[1] $E\left[\left[\ \ \right]\right]$ designates the expectation of the bracketed quantity.

[2] A similar statement holds concerning the effect of filters on the output fluctuation [see Eq. (31)].

Substitution of Eq. (33) into Eq. (30) yields

$$\bar{z} = 2\sum_{\ell=1}^{M}\sum_{k=1}^{M}\int_0^\infty d\omega \left\{ S\, g_S(\omega)\, \sin\left[\omega(k-\ell+M)(t_o-t_1)\right] + I\, g_I(\omega)\, \sin\left[\omega(k-\ell+M)(\Delta-t_1)\right]\right\} \tag{34}$$

Equation (34) will now be evaluated for various signal and interference spectra.

1) White Spectra. Consider first the case of signal and interference spectra white (or prewhitened) over the entire processed frequency band. Then

$$g_S(\omega) = g_I(\omega) = \begin{cases} \dfrac{1}{2\omega_o} & |\omega| < \omega_o \\ 0 & |\omega| \geq \omega_o \end{cases} \tag{35}$$

Equation (34) is now easily integrated, with the result

$$\bar{z} = \sum_{\ell=1}^{M}\sum_{k=1}^{M}\left\{ S\,\frac{1-\cos\left[(k-\ell+M)\omega_o(t_o-t_1)\right]}{(k-\ell+M)\,\omega_o(t_o-t_1)} + I\,\frac{1-\cos\left[(k-\ell+M)\,\omega_o(\Delta-t_1)\right]}{(k-\ell+M)\,\omega_o(\Delta-t_1)}\right\} \tag{36}$$

Since the indices k and ℓ occur only in the combination k-ℓ, it is convenient to introduce the notation

$$k - \ell = r \tag{37}$$

Then Eq. (36) becomes

$$\bar{z} = \sum_{r=-(M-1)}^{M-1}\left\{ S\,\frac{1-\cos\left[(r+M)\omega_o(t_o-t_1)\right]}{(r+M)\,\omega_o(t_o-t_1)} + I\,\frac{1-\cos\left[(r+M)\omega_o(\Delta-t_1)\right]}{(r+M)\omega_o(\Delta-t_1)}\right\}(M-|r|) \tag{38}$$

Introducing the notation

$$x_1 = \omega_o(t_o-t_1) \qquad \text{and} \qquad y_1 = \omega_o(\Delta-t_1) \tag{38a}$$

one can rewrite Eq. (38) in the form

$$\bar{z} = S \sum_{r=-(M-1)}^{M-1} \left\{ \frac{1 - \cos(r+M)x_1}{(r+M)x_1} + \frac{I}{S} \frac{1 - \cos[(r+M)(x_1+y_1)]}{(r+M)(x_1+y_1)} \right\} (M - |r|) \tag{39}$$

Here x_1 is a measure of the array steering angle relative to the target bearing while y_1 is a measure of the interference bearing relative to the target bearing. The relation of these two quantities to the actual target bearing θ_o, interference bearing θ_I, and steering angle θ is specified by the expressions

$$t_o = \frac{d}{c} \sin \theta_o \tag{40}$$

$$\Delta = \frac{d}{c} \sin \theta_I \tag{41}$$

$$t_1 = \frac{d}{c} \sin \theta \tag{42}$$

Figure 3 shows Eq. (39), normalized with respect to S, plotted as a function of x_1 for $\frac{I}{S} = 5$, $M = 20$ (40 element array), and $y_1 = -5$.[1] With a broadside target, $\omega_o = 2\pi \times 5000$ rad/sec, and 1 ft hydrophone spacing, $y_1 = -5$ corresponds to an interference bearing of about 53^o from the target. Figure 4 gives a similar curve for $y_1 = -2$, corresponding to an interference bearing of about 19^o under the same assumptions. Figures 5 and 6 give equivalent curves for $M = 10$ (20 element array). In each case the plot exhibits generally the expected form (see Figure 1) near the target bearing. It shows a similar functional behavior, greater in amplitude, near the interference bearing. Perhaps the most striking feature of the curves is the offset in the axis crossing caused by an interference only 7 db above the signal level, even when the interference is relatively remote in angle from the target. If the tracker indicates a bearing corresponding to the zero of $\bar{z}$, then this effect can lead to appreciable systematic error in indicated bearing. With $M = 10$, $y = -2$

---

[1] The curve on the right gives the complete pattern, while that on the left shows the neighborhood of the origin in expanded form (target response).

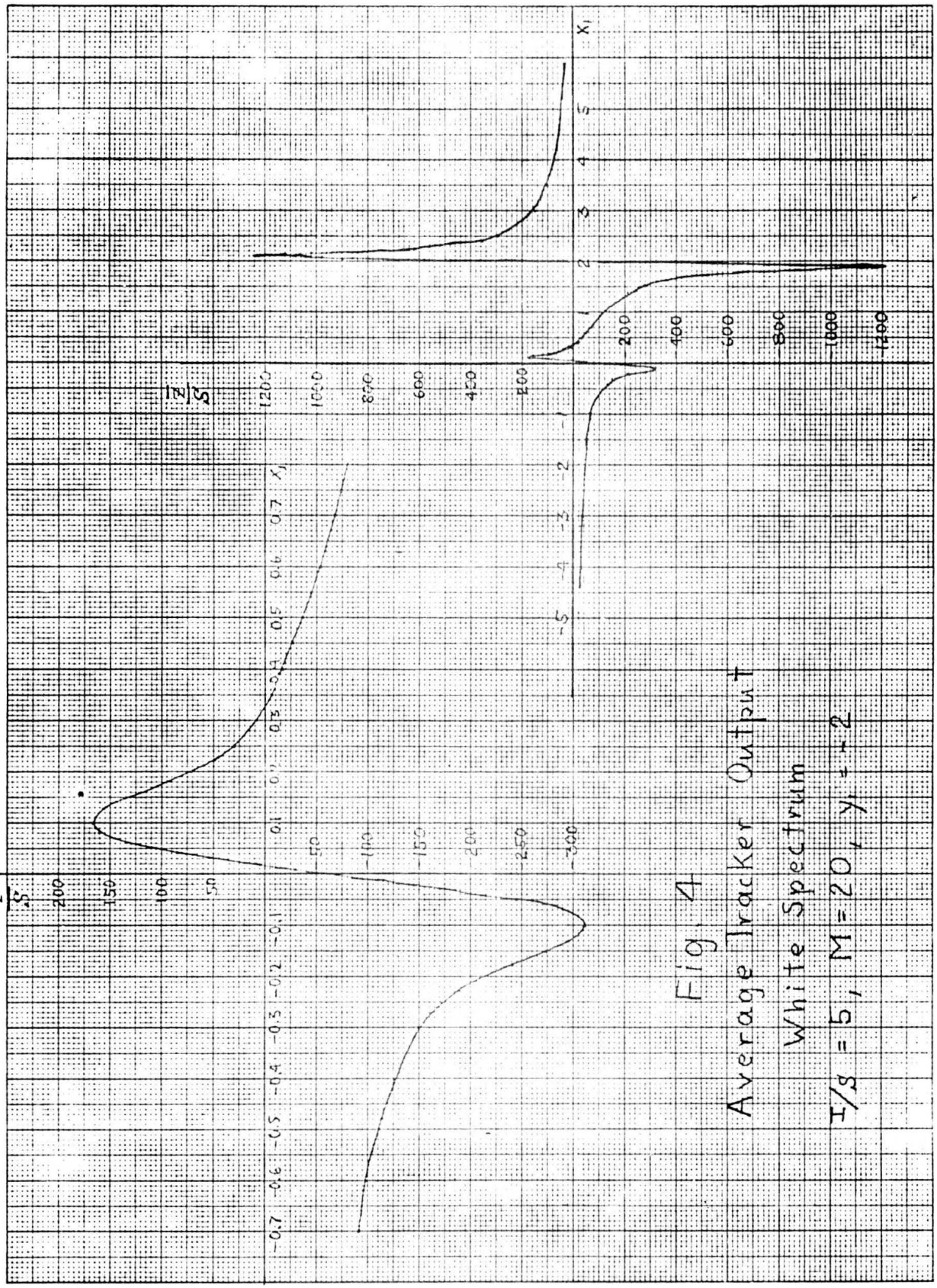

Fig. 4
Average Tracker Output
White Spectrum
$I/s = 5$, $M = 20$, $y_1 = +2$

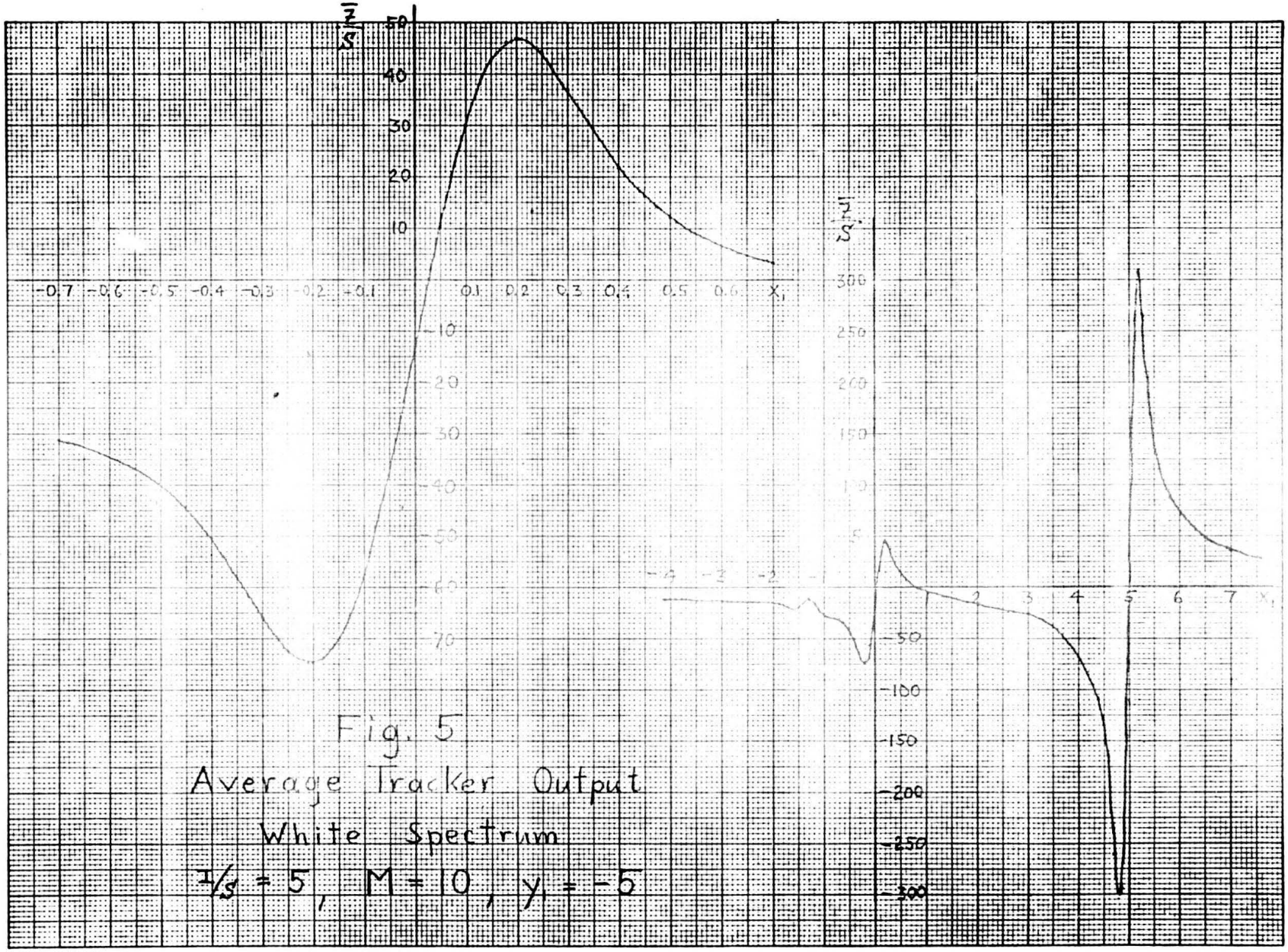

Fig. 5

Average Tracker Output

White Spectrum

$\frac{1}{S} = 5$, $M = 10$, $y_1 = -5$

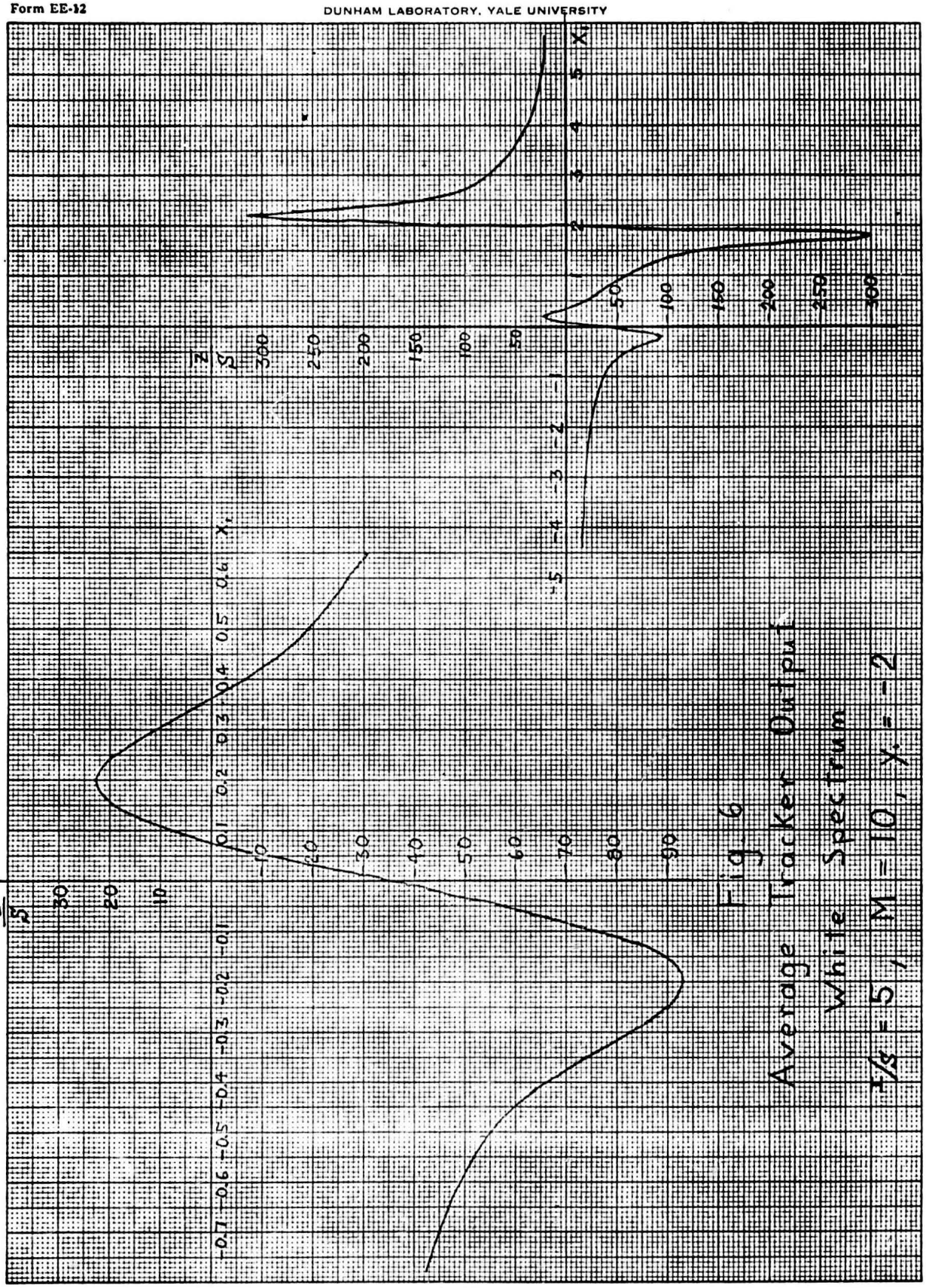
Fig 6
Average Tracker Output
White Spectrum
$\bar{z}/\sigma = 5$, $M = 10$, $y_i = -2$
$\bar{z}/\sigma$
x_i

the zero occurs at $x_1 = 0.078$. With a broadside target, $\omega_o = 2\pi \times 5000$ rad/sec, and d = 1 ft, this is equivalent to a systematic error of 0.71^o. Even with $M = 20$ and $y = -5$ the systematic error is still about 0.06^o. The importance of the problem clearly depends on the relative strength of target and interference. To exhibit this effect more clearly, Figure 7 shows the offset in the zero (systematic error) as a function of $\frac{I}{S}$ for $M = 10$ and $M = 20$ and various values of y_1. With the numerical values of ω_o and d used previously, the vertical scale can be converted to degrees of systematic error through multiplication by $\frac{57.3}{\omega_o \frac{d}{c} \cos \theta_o} = 9.1$. The curves for $y_1 = -1$ and $y_1 = -2$ terminate within the range of the graph because larger values of $\frac{I}{S}$ cause the zero near the true target bearing to disappear entirely. An instrumentation attempting to track this zero would therefore fail.

2) Algebraic Spectra. The relatively large systematic errors introduced in the above calculations by rather remote sources of interference are due at least in part to the slow decay of Eq. (39) away from $x = 0$. That effect, in turn, may be attributed to the sharp decay of $g_S(\omega)$ and $g_I(\omega)$ at ω_o. One suspects that gradually decaying spectral functions would produce more favorable results. More precisely, since the integrals in Eq. (34) are closely related to Fourier transforms of $g_S(\omega)$, less systematic error can be expected from spectra whose Fourier transforms (autocorrelation functions) decay rapidly away from the origin. An analytically convenient function with these general properties is

$$g_S(\omega) = g_I(\omega) = \omega_a^2 \frac{|\omega|}{(\omega^2 + \omega_a^2)^2} \qquad (43)^1$$

[1] Note that this spectral function falls to zero at $\omega = 0$, a feature generally present in practical systems.

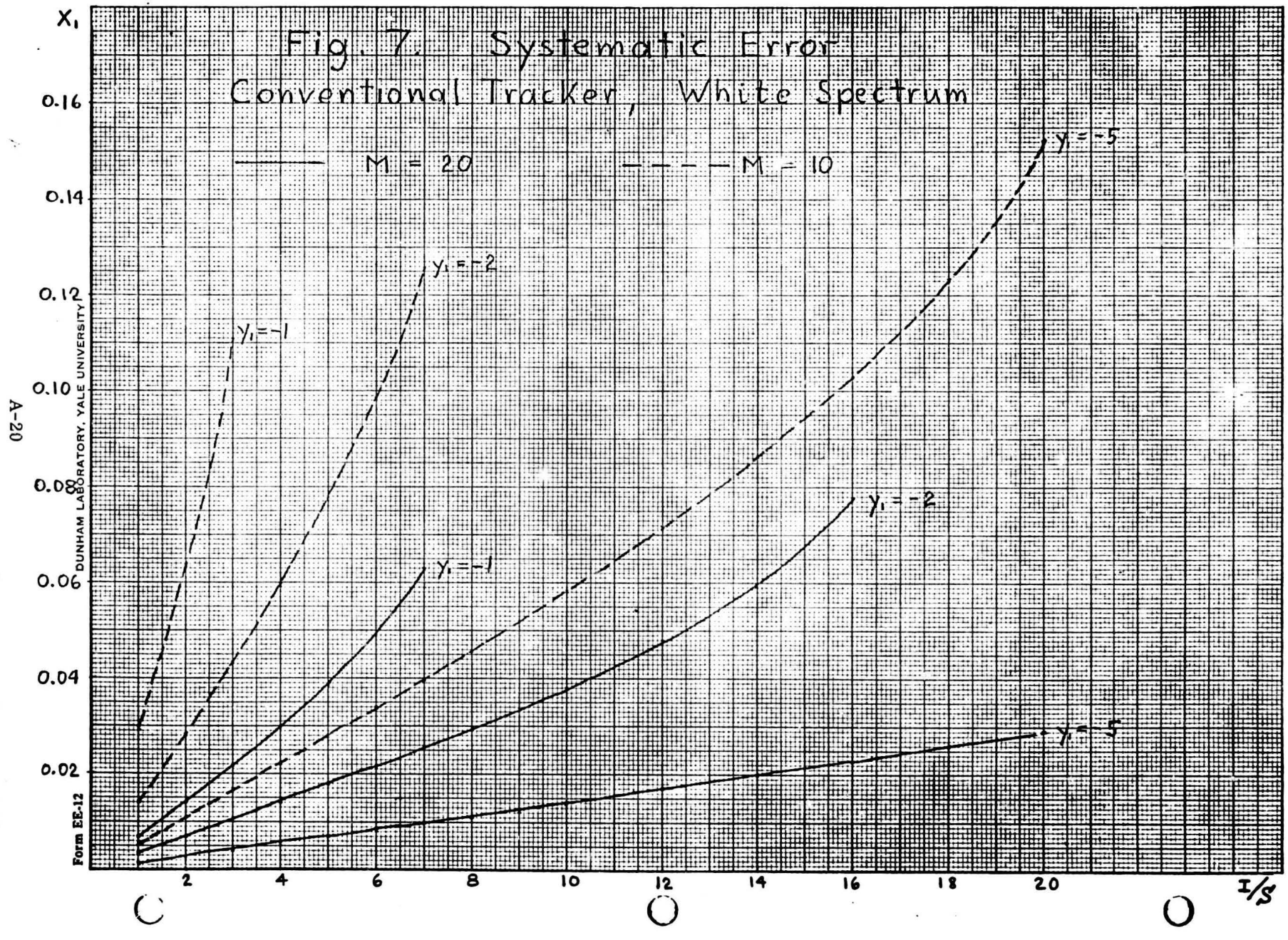

Substituting Eq. (43) into Eq. (34) one obtains

$$\bar{z} = 2\omega_a^2 \sum_{\ell=1}^{M} \sum_{k=1}^{M} \int_0^{\infty} d\omega \frac{\omega}{(\omega^2+\omega_a^2)^2} \left\{ S \sin[\omega(k-\ell+M)(t_o-t_1)] + I \sin[\omega(k-\ell+M)(\Delta-t_1)] \right\}$$

$$= \frac{\pi}{2} \sum_{\ell=1}^{M} \sum_{k=1}^{M} \left\{ S(k-\ell+M)\omega_a(t_o-t_1)\, e^{-|(k-\ell+M)(t_o-t_1)\omega_a|} \right.$$

$$\left. + I(k-\ell+M)\omega_a(\Delta-t_1)\, e^{-|(k-\ell+M)\omega_a(\Delta-t_1)} \right\} \tag{44}$$

Now changing the index, as before,

$$k - \ell = r \tag{45}$$

$$\bar{z} = \frac{\pi}{2} \sum_{r=-(M-1)}^{M-1} \left\{ S(r+M)\omega_a(t_o-t_1)\, e^{-|(r+M)(t_o-t_1)\omega_a|} \right.$$

$$\left. + I(r+M)(\Delta-t_1)\omega_a\, e^{-|(r+M)(\Delta-t_1)\omega_a|} \right\} (M-|r|) \tag{46}$$

Finally, introducing the notation

$$x_2 = \omega_a(t_o-t_1) \quad , \quad y_2 = \omega_a(\Delta-t_o) \tag{47}$$

one obtains

$$\bar{z} = \frac{\pi}{2} \sum_{r=-(M-1)}^{M-1} \left\{ S(r+M)x_2\, e^{-|(r+M)x_2|} + I(r+M)(x_2+y_2)\, e^{-|(r+M)(x_2+y_2)|} \right\} (M-|r|) \tag{48}$$

Figures 8 and 9 present plots of $\bar{z}$ equivalent to Figures 3 and 6. In both cases the plots show a much smaller influence of the interference on the behavior of $\bar{z}$ near the target bearing than was the case with white spectra. Some caution must be used in comparing the systematic errors directly,

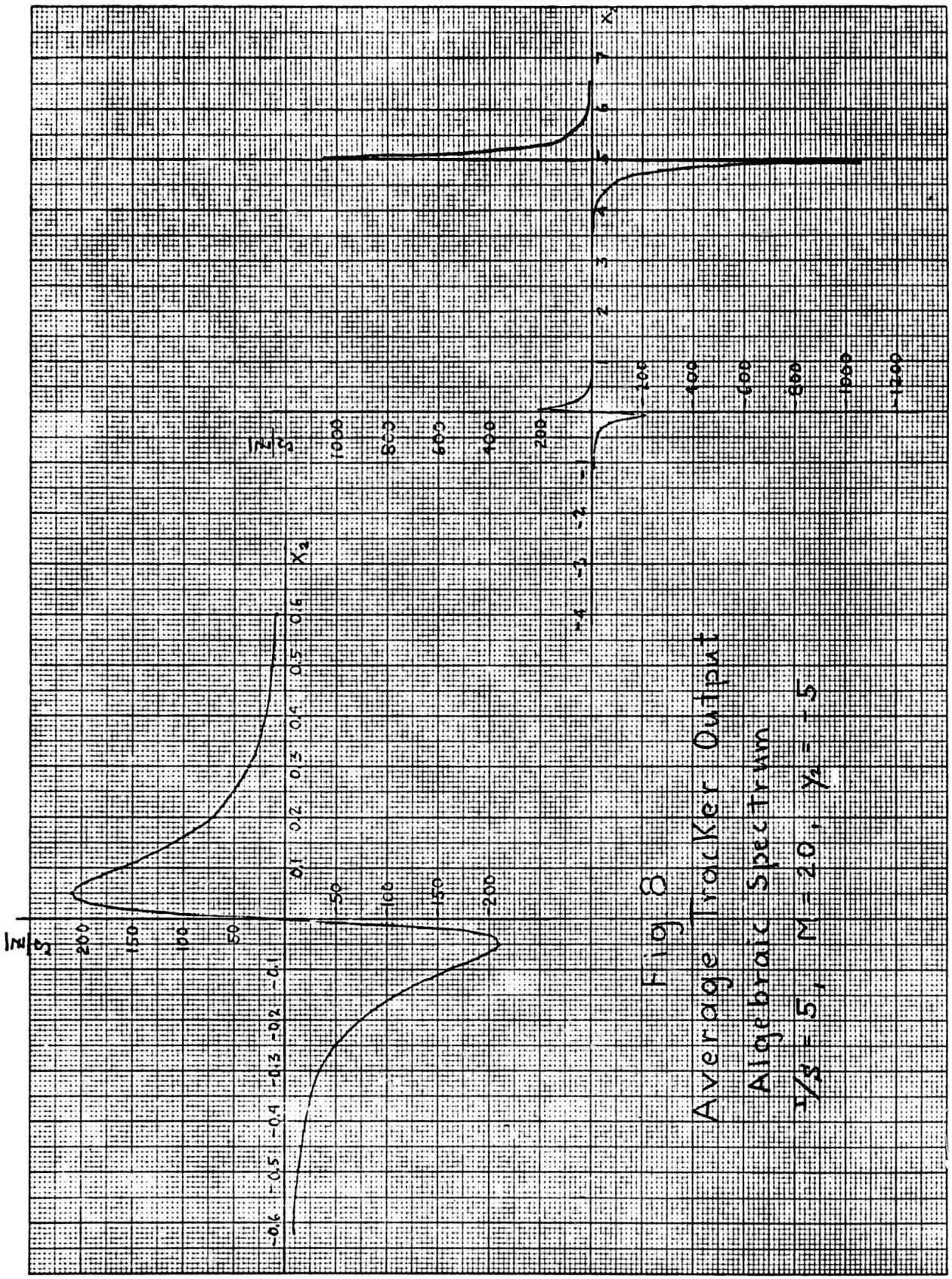
Fig 8
Average Tracker Output
Algebraic Spectrum
$Y_2 = 5$, $M = 20$, $\gamma_2 = -5$
X_2
$|N|^2 S_2$
X_1
$|N|^2 S_1$

Fig. 9

Average Tracker Output

Algebraic Spectrum

$1/S = 5$, $M = 10$, $\gamma_2 = -2$

because the physical meaning of ω_a is not exactly the same as that of ω_o. Since a substantial amount of the total power of the algebraic spectrum lies above ω_a, a fair comparison clearly demands that ω_a be chosen smaller than ω_o. One basis of comparison with a certain intuitive appeal is the following: Suppose that the spectrum is shaped primarily by the filters $H_A(j\omega)$ and $H_B(j\omega)$. Then it is reasonable to assume that the ambient noise has the same spectral form as the signal. We choose ω_a such that the detection index[1] for both types of spectra is the same in the absence of interference. A straightforward computation yields $\omega_a = \frac{\pi}{8}\omega_o$.

Figure 10 presents information analogous to Figure 7, the systematic error for the case of algebraic spectra, plotted as a function of $\frac{I}{S}$ for various values of $y_1 = \frac{8}{\pi} y_2$. Also shown for the sake of comparison are two of the curves from Figure 7 (white spectra). The vertical scale is the displacement of the zero measured in units of $x_1 = \frac{8}{\pi} x_2$. Hence for $\omega_o = 2\pi \times 5000$ rad/sec ($\omega_a = 2\pi \times 1960$ rad/sec) and $d = 1$ ft, the vertical scale must be multiplied by 9.1 to obtain systematic error in degrees (exactly as with Figure 7).

3) Exponential Spectra. Another analytically convenient spectral function, intermediate in its cutoff properties between those of Eqs. (35) and (43), is

$$g_S(\omega) = g_I(\omega) = \frac{1}{2\omega_b} e^{-\frac{|\omega|}{\omega_b}} \tag{49}$$

The resulting expression for $\bar{z}$ is

$$\bar{z} = \sum_{r=-(M-1)}^{M-1} \left\{ S \frac{x_3}{1 + (r+M)^2 x_3^2} + I \frac{(x_3+y_3)}{1 + (r+M)^2 (x_3+y_3)^2} \right\} (M - |r|)(M + r) \tag{50}$$

---

[1] Report No. 3, Eq. (49).

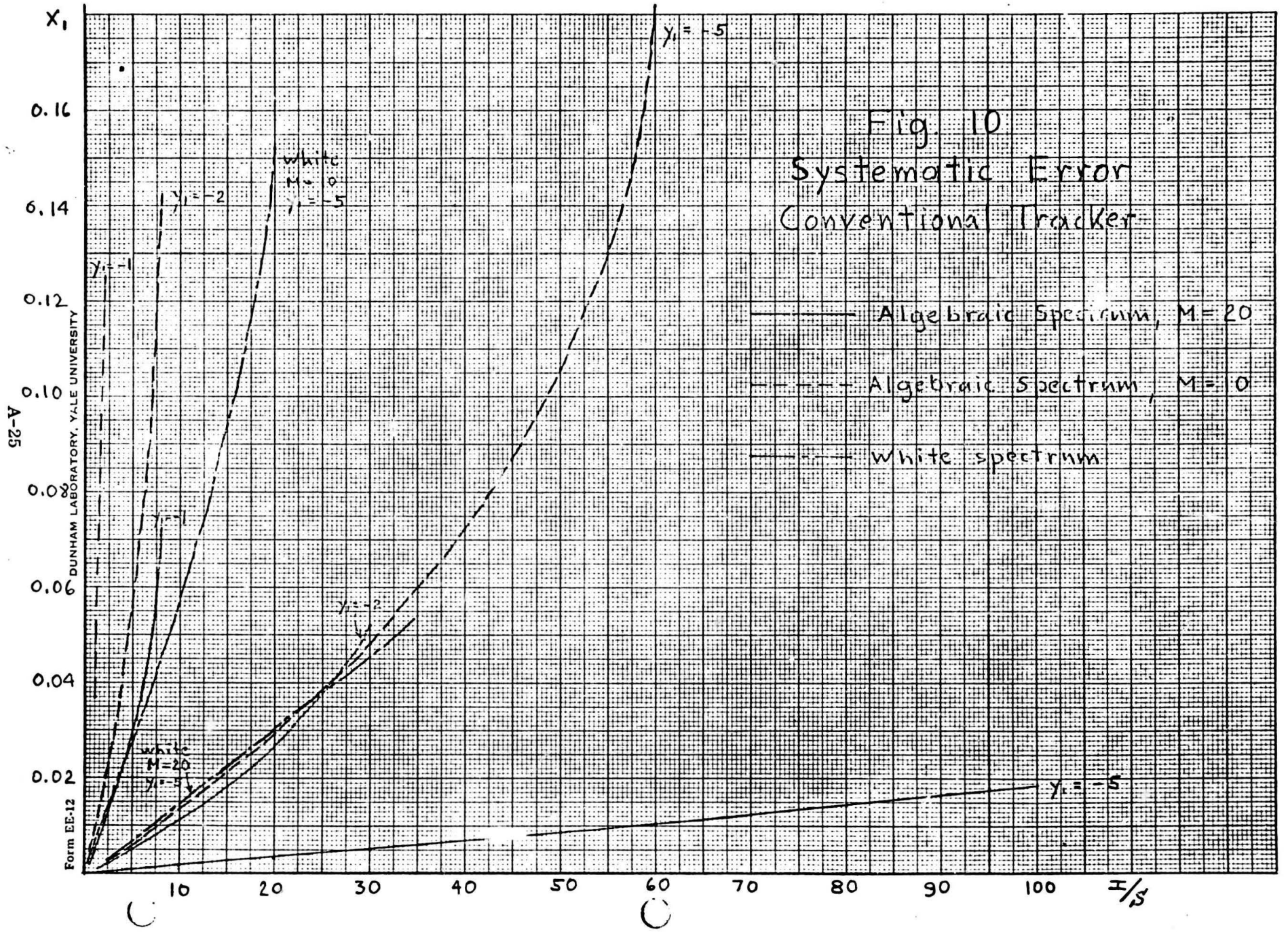
X_1
0.16
0.14
0.12
0.10
0.08
0.06
0.04
0.02
$y_1 = -5$
$y_1 = -2$
$y_1 = -1$
white
M = 0
$y_1 = -5$
$y_1 = -1$
$y_1 = -2$
white
M = 20
$y_1 = -5$
$y_1 = -5$
10
20
30
40
50
60
70
80
90
100
H/S
Fig. 10
Systematic Error
Conventional Tracker
Algebraic Spectrum, M = 20
Algebraic Spectrum, M = 0
White spectrum
DUNHAM LABORATORY, YALE UNIVERSITY
A-25
Form EE-12

where

$$x_3 = \omega_b(t_o - t_1) \qquad \text{and} \qquad y_3 = \omega_b(\Delta - t_o) \tag{51}$$

Figure 11 shows the systematic error plot corresponding to Figures 7 and 10. For proper comparison under a criterion requiring equal detection index in the absence of interference, one finds here that $\omega_b = \frac{\omega_\rho}{2}$. As expected, the systematic error is intermediate to that produced by the other two spectra.[1]

C. Output Fluctuations

According to Eq. (31) one requires the spectra $G_{v_A}(\omega)$ and $G_{v_B}(\omega)$ in addition to the already computed $G_{v_A v_B}(\omega)$ [Eq. (33)]. Computing first the autocorrelation functions, one obtains from Eqs. (13) and (14)

$$R_{v_A}(\tau) = R_{v_B}(\tau) = \overline{v_A(t)\ v_A(t+\tau)} = \overline{v_B(t)\ v_B(t+\tau)}$$

$$= S\sum_{k=1}^{M}\sum_{\ell=1}^{M}\rho_S[\tau+(k-\ell)(t_o-t_1)] + I\sum_{k=1}^{M}\sum_{\ell=1}^{M}\rho_I[\tau+(k-\ell)(\Delta-t_1)] + M\,N\,\rho_N(\tau) \tag{52}$$

$\rho_N(\tau)$ is the normalized autocorrelation of the ambient noise and N is the average ambient noise power.

Fourier transforming to obtain a corresponding expression in terms of spectral functions,

$$G_{v_A}(\omega) = G_{v_B}(\omega) = S\sum_{k=1}^{M}\sum_{\ell=1}^{M} g_S(\omega)\, e^{j(k-\ell)(t_o-t_1)\omega}$$

$$+ I\sum_{k=1}^{M}\sum_{\ell=1}^{M} g_I(\omega)\, e^{j(k-\ell)(\Delta-t_1)\omega} + M\,N\,g_N(\omega) \tag{53}$$

Inserting Eqs. (33) and (53) into Eq. (31) and using the index

$$r = k - \ell \tag{54}$$

---

[1] Note, however, that the curves for exponential spectra consistently terminate at smaller I/S than those for the other spectral types.

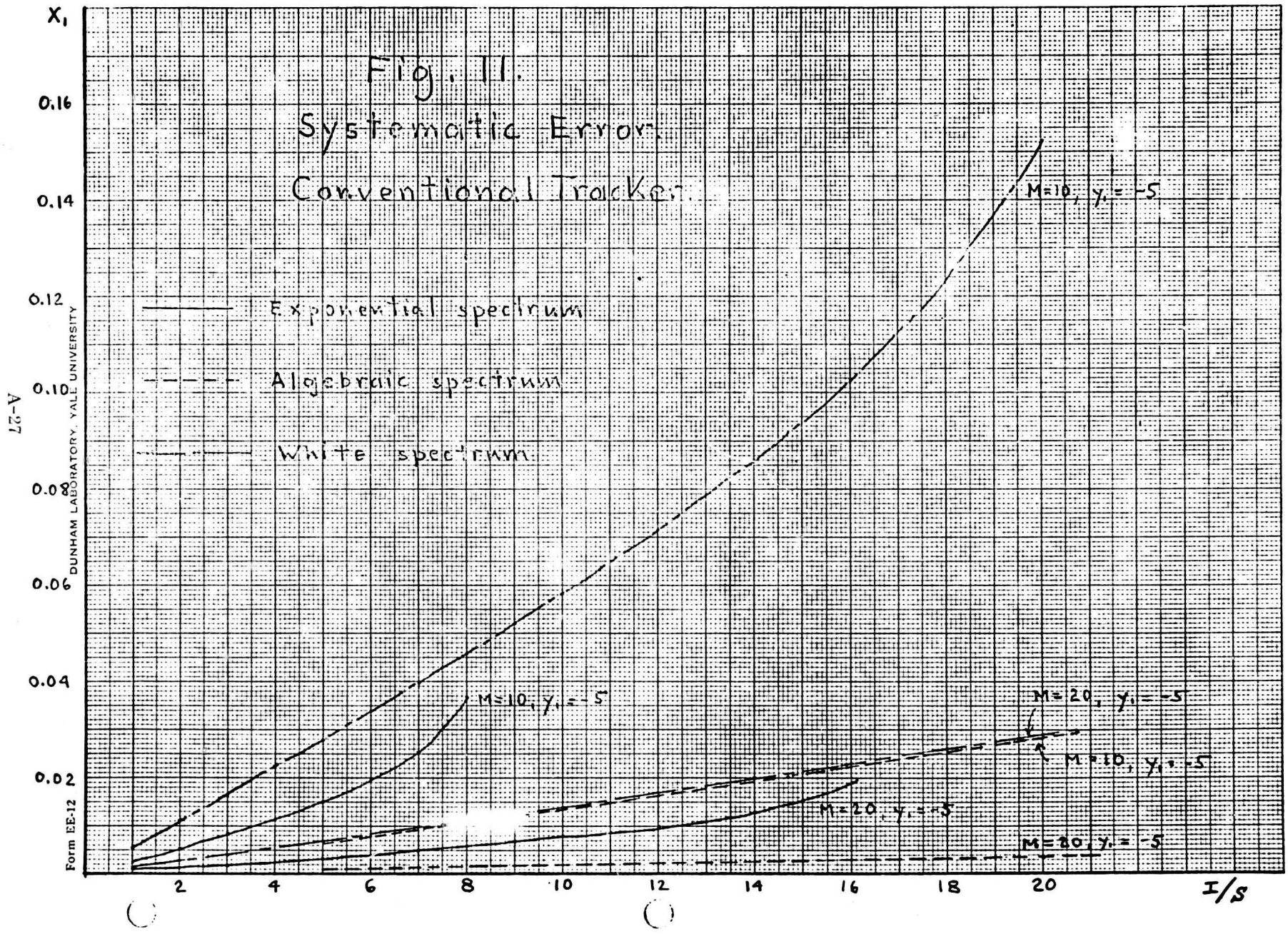
Fig. 11.
Systematic Error:
Conventional Tracker.
Exponential spectrum
Algebraic spectrum
White spectrum
M=10, γ₁=-5
M=10, γ₁=-5
M=20, γ₁=-5
M=10, γ₁=-5
M=20, γ₁=-5
M=20, γ₁=-5
X₁
0.16
0.14
0.12
0.10
0.08
0.06
0.04
0.02
2
4
6
8
10
12
14
16
18
20
I/S
A-27
DUNHAM LABORATORY, YALE UNIVERSITY
Form EE-12

one obtains

$$\sigma_z^2 = \frac{2\pi}{T}\int_{-\infty}^{\infty} d\omega \left\{ \left[S \sum_{r=-(M-1)}^{M-1} g_S(\omega)\, e^{jr(t_o-t_1)\omega}(M-|r|) + I \sum_{r=-(M-1)}^{M-1} g_I(\omega)\, e^{jr(\Delta-t_1)\omega}(M-|r|) + M N\, g_N(\omega) \right]^2 - \left[\sum_{r=-(M-1)}^{M-1} g_S(\omega) e^{j\omega(r+M)(t_o-t_1)}(M-|r|) + I \sum_{r=-(M-1)}^{M-1} g_I(\omega) e^{j\omega(r+M)(\Delta-t_1)}(M-|r|) \right]^2 \right\} \tag{55}$$

In the cases of primary interest here the signal power is much smaller than the interference power. (S may or may not be small compared with N.) In that case the signal contribution to the output variance is negligible and Eq. (55) reduces to

$$\sigma_z^2 = \frac{2\pi}{T}\int_{-\infty}^{\infty} d\omega\, I^2 \sum_{r=-(M-1)}^{M-1} \sum_{q=-(M-1)}^{M-1} g_I^2(\omega) \left| e^{j\omega(r+q)(\Delta-t_1)} - e^{j\omega(r+q+2M)(\Delta-t_1)} \right| (M-|r|)(M-|q|) + 2MNI \sum_{r=-(M-1)}^{M-1} g_I(\omega)\, g_N(\omega)\, e^{j\omega r(\Delta-t_1)}(M-|r|) + M^2N^2 g_N^2(\omega) \Bigg\} \tag{56}$$

Equation (56) must now be evaluated for the various spectra considered previously.

1) White Spectra. Consider first the spectral functions

$$g_I(\omega) = g_N(\omega) = \begin{cases} \dfrac{1}{2\omega_o} & |\omega| < \omega_o \\ 0 & |\omega| \geq \omega_o \end{cases} \tag{57}$$

Substitution into Eq. (56) yields

$$\sigma_z^2 = \frac{2\pi}{4\omega_o^2 T}\int_{-\omega_o}^{\omega_o} d\omega \left\{ I^2 \sum_{r=-(M-1)}^{M-1} \sum_{q=-(M-1)}^{M-1} \left[e^{j\omega(r+q)(\Delta-t_1)} + e^{j\omega(r+q+2M)(\Delta-t_1)} \right] (M-|r|)(M-|q|) \right.$$

$$\left. + 2MNI \sum_{r=-(M-1)}^{M-1} e^{j\omega r(\Delta-t_1)} (M-|r|) + M^2N^2 \right\}$$

$$= \frac{\pi}{\omega_o T} \left\{ I^2 \sum_{r=-(M-1)}^{M-1} \sum_{q=-(M-1)}^{M-1} \frac{\sin[(r+q)(\Delta-t_1)\omega_o]}{(r+q)(\Delta-t_1)\omega_o} - \frac{\sin[(r+q+2M)(\Delta-t_1)\omega_o]}{(r+q+2M)(\Delta-t_1)\omega_o} (M-|r|)(M-|q|) \right.$$

$$\left. + 2MNI \sum_{r=-(M-1)}^{M-1} \frac{\sin[r(\Delta-t_1)\omega_o]}{r(\Delta-t_1)\omega_o} (M-|r|) + M^2N^2 \right\} \qquad (58)$$

With the change of indices $r' = r + M$, $q' = q+M$, Eq. (58) becomes (the primes have been omitted for simplicity of notation):

$$\sigma_z^2 = \frac{\pi I^2}{\omega_o T_o} \sum_{r=1}^{2M-1} \sum_{q=1}^{2M-1} \left[\left[\frac{\sin[(r+q-2M)(x_1+y_1)]}{(r+q-2M)(x_1+y_1)} - \frac{\sin[(r+q)(x_1+y_1)]}{(r+q)(x_1+y_1)} \right] \Lambda \right.$$

$$\left. + 2M\frac{N}{I} \left[M + 2\sum_{r=1}^{M-1} \frac{\sin r(x_1+y_1)}{r(x_1+y_1)} (M-r) \right] + M^2 \frac{N^2}{I^2} \right\} \qquad (59)$$

The symbols x_1 and y_1 are defined in Eq. (38a). $x_1+y_1 = (\Delta-t_1)\omega_o$ is clearly a measure of steering angle relative to the interference bearing. Figure 12 shows a normalized version of σ_z, the square root of Eq. (59), plotted as a function of x_1+y_1 for M = 10, 20 and several values of $\frac{N}{I}$. Dependence on the latter parameter is small, as one would expect in an interference-

$\sigma_2 = \sqrt{\frac{T(\omega_0)}{\pi}} \cdot \frac{1}{\perp}$

Fig 12

Output Fluctuations

Conventional Tracker

White Spectrum

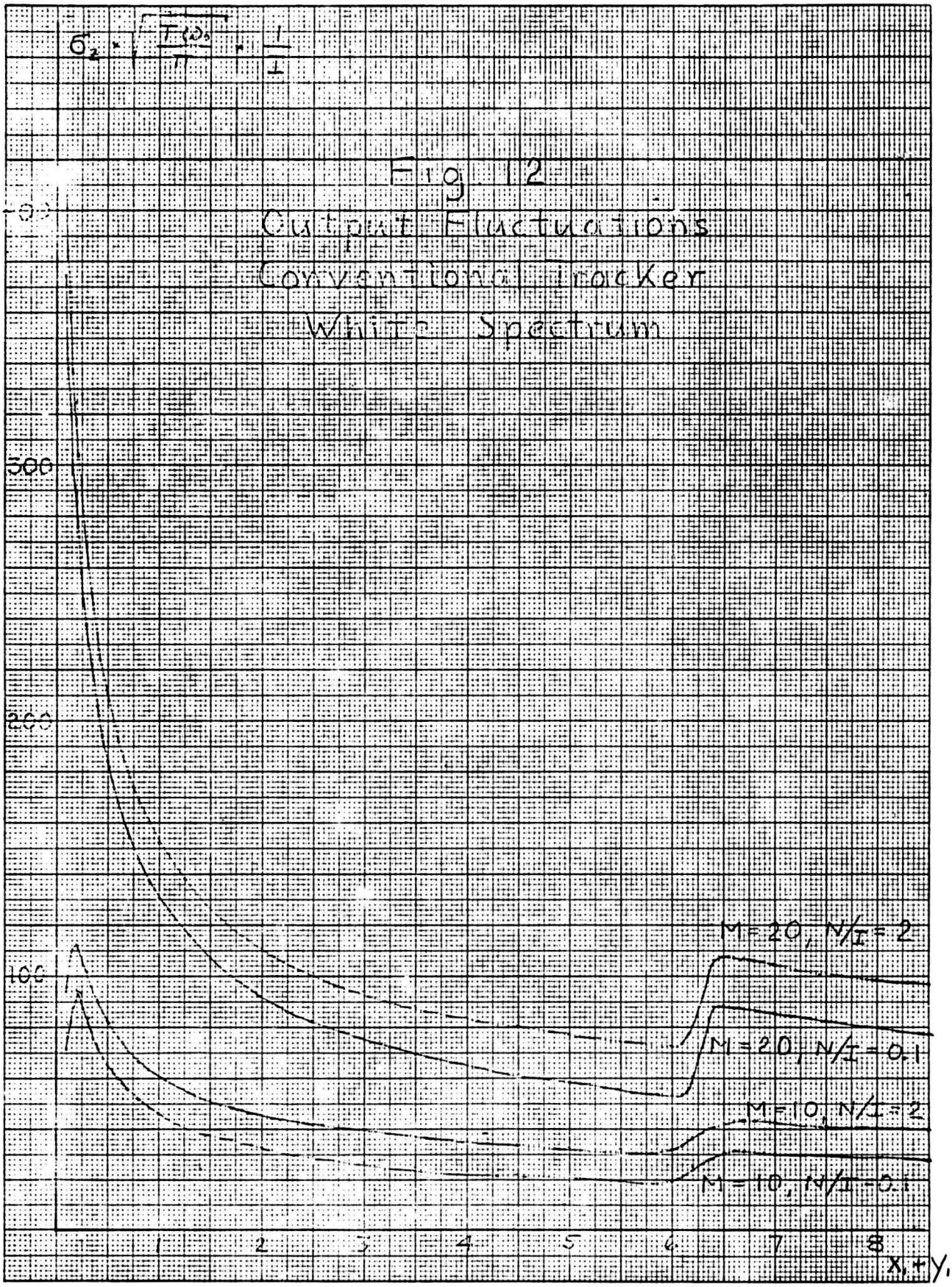

dominated environment. If the tracker is to function properly, σ_z must certainly be small compared with the peak value of $\bar{z}$ near the target bearing. According to Figures 3 and 5 horizontal excursions must therefore be confined to a range small compared with 0.1 and 0.2 for M = 20 and 10 respectively. Over such a range Figure 12 exhibits changes equal to no more than a small fraction of the value of σ_z at any point within the range. Thus the approximation leading to Eq. (9) is amply justified.[1]

For remote interference Eq. (59) reduces to

$$\sigma_z^2 = \frac{2}{3}\frac{\pi}{T\omega_o} I^2 \left\{ M(2M^2+1) + 3\frac{N}{I}M^2 + \frac{3}{2}\left(\frac{N}{I}\right)^2 M^2 \right\} \tag{60}$$

If $M \gg 1$ one can therefore write approximately

$$\sigma_z^2 \simeq \begin{cases} \frac{4}{3}\frac{\pi}{T\omega_o} M^3 I^2 & \text{for} \quad \frac{N}{I} \ll \sqrt{\frac{4}{3}M} \\ \\ \frac{\pi}{T\omega_o} M^2 N^2 & \text{for} \quad \frac{N}{I} \gg \sqrt{\frac{4}{3}M} \end{cases} \tag{61}$$

Much as in the case of detection one finds the fluctuation power varying with M^3 in an interference-dominated environment and with M^2 in an ambient-noise-dominated environment. The dividing line between the two, again as in the case of detection, depends on $\sqrt{M}$, so that even a relatively weak interference can dominate the output fluctuation if the array is sufficiently large.

2) Algebraic Spectra. Next consider again the algebraic spectra

$$g_I(\omega) = g_N(\omega) = \omega_a^2 \frac{|\omega|}{(\omega^2 + \omega_a^2)^2} \tag{62}$$

---

[1] The approximation is poorest for very small x_1+y_1. This is the condition of steering angle very close to interference bearing, where no satisfactory tracking performance would be expected in any case.

Substitution into Eq. (56) yields, after the usual algebraic simplifications,

$$\sigma_z^2 = \frac{\pi^2 I^2}{8\Gamma\omega_a}\left\{\sum_{r=1}^{2M-1}\sum_{q=1}^{2M-1}\left\{e^{-|(r+q-2M)(x_2+y_2)|}\left[1+|(r+q-2M)(x_2+y_2)|-\frac{1}{3}|(r+q-2M)(x_2+y_2)|^3\right]\right.\right.$$

$$\left.\left. - e^{-|(r+q)(x_2+y_2)|}\left[1+|(r+q)(x_2+y_2)| - \frac{1}{3}|(r+q)(x_2+y_2)|^3\right]\right\}(M-|r-M|)(M-|q-M|)\right.$$

$$\left. + 2M\frac{N}{I}\left\{M+2\sum_{r=1}^{M-1} e^{-r|x_2+y_2|}\left[1+|r(x_2+y_2)| - \frac{1}{3}|r(x_2+y_2)|^3\right](M-r)\right\} + M^2\frac{N^2}{I^2}\right\} \qquad (63)$$

For $|x_2+y_2| >> 1$ (steering angle remote from interference) and $\omega_a = \frac{\pi}{8}\omega_o$ Eq. (63) becomes identical with Eq. (60).

Plots of Eq. (63) for several values of M and $\frac{N}{I}$ are shown in Figure 13. Here, as in Figure 12, the approximation leading to Eq. (9) is clearly satisfied.

D. Random Bearing Error

According to Eq. (9) the random component of bearing error is

$$\frac{\sigma_z}{\left|\frac{\partial\bar{z}}{\partial\theta}\right|} \qquad (64)$$

evaluated at the target bearing. Only the slope of the average response curve (the sensitivity) remains to be calculated. For white spectra one obtains from Eq. (39)

$$\left.\frac{\partial\bar{z}}{\partial\theta}\right|_0 = \left.\frac{\partial\bar{z}}{\partial x_1}\frac{\partial x_1}{\partial\theta}\right|_0 =$$

$$S\omega_o\frac{d}{c}\cos\theta_o\left\{\frac{1}{2}M^3 + \frac{I}{S}\sum_{r=-(M-1)}^{M-1}\left[\frac{\sin(M+r)y_1}{(M+r)y_1} - \frac{1-\cos(M+r)y_1}{(M+r)^2y_1^2}\right](M-|r|)(M+r)\right\} \qquad (65)$$

$\sigma_2 = \sqrt{F\omega_n}\ \frac{2}{\pi}\sqrt{\frac{2}{I}}$

Fig. 13
Output Fluctuations
Conventional Tracker
Algebraic Spectrum

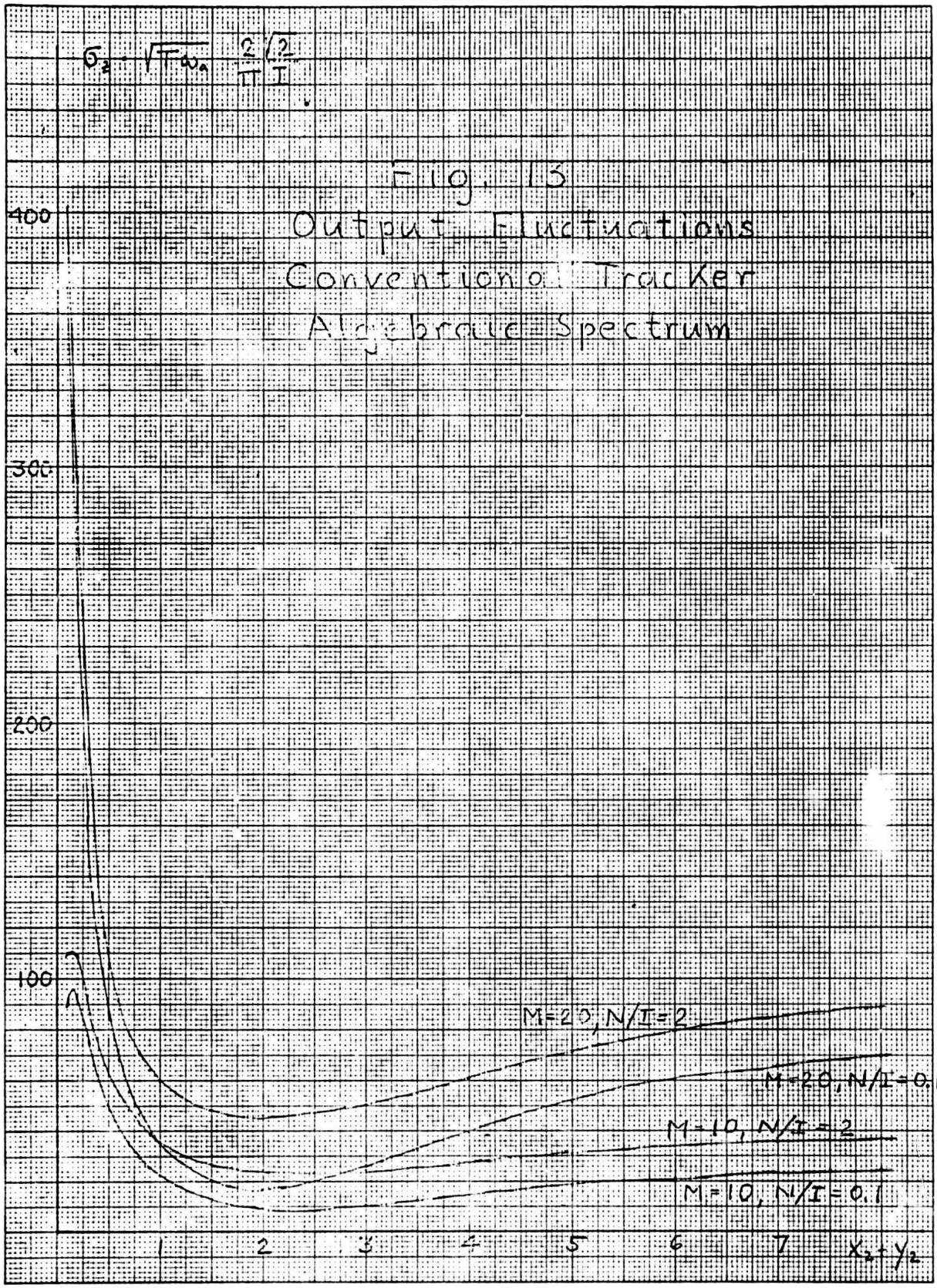

A similar computation for the case of algebraic spectra yields

$$\left.\frac{\partial \bar{z}}{\partial \theta}\right|_0 = \frac{\partial \bar{z}}{\partial x_2}\left.\frac{\partial x_2}{\partial \theta}\right|_0 =$$

$$\pi S \omega_a \frac{d}{c}\cos\theta_o \left\{ \frac{1}{2}M^3 + \frac{1}{2S}\sum_{r=-(M-1)}^{M-1}\left[1-(M+r)|y_2|\right]e^{-(M+r)|y_2|}(M-|r|)(M+r)\right\} \tag{66}$$

For remote interference and $\omega_a = \frac{\pi}{8}\omega_o$, Eqs. (65) and (66) are related by

$$\left.\frac{\partial \bar{z}}{\partial \theta}\right|_{\text{algeb.}} = \frac{\pi^2}{8}\left.\frac{\partial \bar{z}}{\partial \theta}\right|_{\text{white}} \tag{67}$$

Normalized plots of Eqs. (65) and (66) for various values of M and $\frac{1}{S}$ are shown in Figures 14 and 15 respectively. In each case, but particularly for the algebraic spectrum, the sensitivity quickly approaches its asymptotic value once the separation of interference and target exceeds the basic beamwidth of the array.

Normalized plots of random bearing error [Eq. (64)] are shown in Figures 16 and 17. Since the values of $\frac{N}{I}$ all correspond to an interference-dominated environment, the dependence on this parameter is quite weak.[1] Since S/I appears only in the expression for sensitivity it is clear from Figures 14 and 15 that this parameter has little influence on the random bearing error except for interferences within a beam width of the target - in which case discussion of the fluctuation error becomes an academic matter because the postulated tracker can no longer distinguish between target and interference. Conversion of the vertical scale of Figure 16 into degrees of rms error is accomplished through multiplication by

$$57.3\sqrt{\frac{\pi}{T\omega_o}}\,\frac{I}{S}\,\frac{1}{\omega_o \frac{d}{c}\cos\theta_o} \tag{68}$$

[1] Note $N/I = 2$, $M = 10$ is fairly close to the borderline of ambient noise domination, hence the deviation is greatest in this case.

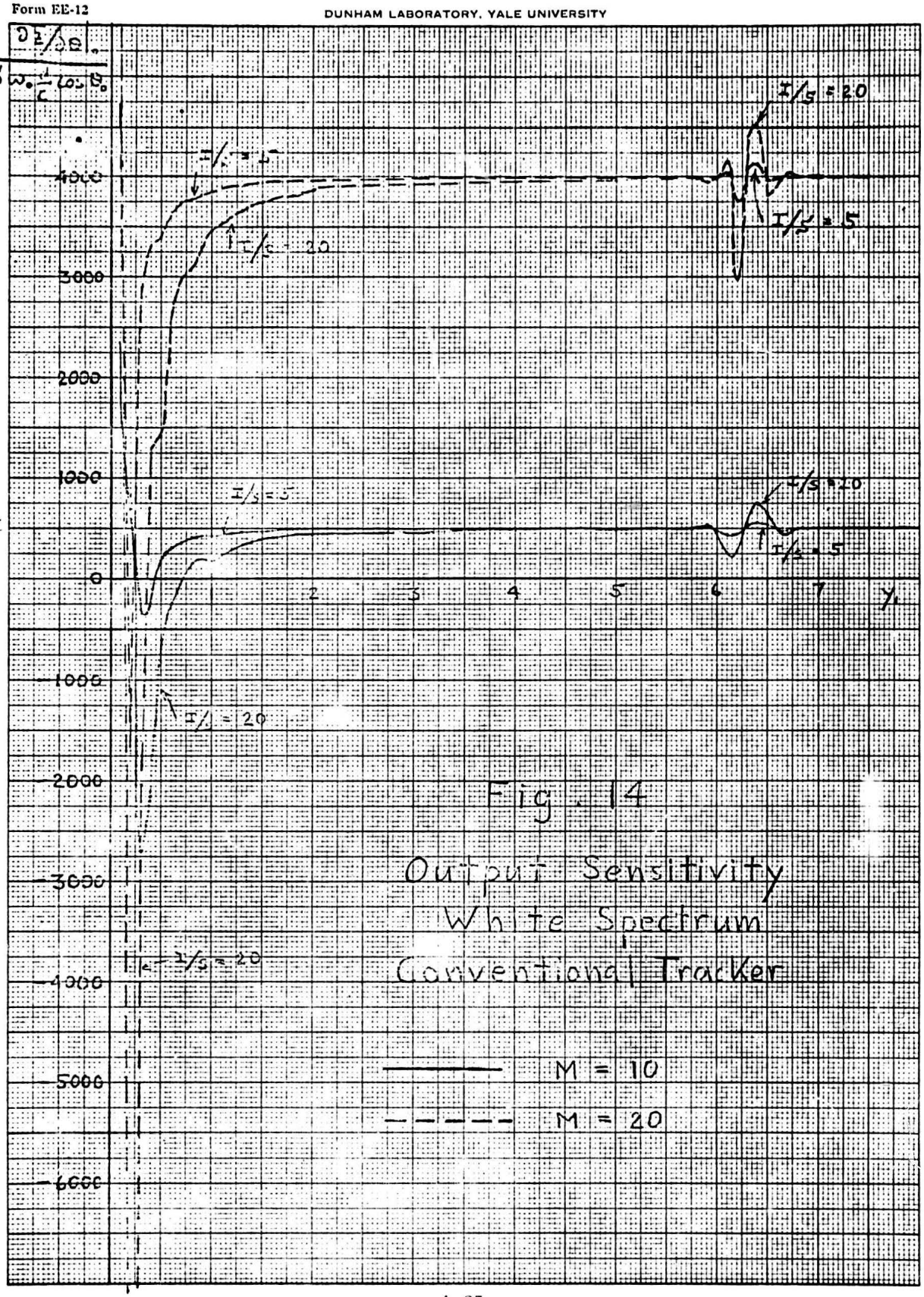

Fig. 14

Output Sensitivity
White Spectrum
Conventional Tracker

——— M = 10

– – – – – M = 20

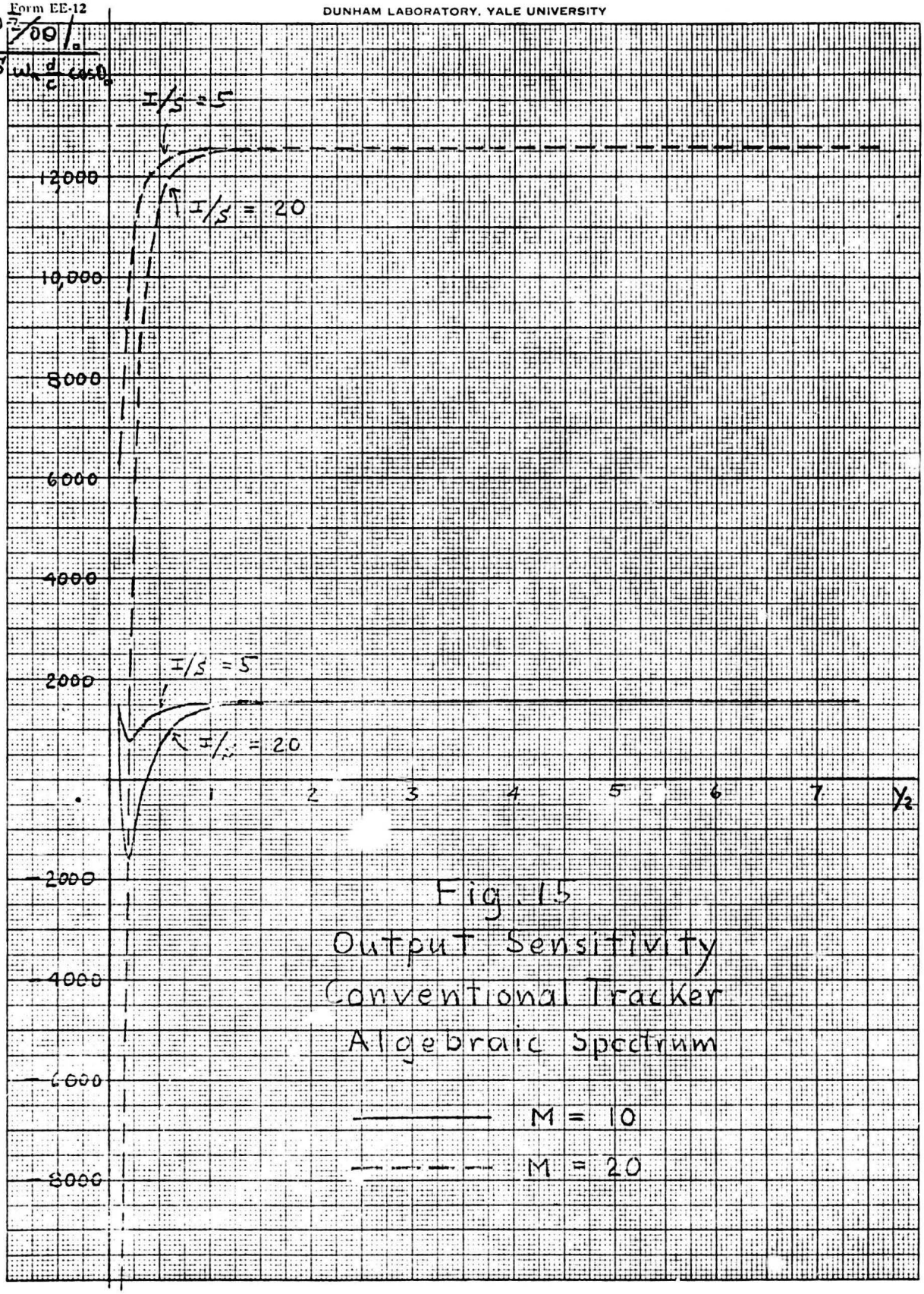

Fig. 15
Output Sensitivity
Conventional Tracker
Algebraic Spectrum

$$(\text{rad. rms error}) = \sqrt{\frac{T\omega_0}{\pi}}\,\frac{S}{H}\,\omega_0\,\frac{d}{c}\cos\theta_0$$

Fig. 16

Random Bearing Error

Conventional Tracker

White Spectrum

M = 10

M = 20

I/S = 5, N/I = 2

I/S = 10, N/I = 0.1

I/S = 5, N/I = 2

I/S = 10, N/I = 0.1

0.22 0.20 0.18 0.16 0.14 0.12 0.10 0.08 0.06 0.04 0.02

1 2 3 4 5 6 7 8 y_1

$$(\text{rad rms error}) = 2\sqrt{2}\sqrt{T\omega_n}\,\frac{S}{I}\,\omega_n\frac{d}{c}\cos\Theta$$

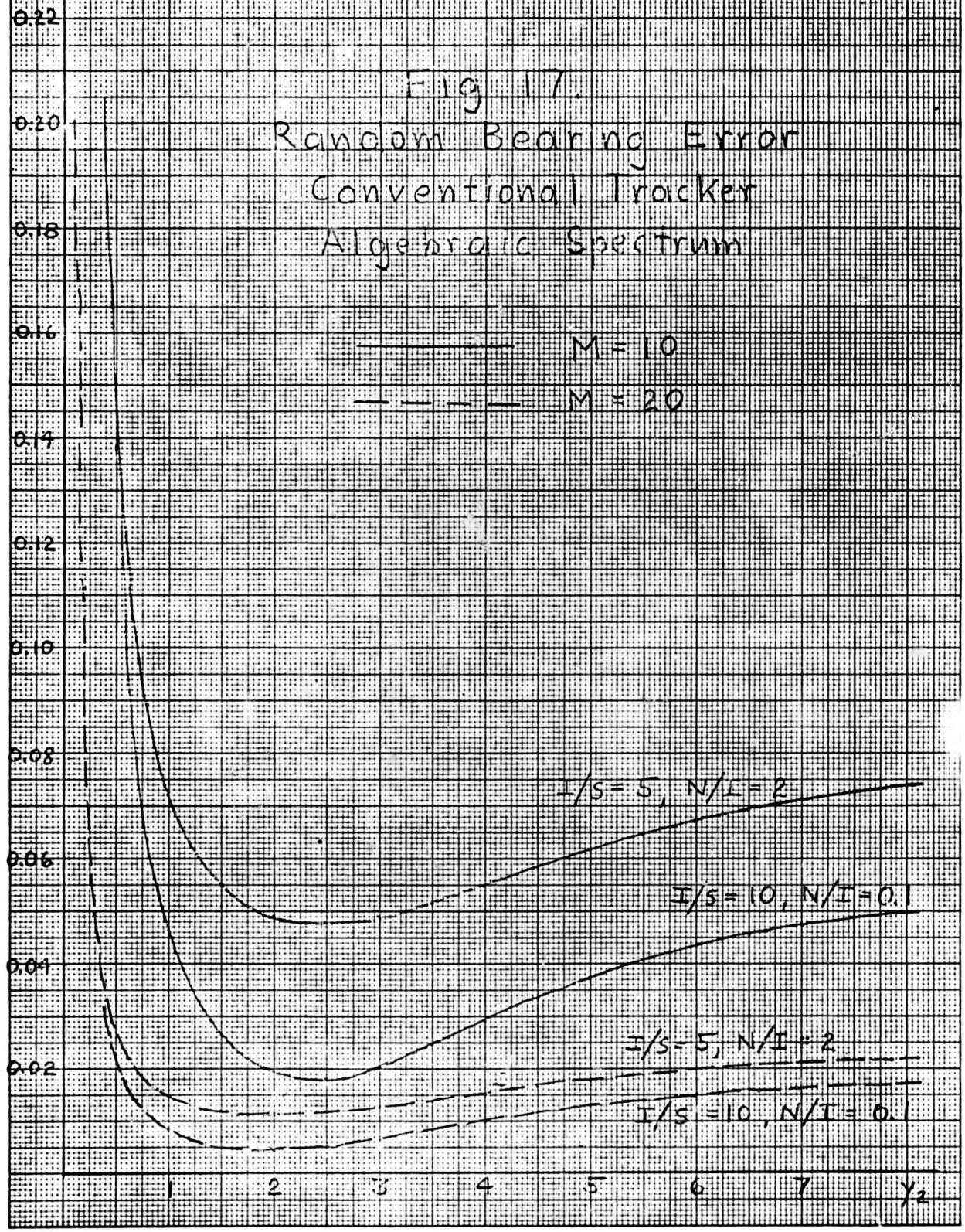

Of considerable practical importance is the question whether the random component of error currently under discussion is larger or smaller than the systematic error investigated in Section II.B. In order to avoid tedious comparison of a large number of cases, the following approximate analysis is carried out:

If the tracker is to function properly the shift in the null (systematic error) should be confined to a region sufficiently close to the true bearing so that the average bearing response pattern (Figure 1) may be regarded as linear over the region in question. In that case one can write

$$\text{Systematic error (in radians)} = -\frac{\bar{z}_o}{\left.\frac{\partial \bar{z}}{\partial \theta}\right|_0} \qquad (69)^1$$

where $\bar{z}_o$ is the on-target value of the average bearing response. Hence from Eqs. (64) and (69)

$$\frac{\text{systematic error}}{\text{rms random error}} = \frac{\bar{z}_o}{\sigma_{z_o}} \qquad (70)$$

$\bar{z}_o$ is obtained by setting $x_1 = 0$ in Eq. (39) and $x_2 = 0$ in Eq. (48). Similarly Equations (50) and (63) yield σ_{z_o}. Figures 18 and 19 show normalized plots of Eq. (70) on a logarithmic scale for white and algebraic spectra respectively. An interference-dominated environment is assumed, so that dependence of the noise level on N may be ignored. Except for the neighborhood of $y_1 = 2\pi$ the curves for white spectra (Figure 18) are essentially straight lines with a slope of $(-\frac{1}{2})$, once the interference is separated from the target by more than the width of the beam pattern.[2] This behavior has important practical implications. The abscissa y_1 is related to target and interference bearing through the equation

---

[1] This is clearly equivalent to the approximation of Equation (9).

[2] Each of the curves exhibits a sharp downward excursion near $y_1 = 2\pi$. To avoid confusion on the graph this has been shown only for $M = 5$.

NO. 3123. LOGARITHMIC: 2¾ BY 2 3¾-INCH CYCLES.
CODEX BOOK COMPANY, INC. NORWOOD, MASSACHUSETTS.
PRINTED IN U. S. A.

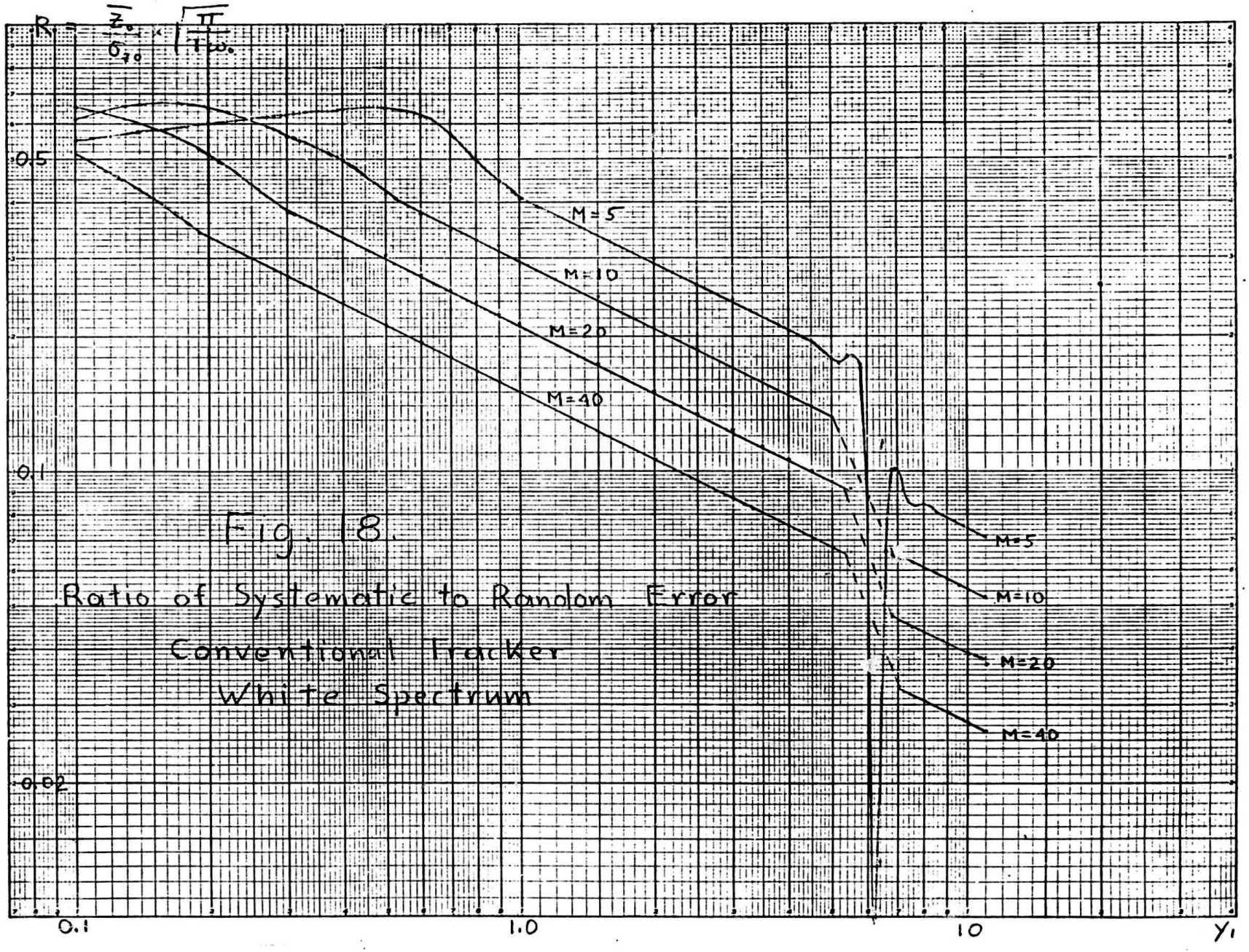

Fig. 18.

Ratio of Systematic to Random Error

Conventional Tracker

White Spectrum

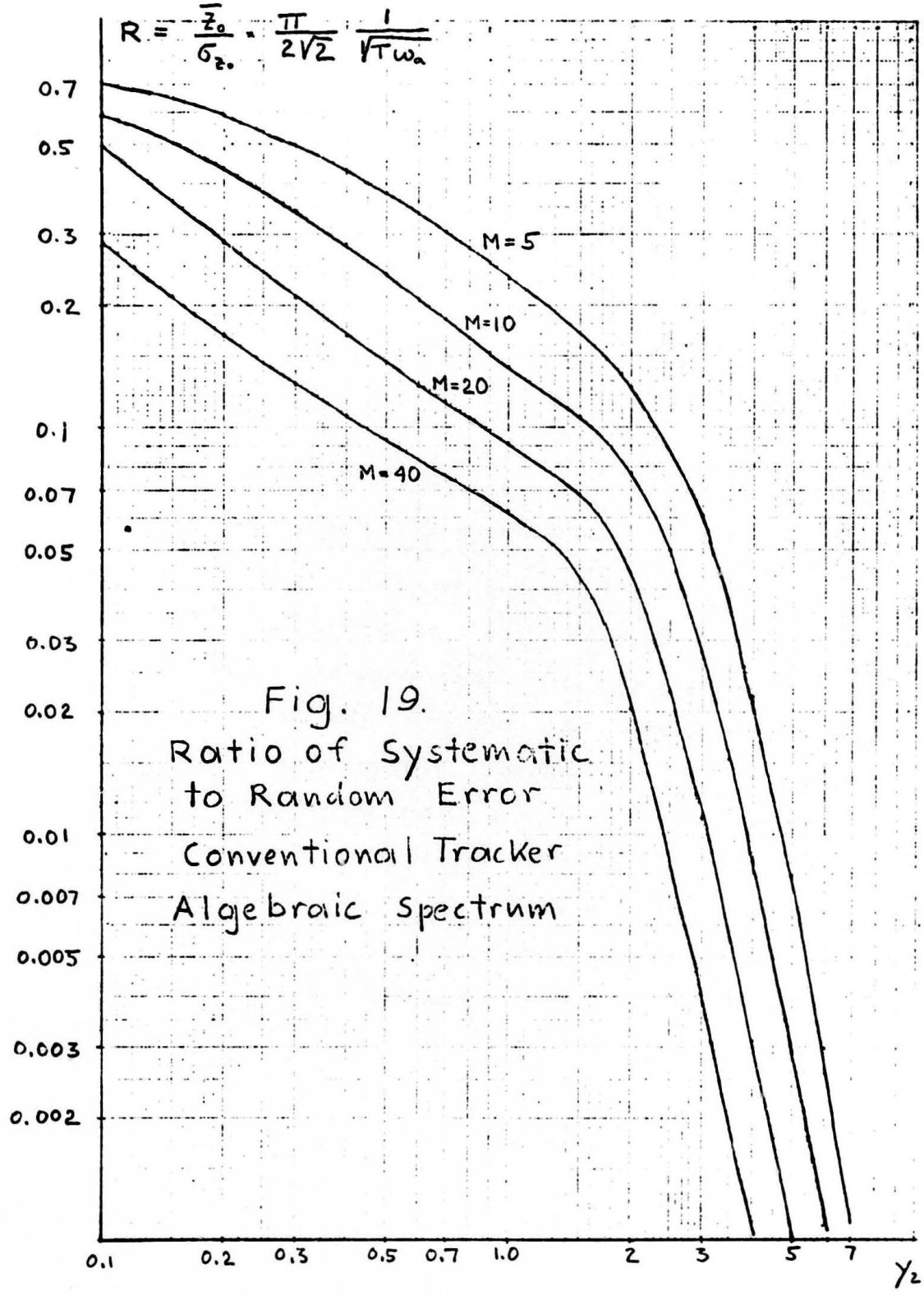

Fig. 19.
Ratio of Systematic to Random Error
Conventional Tracker
Algebraic Spectrum

$$y_1 = \omega_o(\Delta - t_o) = \omega_o \frac{d}{c}(\sin \theta_I - \sin \theta_T) \tag{71}$$

The error ratio [Eq. (70)] is related to the normalized R plotted in Figure 18 through

$$\frac{\text{systematic error}}{\text{rms random error}} = \sqrt{\frac{T\omega_o}{\pi}}\, R \tag{72}$$

If $\omega_o' = K\omega_o$, the corresponding y_1' is Ky_1. Because of the $(-\frac{1}{2})$ slope this results in $R' = K^{-1/2}R$. Hence

$$\frac{\sqrt{T\omega_o'}}{\sqrt{\pi}} R' = \frac{\sqrt{T\omega_o}}{\sqrt{\pi}} R \tag{73}$$

so that the error ratio remains unchanged. In other words, the error ratio is independent of the cutoff frequency ω_o as long as y_1 lies on the linear portion of the curves. Furthermore, note that the horizontal spacing between curves is essentially constant at a value corresponding to a factor of 2. An increase in the number of hydrophones decreases the error ratio if all other parameters remain fixed. This implies that the total array length increases linearly with M. In practice, it may be more realistic to consider the array length fixed and to vary the hydrophone spacing d inversely with M. Assuming that phone-to-phone independence of the ambient noise is maintained during these changes one finds that to double M implies cutting y_1 in half. Hence the error ratio is unaffected by the change. One concludes that for fixed overall array length the error ratio is independent of the number of hydrophones as long as y_1 lies on the linear portion of the curves.

The next question is clearly whether y_1 does or does not lie on the linear portion of the curves in situations of practical interest. One need not be greatly concerned with the nonlinearity for small y_1, for one

would hardly expect to operate the system with interferences separated from the target by less than a beam width. To obtain an upper bound on y_1 consider d = 1, $\omega_o = 2\pi \times 5000$ rad/sec. With a broadside target ($\theta_T = 0$) Eq. (71) yields a maximum y_1 of 2π . Thus all but a small range of interference bearings near endfire produces values of y_1 within the linear portion of Figure 18.

It is now possible to determine the value of the error ratio in the linear region, which is independent of all parameters except overall array length, smoothing time, and bearing angles.

$$\frac{\text{systematic error}}{\text{rms random error}} \simeq 53 \sqrt{\frac{T}{L}} \frac{1}{|\sin \theta_I - \sin \theta_o|^{\frac{1}{2}}} \tag{74}$$

where L is the array length in feet. For smoothing times of the order of seconds and moderate array length this ratio is clearly larger than unity.

The error ratio curves for algebraic spectra [Figure (19)] do not exhibit all of the invariance properties present in the white noise case. Confining attention to the region $y_2 \leq 2$ (corresponding to $y_1 = \frac{16}{\pi}$) one still finds a horizontal spacing roughly proportional to M and hence approximate invariance of the error ratio relative to M (for fixed array length). However, the slope of the curves below $y_2 = 2$ exceeds $\frac{1}{2}$. The reasoning of Equations (71) - (73) therefore leads to the conclusion that the error ratio is a monotone decreasing function of ω_a . The conversion from the normalized R plotted in Figure 19 to actual error ratio is accomplished through the relation:

$$\frac{\text{systematic error}}{\text{rms random error}} = \frac{2\sqrt{2}}{\pi} \sqrt{T\omega_a} \; R \tag{75}$$

With a 40 ft. array, 1 ft. hydrophone spacing, and ω_a = 10,000 rad/sec

this leads to

$$\frac{\text{systematic error}}{\text{rms random error}} \geq 4\sqrt{T}, \text{ for } y_2 \leq 2 \tag{76}$$

Thus the error ratio is still in excess of unity for most reasonable smoothing times. Only with larger arrays or wider bandwidth is the random error likely to become dominant.

III. Nulling Trackers

A. General Relations

Figure 20 shows one possible implementation of a split beam tracker with provisions for nulling a plane wave interference. The block diagram

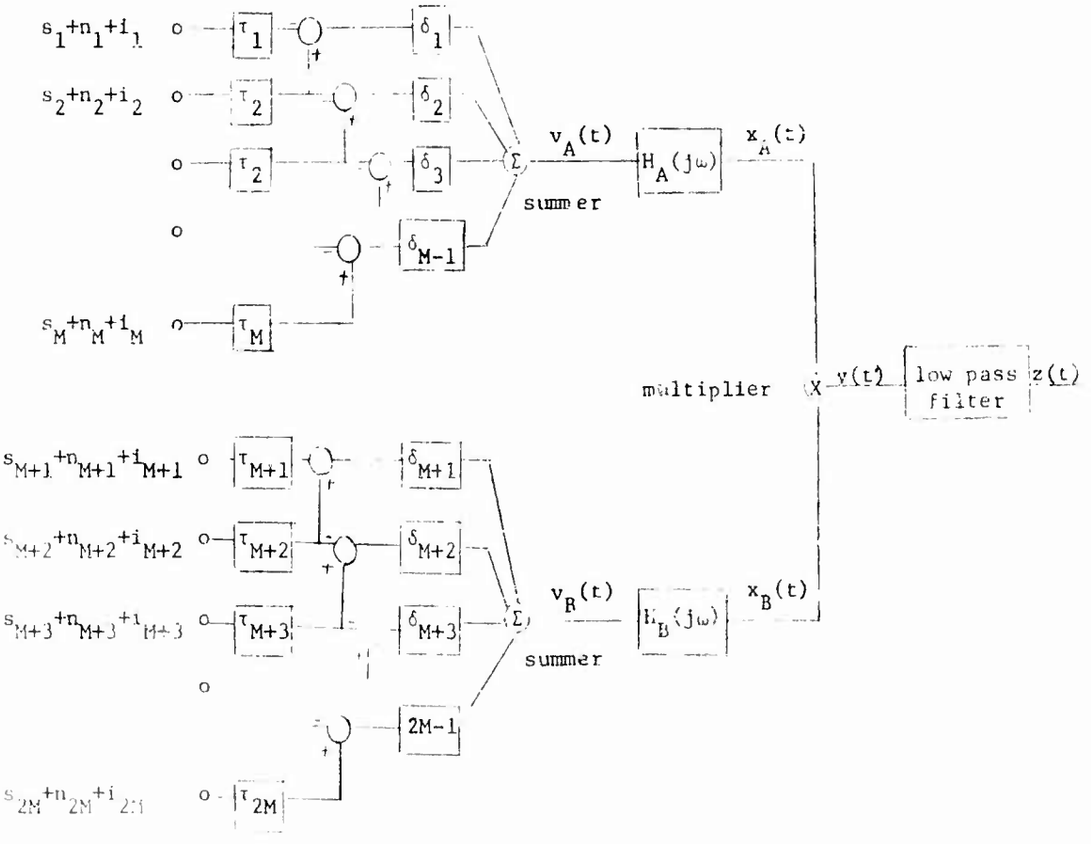

Figure 20

represents a split beam version of the simplest configuration analysed in Report No. 21 (see Figure 1 of that report). The delays τ_i are adjusted in accordance with the interference delay from hydrophone to hydrophone,

so that the subsequent subtractions achieve in principle complete elimination of the interference. The delays δ_i align the remaining signal components. From this point on the instrumentation is identical with that of the conventional tracker (Figure 2). Thus, as pointed out previously, Equations (39) and (27) [or, with the previous assumptions concerning H_A and H_B, Equations (30) and (31)] remain valid. The spectral functions $G_{v_A}(\omega)$, $G_{v_B}(\omega)$ and $G_{v_A v_B}(\omega)$ must now be computed.

From Report No. 21, Equation (27) :

$$v_A(t) = \sum_{k=1}^{M-1} \left\{ s_1\left[t+k(t_o-t_1)\right] - s_1\left[t+k(t_o-t_1)-(t_o-\Delta)\right] + n_{k+1}(t-kt_1) - n_k(t-kt_1+\Delta) \right\} \tag{77}$$

$$\text{and } v_B(t) = \sum_{k=1}^{M-1} \left\{ s_1\left[t + (k+m)(t_o-t_1)\right] - s_1\left[t + (k+m)(t_o-t_1)-(t_o+\Delta)\right] + n_{m+k+1}\left[t - (m+k)t_1\right] - n_{m+k}\left[t-(m+k)t_1 + \Delta\right] \right\} \tag{78}$$

It follows that

$$R_{v_A}(\tau) = R_{v_B}(\tau) = S \sum_{k=1}^{M-1} \sum_{\ell=1}^{M-1} \left\{ 2\rho_s\left[\tau+(k-\ell)(t_o-t_1)\right] - \rho_s\left[\tau+(k-\ell)(t_o-t_1)+(t_o-\Delta)\right] - \rho_s\left[\tau+(k-\ell)(t_o-t_1)-(t_o-\Delta)\right] \right\}$$
$$+ N\left\{ 2(M-1)\rho_N(\tau) - (M-2)\rho_N\left[\tau+(t_1-\Delta)\right] - (M-2)\rho_N\left[\tau-(t_1-\Delta)\right] \right\} \tag{79}$$

Fourier transforming:

$$G_{v_A}(\omega) = G_{v_B}(\omega) = S\, g_s(\omega) \sum_{k=1}^{M-1} \sum_{\ell=1}^{M-1} \left\{ 2\, e^{j\omega(k-\ell)(t_o-t_1)} - e^{j\omega\left[(k-\ell)(t_o-t_1)+(t_o-\Delta)\right]} - e^{j\omega\left[(k-\ell)(t_o-t_1)-(t_o-\Delta)\right]} \right\}$$
$$+ N\, g_N(\omega) \left\{ 2(M-1) - (M-2)\, e^{j\omega(t_1-\Delta)} - (M-2)\, e^{-j\omega(t_1-\Delta)} \right\} \tag{80}$$

Furthermore,

$$R_{v_A v_B}(\tau) = S \sum_{k=1}^{M-1} \sum_{\ell=1}^{M-1} \Big\{ 2\rho_s\Big[\tau+(M+k-\ell)\ (t_o-t_1)\Big] - \rho_s\Big[\tau+(M+k-\ell)\ (t_o-t_1) + (t_o-\Delta)\Big] - \rho_s\Big[\tau+(M+k-\ell)\ (t_o-t_1) - (t_o-\Delta)\Big]\Big\} \quad (81)$$

Hence

$$G_{v_A v_B}(\omega) = S\, g_s(\omega) \sum_{k=1}^{M-1} \sum_{\ell=1}^{M-1} \Big\{ 2\, e^{j\omega(M+k-\ell)\ (t_o-t_1)} - e^{j\omega\left[(M+k-\ell)\ (t_o-t_1) + (t_0-\Delta)\right]} - e^{j\omega\left[(M+k-\ell)\ (t_o-t_1) - (t_o-\Delta)\right]}\Big\} \quad (82)$$

As in the case of the conventional tracker, it is clear from Equations (19), (27), (80) and (82) that multiplication of $H_A(j\omega)$ and $H_B(j\omega)$ by $H(j\omega)$ is entirely equivalent to multiplication of $g_s(\omega)$ and $g_N(\omega)$ by $\left|H(j\omega)\right|^2$.

Substituting Equation (82) into Equation (30) one obtains the expression for the average tracker output

$$\bar{z} = 2S \sum_{k=1}^{M-1} \sum_{\ell=1}^{M-1} \int_o^\infty d\omega\, g_s(\omega) \Big\{ 2 \sin \omega(M+k-\ell)\ (t_o-t_1) - \sin \omega\Big[(M+k-\ell)\ (t_o-t_1) + (t_o-\Delta)\Big] - \sin \omega\Big[(M+k-\ell)\ (t_o-t_1) - (t_o-\Delta)\Big]\Big\} \quad (83)$$

with the change of index $k-\ell = r$ this becomes

$$\bar{z} = 2S \sum_{r=-(M-2)}^{M-2} \int_o^\infty d\omega\, g_s(\omega) \Big\{ 2 \sin \Big[\omega(r+M)\ (t_o-t_1)\Big] - \sin \omega\Big[(r+M)\ (t_o-t_1) + (t_o-\Delta)\Big] - \sin \omega\Big[(r+M)\ (t_o-t_1) - (t_o-\Delta)\Big]\Big\} (M-1-|r|) \quad (84)$$

The corresponding expression for the output variance is obtained formally by substituting Equations (80) and (82) into Equation (31). However, in the cases of primary interest here the signal power will be small compared with the ambient noise so that one can ignore the signal contribution to

the output fluctuation.[1] Then the variance of z becomes

$$\sigma_z^2 = \frac{2\pi N^2}{T} \int_{-\infty}^{\infty} d\omega \; g_N^2(\omega) \left\{ 2(M-1) - (M-2)\, e^{j\omega(t_1-\Delta)} - (M-2)\, e^{-j\omega(t_1-\Delta)} \right\}^2 \qquad (85)$$

Equations (84) and (85) must now be evaluated for the various spectral functions under study.

B. Average Tracker Output

Consider first the white spectrum specified by Equation (35). Integration of Equation (84) yields after some algebraic simplification

$$\bar{z} = S \sum_{r=-(M-2)}^{M-2} \left\{ 2\,\frac{1-\cos(M+r)\,x_1}{(M+r)\,x_1} - \frac{1-\cos\left[(M+r)\,x_1-y_1\right]}{(M+r)\,x_1-y_1} - \frac{1-\cos\left[(M+r)\,x_1+y_1\right]}{(M+r)\,x_1+y_1} \right\} \{M-1-|r|\} \qquad (86)$$

x_1 and y_1 are defined in Equation (38a).

The equivalent expression for the algebraic spectrum [Equation (43)] is

$$\bar{z} = \frac{\pi}{2} S \sum_{r=-(M-2)}^{M-2} \left\{ 2(M+r)\,x_2\, e^{-|(M+r)\,x_2|} - \left|(M+r)\,x_2-y_2\right| e^{-|(M+r)\,x_2-y_2|} - \left|(M+r)\,x_2+y_2\right| e^{-|(M+r)\,x_2+y_2|} \right\} (M-1-|r|) \qquad (87)$$

x_2 and y_2 are defined in Equation (47).

Plots of Equations (86) and (87) for selected parameter values are given in Figures (21) and (22) respectively. Only the neighborhood of the target is shown, because the average output elsewhere is too small to be significant on the scales of the two graphs. The most important

---

[1] With $S \geq N$ there is presumably very little difficulty in tracking once the interference has been eliminated.

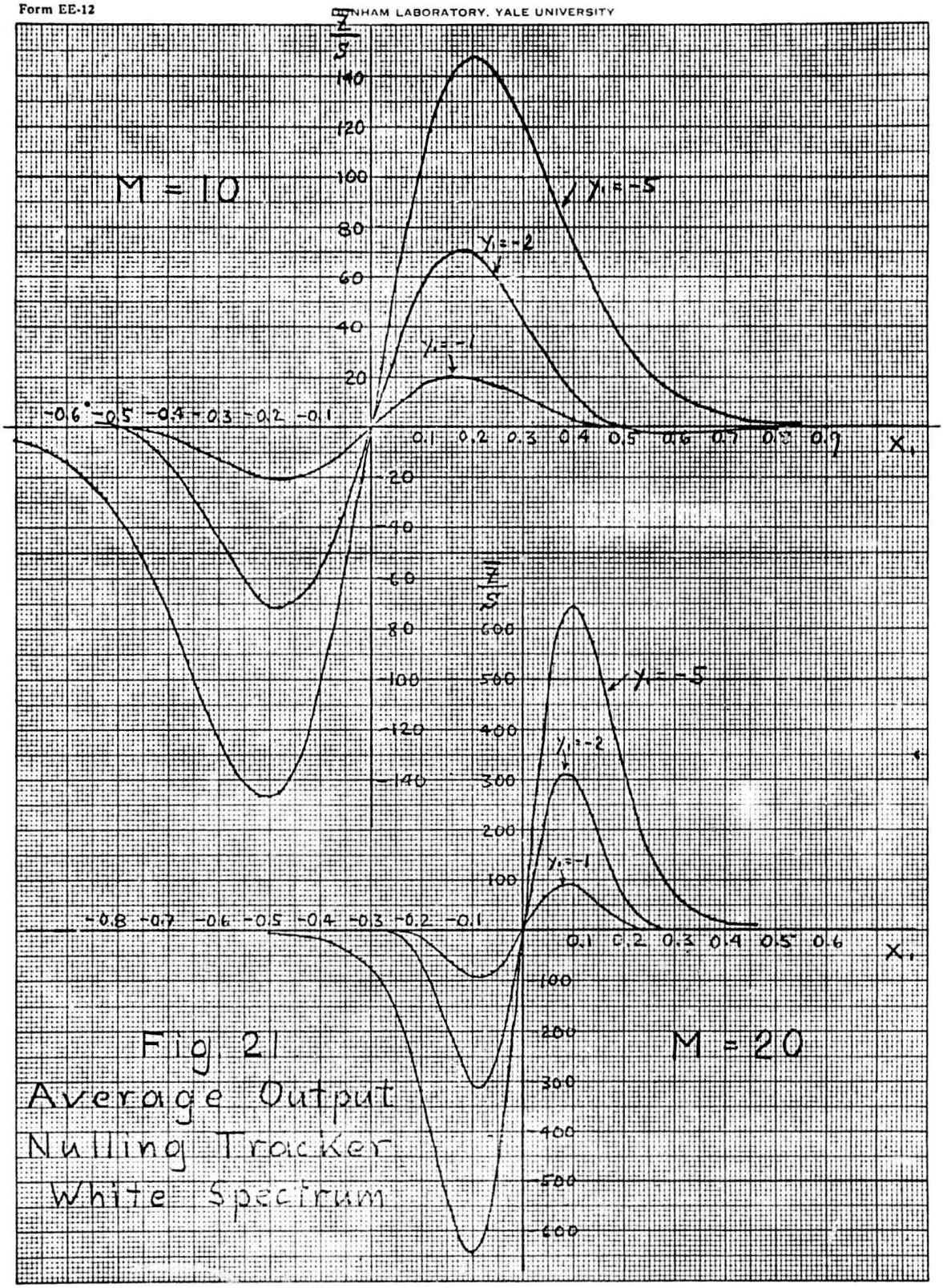

Fig 21
Average Output
Nulling Tracker
White Spectrum

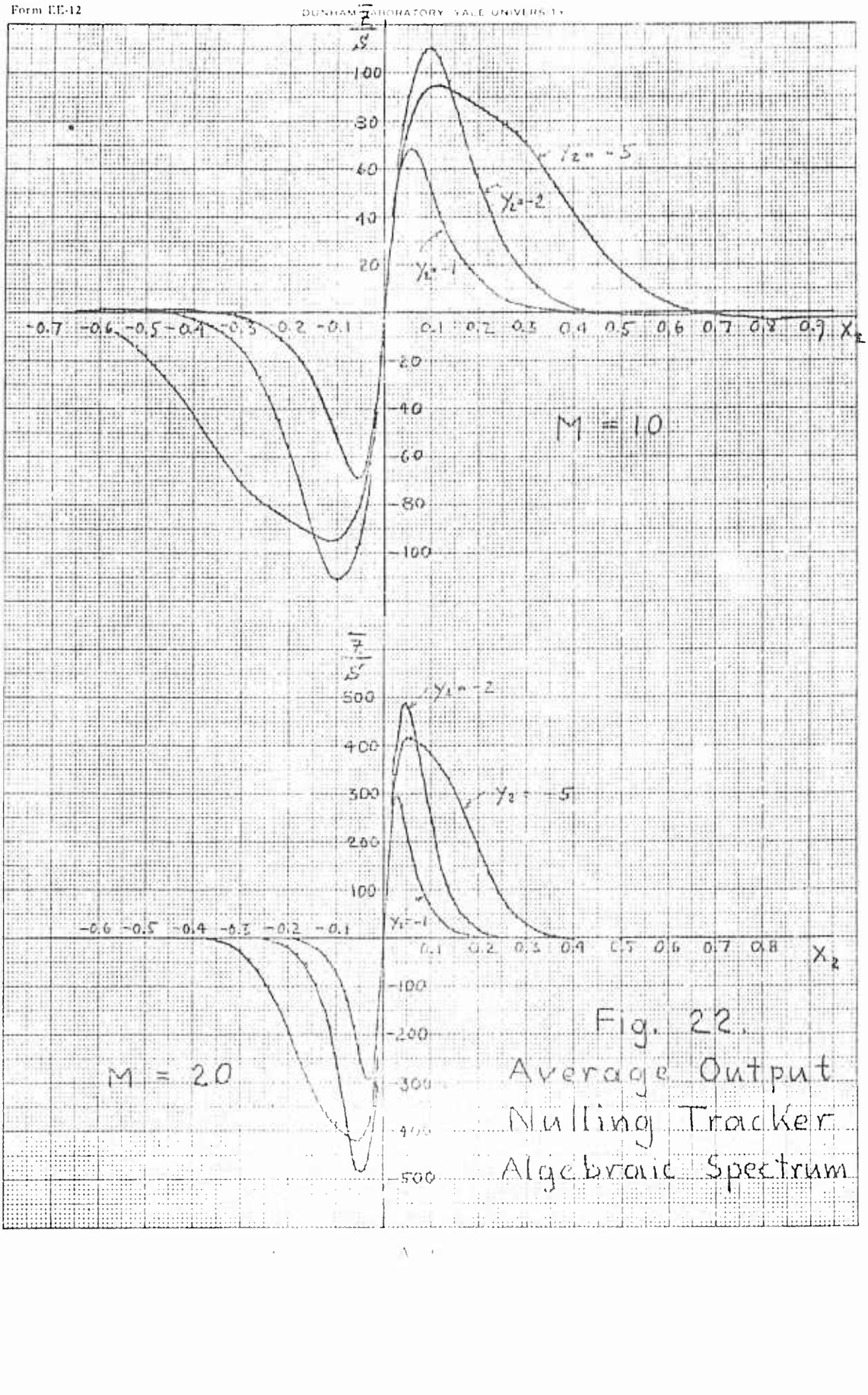

Fig. 22.
Average Output
Nulling Tracker
Algebraic Spectrum

aspect of the curves is the complete absence of any offset in the null (systematic error), a conclusion also apparent from the equations upon setting $x_1 = 0$ in (86) and $x_2 = 0$ in (87). In comparing Figures (21) and (22) one must, of course, keep in mind that $y_2 = (\frac{\pi}{8})y_1$ for equal detection index, so that $y_2 = -2$ corresponds very nearly to $y_1 = -5$.

C. Output Fluctuations

Substitution of the white noise spectrum [Equation (57)] into Equation (85) yields after algebraic simplification

$$\sigma_z^2 = \frac{4\pi N^2}{T\omega_o}\left\{(M-1)^2 + \tfrac{1}{2}(M-2)^2 - 2(M-1)\ (M-2)\ \frac{\sin(x_1+y_1)}{(x_1+y_1)} + \tfrac{1}{2}(M-2)^2\ \frac{\sin 2(x_1+y_1)}{2(x_1+y_1)}\right\} \tag{88}$$

The equivalent expression for the algebraic spectrum is

$$\sigma_z^2 = \frac{\pi^2 N^2}{2T\omega_a}\left\{(M-1)^2 + \tfrac{1}{2}(M-2)^2 - 2(M-1)\ (M-2)\ e^{-|x_2+y_2|}\left[1+|x_2+y_2| - \tfrac{1}{3}|x_2+y_2|^3\right] + \tfrac{1}{2}(M-2)^2\ e^{-2|x_2+y_2|}\left[1+2|x_2+y_2| - \tfrac{8}{3}|x_2+y_2|^3\right]\right\} \tag{89}$$

Figures (23) and (24) show the standard deviation σ_z plotted in normalized form as a function of (x_1+y_1) and (x_2+y_2) respectively. (x_1+y_1) and (x_2+y_2) are, of course, measures of steering angle relative to the interference bearing.

D. Random Bearing Error

The sensitivity of the tracker is obtained by differentiating Equations (86) and (87) with respect to θ and evaluating the derivatives at the target bearing. The result is:

Fig 23
Output Fluctuations
Nulling Tracker
White Spectrum

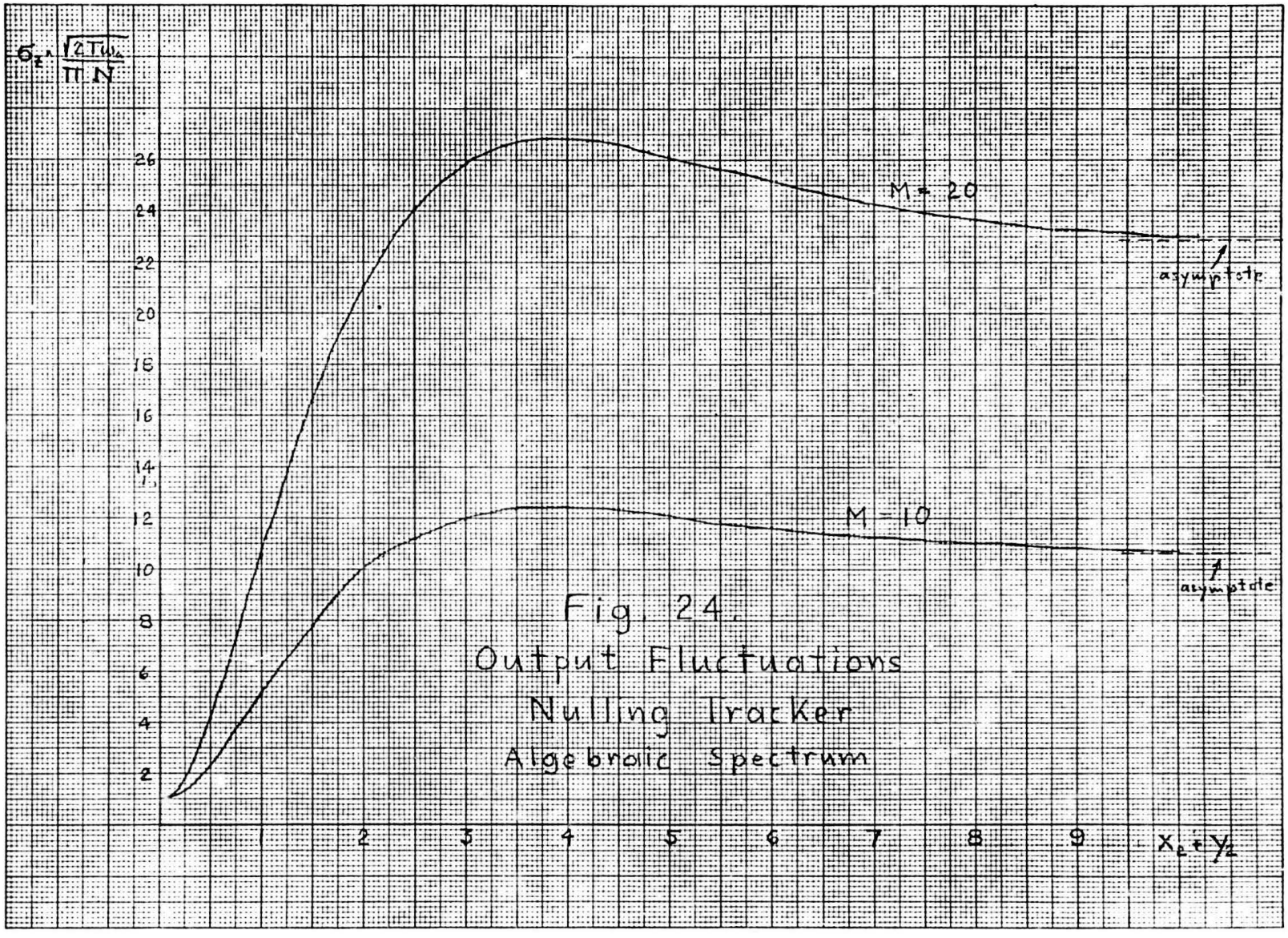

Fig. 24.
Output Fluctuations
Nulling Tracker
Algebraic Spectrum

For the white spectrum

$$\left.\frac{\partial \bar{z}}{\partial \theta}\right|_o = \omega_o S \frac{d}{c} \cos \theta_o \left[1-2 \frac{\sin y_1}{y_1} + 2 \frac{1-\cos y_1}{y_1^2}\right] M(M-1)^2 \tag{90}$$

For the algebraic spectrum

$$\left.\frac{\partial \bar{z}}{\partial \theta}\right|_o = \pi\omega_a S \frac{d}{c} \cos \theta_o \left[1-(1-|y_2|)\, e^{-|y_2|}\right] M(M-1)^2 \tag{91}$$

For remote interference and $\omega_a = (\pi/8)\,\omega_o$ **(the basis of comparison used before) Equations (90) and (91) are related by**

$$\left.\frac{\partial \bar{z}}{\partial \theta}\right|_{\text{algeb.}} = \frac{\pi^2}{8} \left.\frac{\partial \bar{z}}{\partial \theta}\right|_{\text{white}} \tag{92}$$

exactly as in the case of the conventional tracker. For bearings remote from the interference and $\omega_a = (\pi/8)\omega_o$, σ_z **approaches the same value for both types of spectra [see Equations (88) and (89)]. Hence the asymptotic ratio of fluctuation errors is**

$$\frac{\text{rms error with algebraic spectrum}}{\text{rms error with white spectrum}} = \frac{8}{\pi^2} \quad \text{for remote interference} \tag{93}$$

Plots of normalized rms error versus interference bearing relative to target bearing (measured by y_1 **and** y_2**) are given in Figures 25 and 26. The qualitative differences between the two sets of curves is due in large measure to the very rapid approach to the asymptotic value of the sensitivity for algebraic spectra. In other words, once the interference is separated from the target by more than a small minimum angle, the sensitivity at the target bearing is almost independent of the interference bearing (for algebraic spectra). This is, of course, precisely the lack of influence of the interference on average response which**

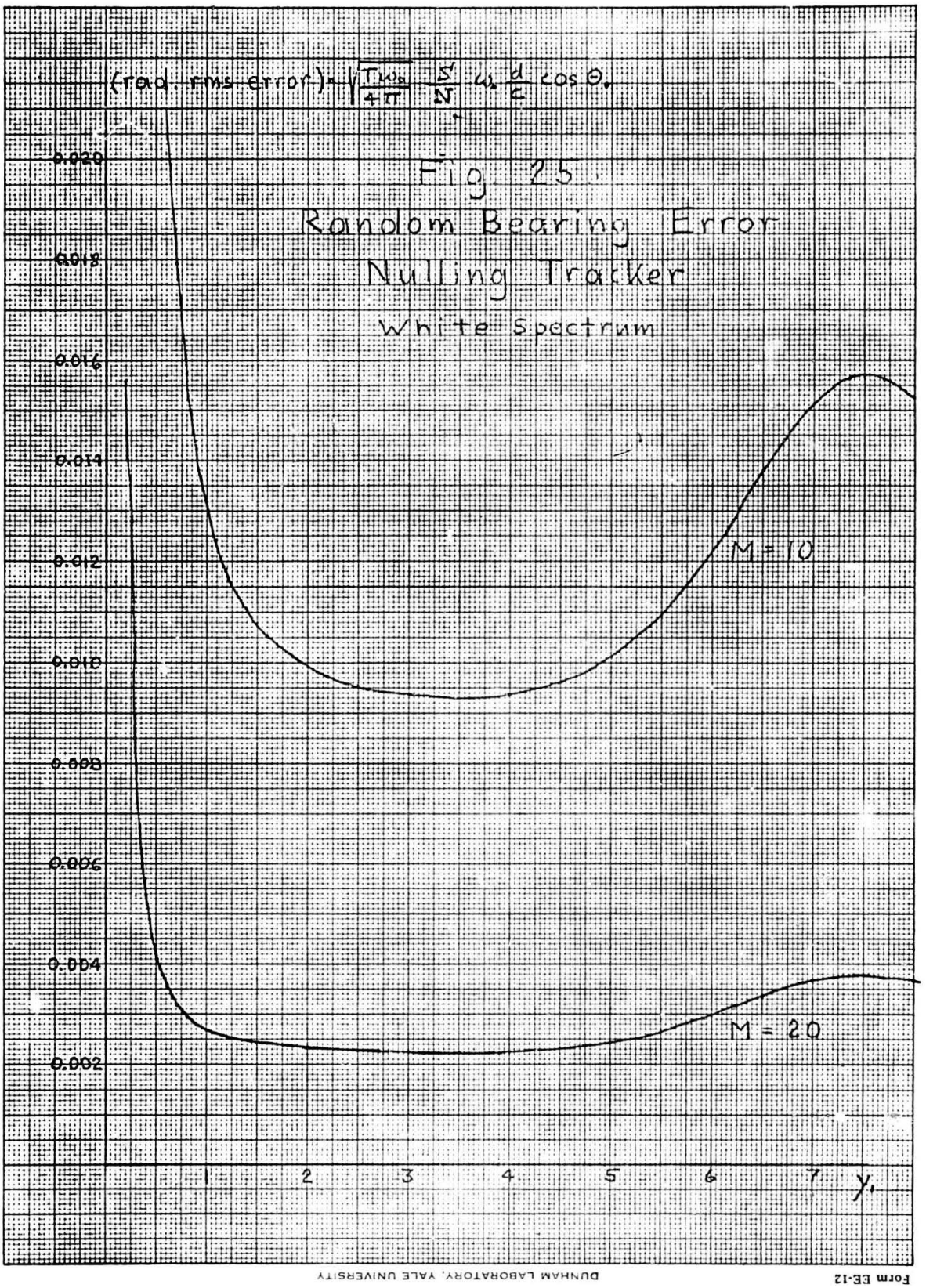

DUNHAM LABORATORY, YALE UNIVERSITY

Form EE-12

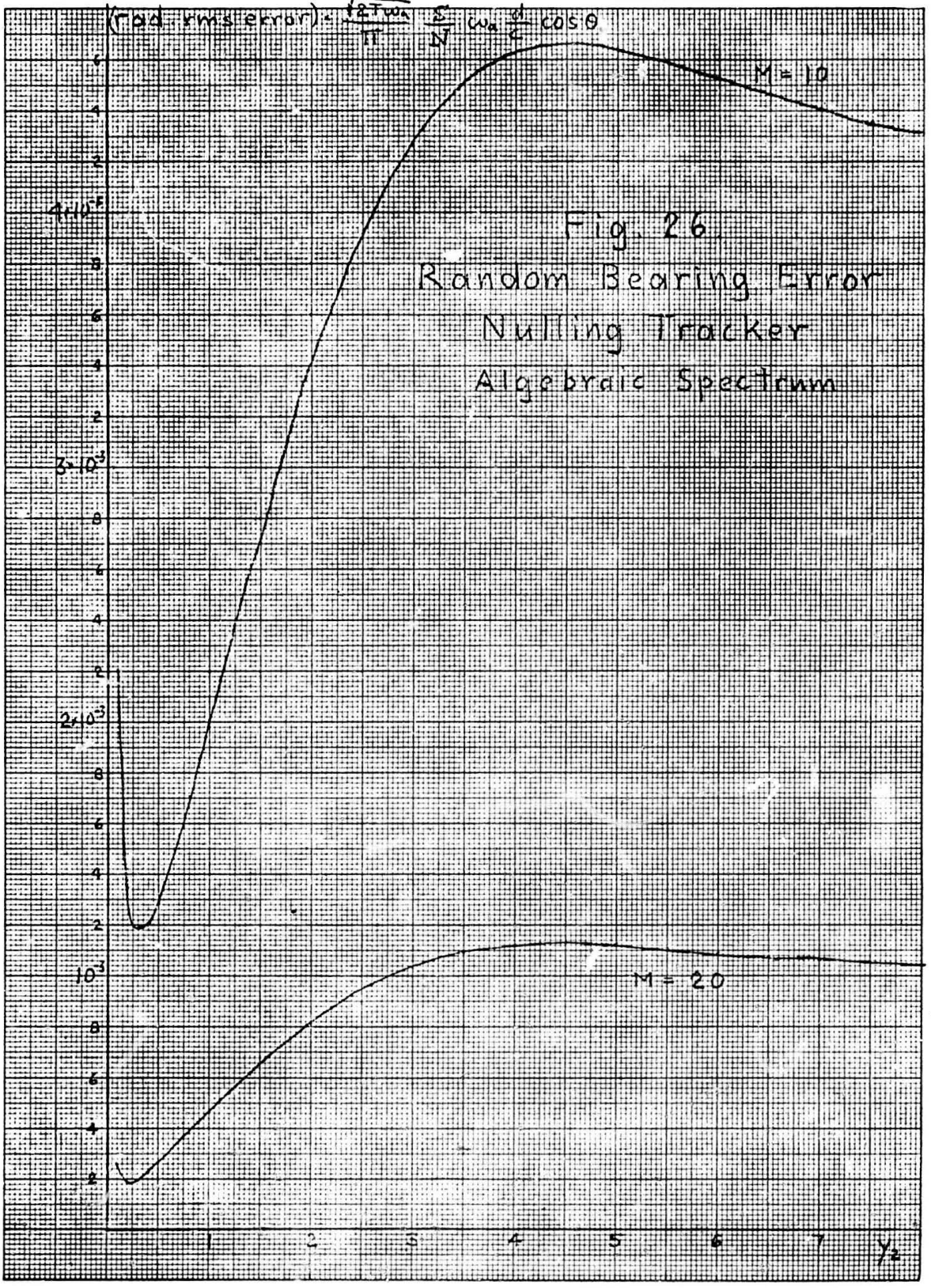

Fig. 26.
Random Bearing Error
Nulling Tracker
Algebraic Spectrum

motivated the investigation of algebraic spectra in the first place.

As a final point of interest, it may be useful to compare the rms error of the conventional tracker with that of the nulling tracker. From Equations (59), (65), (88) and (90) (white spectra) or (63), (66), (89) and (91) (algebraic spectra) one obtains for remote interference

$$\frac{\text{rms error of nulling tracker}}{\text{rms error of conventional tracker}} =$$

$$\frac{\sqrt{3}}{2}\frac{N}{I}\;\frac{M^2}{(M-1)^2}\sqrt{\frac{(M-1)^2+\frac{1}{2}(M-2)^2}{\frac{1}{2}M(2M^2+1)+\frac{3}{2}\frac{N}{I}M^2+\frac{3}{4}\left(\frac{N}{I}\right)^2M^2}} \tag{94}$$

With $M \gg 1$ this reduces to

$$\frac{\text{rms error of nulling tracker}}{\text{rms error of conventional tracker}} = \sqrt{\frac{9}{8}}\frac{N}{I}\;\frac{1}{\sqrt{M+\frac{3}{2}\frac{N}{I}+\frac{3}{4}\left(\frac{N}{I}\right)^2}} \tag{95}$$

In the limiting cases of ambient noise dominated and interference dominated environments one obtains finally

$$\frac{\text{rms error of nulling tracker}}{\text{rms error of conventional tracker}} = \begin{cases} \sqrt{\frac{3}{2}} & \text{for } \frac{N}{I} \gg \sqrt{\frac{4}{3}M} \\ \sqrt{\frac{9}{8}}\,M^{-\frac{1}{2}}\frac{N}{I} & \text{for } \frac{N}{I} \ll \sqrt{\frac{4}{3}M} \end{cases} \tag{96}$$

It is interesting that the superiority (if any) of the nulling tracker over the conventional tracker is measured by $M^{-\frac{1}{2}}\frac{N}{I}$, the parameter which also measures directly the extent to which the environment is interference dominated. Only in a strongly interference dominated environment is there a significant reduction in rms error due to nulling. The slight inferiority of the nulling tracker in an ambient noise dominated environment is, of course, due to the suboptimal nature of the primitive interference nulling scheme employed in the postulated instrumentation.

IV. Concluding Remarks

The report has analyzed the performance of split beam (phase) trackers with and without provisions for null steering in an environment composed of plane wave interference as well as isotropic ambient noise. Two types of error can arise,

1) Systematic error. This is a displacement in the null of the average tracker output from the true target bearing. It is caused by the asymmetry in the noise field due to the interference.
2) Random error. This is the rms fluctuation of the instantaneous tracker output about its average value. Its cause is the inability of a filter with finite smoothing time to eliminate fluctuations completely.

In the conventional tracker the interference contributes to both types of error. In the nulling tracker it contributes to neither, because the null steering feature totally eliminates (at least in principle) the interference at the very beginning of the data processing procedure. This dual effect of nulling tends to obscure questions of crucial importance to the ultimate decision whether the benefits of null steering are sufficient to justify the added system complexity. To clarify this point, consider the following conclusions from the conventional tracker analysis:

1) The interference contributes significantly to the random error only if the environment is interference dominated $\left[N/I << \sqrt{\frac{4}{3}}\,B\right]$.
2) If the environment is interference dominated, the systematic error exceeds the random error under most reasonable operating conditions, often by a very substantial amount.

According to 1) the use of nulling to reduce random error can be justified only if operation in a strongly interference dominated environment

is a common occurrence. If this is not the case one is interested primarily in eliminating the systematic error. Since the latter depends only on interference bearing and such average properties as interference power (but not on the detailed interference time function) one can envision much simpler schemes than nulling to achieve the necessary correction.

Even when the environment is interference dominated one may be concerned primarily with the simpler problem of systematic error correction. According to 2) the largest error component is likely to be systematic and failure to track may well be due largely to this component. Elimination of the systematic error alone may then result in satisfactory operation, even though random error reduction through nulling or related schemes might achieve further improvements in accuracy. In view of the inherent complexity of all schemes designed to eliminate time functions of interference or other spatially coherent components of the noise field, it appears desirable to study further whether simple modifications of the conventional tracker, utilizing only statistical information about the interference, may not achieve satisfactory performance.

The basic difference between systematic and random error compensation appears in a somewhat different guise in the detection problem. The average bearing response of a conventional detector operating in the presence of interference might assume the form sketched in Figure 27. The proximity

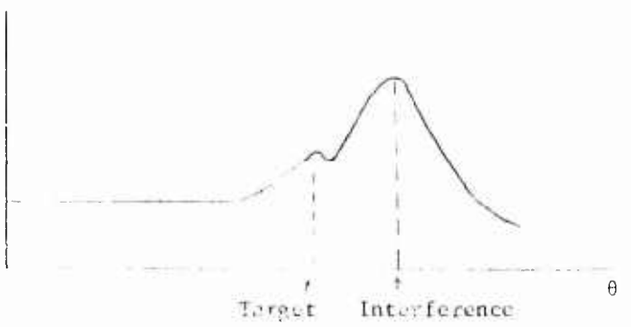

Figure 27

of the interference imposes a sloping background on the target peak. Depending on the method chosen to display the information this may or may not affect the ability of an operator to detect the target. Ignoring such display problems, however, a fundamental difficulty arises only when the rms fluctuation becomes comparable with the target peak, i.e., when the "on target" signal-to-noise ratio at the detector output falls to the neighborhood of unity. If the interference-free output signal-to-noise ratio is well in excess of unity, then the introduction of an interference separated from the target by more than a beamwidth can achieve reduction of the output signal-to-noise ratio to a level of unity only if the interference is strong enough to dominate the environment. In such cases nulling can clearly be beneficial. Otherwise the problem is primarily one of display, and while this counterpart of the systematic error problem is clearly resolved as a by-product of any nulling procedure, one should recognize that simpler techniques may be available to compensate for the average effect of the interference.

THE EFFECT OF MULTIPLE OR DISTRIBUTED INTERFERENCES ON THE PERFORMANCE OF A CONVENTIONAL PASSIVE SONAR DETECTOR

by

Verne H. McDonald

Progress Report No. 30

General Dynamics/Electric Boat Research

(8050-31-55001)

January 1967

DEPARTMENT OF ENGINEERING

AND APPLIED SCIENCE

YALE UNIVERSITY

Summary

A straightforward extension of the methods of Report No. 17 is employed to obtain general expressions for the index of performance of a conventional detector when multiple independent point source interferences are present. As in Report No. 17, autocorrelation functions of the form $e^{-\omega_0|\tau|}$ are assumed for the noise and interference processes, and the index of performance is derived for cases where all interferences differ at least several degrees in bearing from the target.

An interference distributed over an arc of several degrees is represented as a limiting case of a large number of closely spaced point interferences. Computer calculations relevant to determination of the index of performance in cases of multiple or distributed interferences are presented.

If the total interference power substantially exceeds the ambient noise power, the magnitude of the total interference power determines the order of magnitude of the index of performance. If a fixed value of total interference power I is considered, the case of a single point interference of power I may be compared with the cases of distributed or multiple interferences of total power I. Assuming the average bearings of interferences to be comparable, one finds that the index of performance is somewhat higher for multiple or distributed interferences than for a single point source of interference. The factor by which the index of performance with multiple or distributed interferences may exceed that for one point interference is found to have a hypothetical maximum of approximately $\sqrt{2M/3}$, where M is the number of hydrophones. The computed results indicate, however, that the improvement factor in most realistic situations is no greater than 2 or 3 for multiple point source interferences and between 1 and 2 for a distributed interference.

Finally the report points out the omission of a term in the basic expression in Report No. 17 for the variance of the output of a standard detector

in the presence of ambient noise and a point source interference. The term in question involves the product IN of interference power and ambient noise power. Calculations are performed which indicate that the error introduced in the output signal-to-noise ratio (index of performance) by neglecting this term is at most a few percent for the values of N/I and number of hydrophones M considered in Report No. 17. The effect of the term is found to decrease as either M or I/N increases.

I. Introduction

The present report is essentially an amendment and extension to the portion of Report No. 17 which treats the conventional detector. The expression in that report for the variance of the detector output is modified, and the case of a single interference is extended to consider any number of interferences.

This report considers only a linear array of M equally spaced omnidirectional hydrophones. Processing consists of summing the outputs of the hydrophones, squaring the sum, and low-pass filtering the square. The target signal, the ambient noise, and the one or many interferences are taken to be mutually independent random processes.

The ambient noise components from different hydrophones are assumed to be independent. We shall also assume signal and interference wavefronts to be plane. Consequently, at any given time the signal and interference components of the M hydrophone outputs represent samples of these random processes at M different points in time. If the array is steered on target, the M signal components are identical at any time. The signal, ambient noise, and interference components of voltage at each hydrophone are all assumed to be zero-mean Gaussian variables. The average power of any of these distinct processes is assumed not to vary from hydrophone to hydrophone.

The nomenclature of the present report is adopted from Report No. 17, and where specific assumptions are made regarding magnitude or functional form of variables, the assumptions are those of that report. The case of an interference very close in bearing to the target is not discussed in detail.

II. Output Variance with Ambient Noise and a Single Interference Present

It is desired to calculate the output variance $D^2(\text{output})$ for the situation depicted in Figure 1. The variables $i_j(t)$ and $n_j(t)$ represent the interference and noise components, respectively, of the jth hydrophone output.

This report follows the procedure established in Report No. 3, section IV.

Under the assumption that the array is steered on target but that signal power is negligible compared with ambient noise or interference power, the autocorrelation function of the output is

$$R_z(\tau) = E\left\{ \left[\sum_{h=1}^{M} i_h(t) + n_h(t) \right] \left[\sum_{j=1}^{M} i_j(t) + n_j(t) \right] \times \left[\sum_{k=1}^{M} i_k(t+\tau) + n_k(t+\tau) \right] \left[\sum_{\ell=1}^{M} i_\ell(t+\tau) + n_k(t+\tau) \right] \right\} =$$

$$\sum_{h=1}^{M} \sum_{j=1}^{M} \sum_{k=1}^{M} \sum_{\ell=1}^{M} E\left\{ \left[i_h(t) + n_h(t) \right] \left[i_j(t) + n_j(t) \right] \left[i_k(t+\tau) + n_k(t+\tau) \right] \times \left[i_\ell(t+\tau) + n_\ell(t+\tau) \right] \right\} \quad (1)$$

Since all variables are Gaussian, the products may be grouped as follows:

$$R_z(\tau) = \sum_{h=1}^{M} \sum_{j=1}^{M} \sum_{k=1}^{M} \sum_{\ell=1}^{M} \left\{ \left\langle \left[i_h(t) + n_h(t) \right] \left[i_j(t) + n_j(t) \right] \right\rangle \times \left\langle \left[i_k(t+\tau) + n_k(t+\tau) \right] \left[i_\ell(t+\tau) + n_\ell(t+\tau) \right] \right\rangle + \right.$$

$$\left\langle \left[i_h(t)+n_h(t) \right] \left[i_k(t+\tau)+n_k(t+\tau) \right] \right\rangle \left\langle \left[i_j(t)+n_j(t) \right] \left[i_\ell(t+\tau)+n_\ell(t+\tau) \right] \right\rangle +$$

$$\left. \left\langle \left[i_h(t)+n_h(t) \right] \left[i_\ell(t+\tau)+n_\ell(t+\tau) \right] \right\rangle \left\langle \left[i_j(t)+n_j(t) \right] \left[i_k(t+\tau)+n_k(t+\tau) \right] \right\rangle \right\} \quad (2)$$

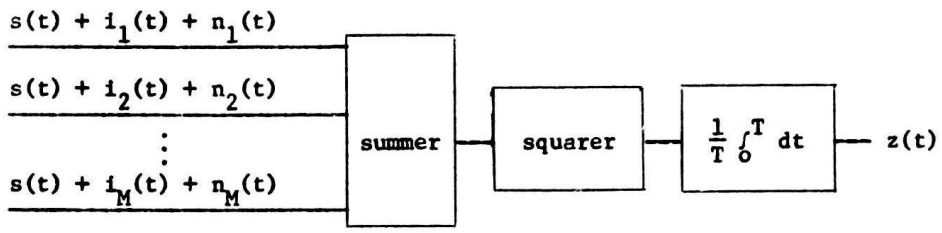

Fig. 1

The last two of the three expressions in brackets above are identical except for indexing. Since noise and interference are independent, the autocorrelation function may be written

$$R_z(\tau) = \sum_{h=1}^{M} \sum_{j=1}^{M} \sum_{k=1}^{M} \sum_{\ell=1}^{M} \left\{ \left[\left\langle i_h(t)\, i_j(t) \right\rangle + \left\langle n_h(t)\, n_j(t) \right\rangle \right] \left[\left\langle i_k(t+\tau)\, i_\ell(t+\tau) \right\rangle + \left\langle n_k(t+\tau)\, n_\ell(t+\tau) \right\rangle \right] + 2 \left[\left\langle i_h(t)\, i_k(t+\tau) \right\rangle + \left\langle n_h(t)\, n_k(t+\tau) \right\rangle \right] \left[\left\langle i_j(t)\, i_\ell(t+\tau) \right\rangle + \left\langle n_j(t)\, n_\ell(t+\tau) \right\rangle \right] \right\} \quad (3)$$

One may define the following normalized correlation functions with N the average noise power at any hydrophone and I the average interference power.

$$I\, q^i_{hj}(\tau) = E\left[i_h(t)\, i_j(+\tau) \right], \quad N\, q^n_{hj}(\tau) = E\left[n_h(t)\, n_j(t+\tau) \right] \quad (4)$$

In terms of the q function, the autocorrelation function is

$$R_z(\tau) = \sum_{h=1}^{M} \sum_{j=1}^{M} \sum_{k=1}^{M} \sum_{\ell=1}^{M} \left\{ \left[I\, q^i_{hj}(0) + N\, q^n_{hj}(0) \right] \left[I\, q^i_{k\ell}(0) + N\, q^n_{k\ell}(0) \right] + 2 \left[I\, q^i_{hk}(\tau) + N\, q^n_{hk}(\tau) \right] \left[I\, q^i_{j\ell}(\tau) + N\, q^n_{j\ell}(\tau) \right] \right\} \quad (5)$$

The q terms with zero argument represent DC power. Define $R_z'(\tau)$ as $\left[R_z(\tau) - (\text{DC terms}) \right]$:

$$R_z'(\tau) = \sum_{h=1}^{M} \sum_{j=1}^{M} \sum_{k=1}^{M} \sum_{\ell=1}^{M} \left\{ 2\, I^2\, q^i_{hk}(\tau)\, q^i_{j\ell}(\tau) + 2\, N^2\, q^n_{hk}(\tau)\, q^n_{j\ell}(\tau) + 4\, IN\, q^i_{hk}(\tau)\, q^n_{j\ell}(\tau) \right\} \quad (6)$$

From Eqs. (39) and (40) of Report No. 3, we obtain the following formula for the variance of the output.

$$D^2(z) = \frac{1}{T} \int_{-\infty}^{\infty} R_z'(\tau)\, d\tau \quad (7)$$

CONFIDENTIAL

Now let $\rho_n(\tau)$ and $\rho_i(\tau)$ represent the normalized autocorrelation function of the ambient noise and interference components of hydrophone output, respectively. Since the noise components of different hydrophones are assumed to be independent, the following relation results:

$$q^n_{hj}(\tau) = \delta_{hj}\,\rho_n(\tau) \qquad \delta_{hj} = \begin{cases} 1 & h = j \\ 0 & h \neq j \end{cases} \tag{8}$$

At a given instant, the interference components at hydrophones h and j respectively represent samples of the same random process taken at an interval of τ_{hj} seconds apart, where τ_{hj} is the delay from hydrophone h to hydrophone k. It is therefore true that

$$q^i_{hj}(\tau) \quad \rho_i(\tau_{hj} + \tau) \tag{9}$$

By Eq. (6) through Eq. (9),

$$D^2(z) = \frac{2I^2}{T} \sum_{h=1}^{M} \sum_{j=1}^{M} \sum_{k=1}^{M} \sum_{\ell=1}^{M} \int_{-\infty}^{\infty} \rho_i\,(\tau_{hk} + \tau)\ \rho_i(\tau_{j\ell} + \tau)\ d\tau$$

$$+ \frac{2N^2}{T} M^2 \int_{-\infty}^{\infty} \rho_n^{\,2}\,(\tau)\ d\tau + \frac{4IN}{T} \sum_{h=1}^{M} \sum_{j=1}^{M} \int_{-\infty}^{\infty} \rho_i\,(\tau_{hj} + \tau)\ M\ \rho_n(\tau)\ d\tau \tag{10}$$

The term above containing the product IN does not appear in Eq. (2) of Report No. 17. For situations where the ratio I/N is substantially greater than unity, this term does not significantly affect the value of $D^2(z)$. Even with I/N near or less than unity, the term has little effect for sufficiently large M. Some calculations appear in Table 1 of Section III which indicate the relative magnitude of terms in the expression for $D^2(z)$ when exponential ρ functions are assumed.

III. Detector Performance with Ambient Noise and Two Interferences

If two uncorrelated interferences of power I_1 and I_2 are present at different bearings, one may infer the expression for $D^2(z)$ from Eq. (10).

Ambient noise power is assumed small in comparison with both I_1 and I_2.

$$D^2(z) = \frac{2I_1^2}{T} \sum_{h=1}^{M} \sum_{j=1}^{M} \sum_{k=1}^{M} \sum_{\ell=1}^{M} \int_{-\infty}^{\infty} \rho_1 (\tau_{hk}^{(1)} + \tau)\, \rho_1 (\tau_{j\ell}^{(1)} + \tau)\, d\tau$$

$$+ \frac{2I_2^2}{T} \sum_{h=1}^{M} \sum_{j=1}^{M} \sum_{k=1}^{M} \sum_{\ell=1}^{M} \int_{-\infty}^{\infty} \rho_2 (\tau_{hk}^{(2)} + \tau)\, \rho_2 (\tau_{j\ell}^{(2)} + \tau)\, d\tau + \frac{2N^2}{T} M^2 \int_{-\infty}^{\infty} \rho_n^2 (\tau)\, d\tau$$

$$+ \frac{4I_1 I_2}{T} \sum_{h=1}^{M} \sum_{j=1}^{M} \sum_{k=1}^{M} \sum_{\ell=1}^{M} \int_{-\infty}^{\infty} \rho_1 (\tau_{hk}^{(1)} + \tau)\, \rho_2 (\tau_{j\ell}^{(2)} + \tau)\, d\tau$$

$$+ \frac{4I_1 N}{T} \sum_{h=1}^{M} \sum_{j=1}^{M} \int_{-\infty}^{\infty} \rho_1 (\tau_{hj}^{(1)} + \tau)\, M\rho_n (\tau)\, d\tau + \frac{4I_2 N}{T} \sum_{h=1}^{M} \sum_{j=1}^{M}$$

$$\int_{-\infty}^{\infty} \rho_2 (\tau_{hj}^{(2)} + \tau)\, M\rho_n (\tau)\, d\tau \qquad (11)$$

In general terms, $\rho_\mu (\tau_{hj}^{(\mu)} + \tau)$ refers to the normalized autocorrelation of the μth interference.

The procedure of Report No. 17 will now be followed to obtain specific results for the figure of merit $\frac{\Delta \text{ (DC output)}}{D \text{ (output)}}$. The following normalized autocorrelation functions are assumed:

$$\rho_1(\tau) = e^{-\omega_1|\tau|} \qquad \rho_2(\tau) = e^{-\omega_2|\tau|} \qquad \rho_n(\tau) = e^{-\omega_o|\tau|} \qquad (12)$$

As explained in Report No. 17, for the cases of interest, the frequencies ω_o, ω_1, ω_2 are comparable. Because the array is linear and the interference wavefronts plane,

$$\tau_{hk}^{(1)} = (h-k)\,\tau_1 \qquad \tau_{hk}^{(2)} = (h-k)\,\tau_2 \qquad (13)^1$$

---

[1] Assuming the delays τ_1 and τ_2 to be positive numbers proves convenient in writing many subsequent expressions, even though Eq. (13) actually permits negative τ's. In all expressions derived, no error is incurred by assuming the τ's positive, even if Eq. (13) indicates that one or both are negative for the geometry and indexing of a particular situation.

For convenience, define the coefficients

$$C^{uv}_{h-j,\ k-\ell} = \int_{-\infty}^{\infty} \rho_u (\tau^{(u)}_{hj} + \tau)\ \rho_v\ (\tau^{(v)}_{k\ell} + \tau)\ d\tau \tag{14}$$

The fact that autocorrelation functions are even functions leads to the results

$$C^{uu}_{rs} = C^{uu}_{sr} = C^{uu}_{-r,\ -s} \qquad\qquad C^{uv}_{rs} = C^{vu}_{sr} = C^{uv}_{-r,\ -s} \tag{15}$$

Consideration of Eq. (7) through Eq. (10) in Report No. 17 and the above Eq. (15) leads to the result

$$\sum_{h=1}^{M}\sum_{j=1}^{M}\sum_{k=1}^{M}\sum_{\ell=1}^{M} C^{uv}_{h-j,\ k-\ell} = M^2\, C^{uv}_{oo} + 2M \sum_{s=1}^{M-1} (M-s)\, C^{uv}_{os} + 2M \sum_{r=1}^{M-1} (M-r)\, C^{uv}_{ro}$$

$$+ 2 \sum_{r=1}^{M-1}\sum_{s=1}^{M-1} (M-r)\ (M-s) \left[C^{uv}_{rs} + C^{uv}_{-rs} \right] \tag{16}$$

By analogy with Eq. (14), define the coefficients

$$D^{u}_{h-j} = \int_{-\infty}^{\infty} \rho_u\ (\tau^{(u)}_{hj} + \tau)\ \rho_n\ (\tau)\ d\tau \tag{17}$$

Using the fact that $D^u_r = D^u_{-r}$, one may show that

$$\sum_{h=1}^{M}\sum_{j=1}^{M} D^{u}_{h-j} = M\, D^u_o + 2 \sum_{r=1}^{M-1} (M-r)\, D^u_r \tag{18}$$

The coefficients are calculated from Eq. (12) through Eq. (14). Details of the calculation appear in Appendix A.

$$C^{uv}_{rs} = \int_{-\infty}^{\infty} e^{\left[-\omega_u |\tau + r\tau_u| \ -\omega_v |\tau + s\tau_v| \right]} =$$

$$\frac{e^{-\omega_u \Delta} + e^{-\omega_v \Delta}}{\omega_u + \omega_v} + \frac{e^{-\omega_u \Delta} - e^{-\omega_v \Delta}}{\omega_v - \omega_u} \tag{19}$$

where, by definition,

$$\Delta = |\ r\,\tau_u - s\,\tau_v\ | \tag{20}$$

If $\omega_u = \omega_v$, the coefficient takes a simpler form,

$$C_{rs}^{uv} = \frac{1}{\omega_u}(1 + \omega_u|r\tau_u - s\tau_v|)e^{-\omega_u|r\tau_u - s\tau_v|} \qquad (\omega_u = \omega_v) \tag{21}$$

From Eq. (14) of Report No. 17,

$$C_{rs}^{uu} = \frac{1}{\omega_u}(1 + |r-s|\omega_u\tau_u)e^{-|r-s|\,\omega_u\tau_u} \qquad (u=v) \tag{22}$$

By setting τ_v equal to zero in Eq. (19) one may infer the value of the D coefficients, defined in Eq. (17) .

$$D_r^u = \frac{e^{-\omega_u|r\tau_u|} + e^{-\omega_o|r\tau_u|}}{\omega_u + \omega_o} + \frac{e^{-\omega_u|r\tau_u|} - e^{-\omega_o|r\tau_u}}{\omega_o - \omega_u} \tag{23}$$

If $\omega_u = \omega_o$, the result simplifies.

$$D_r^u = \frac{1}{\omega_u}(1 + \omega_u|r\tau_u|)e^{-\omega_u|r\tau_u|} \tag{24}$$

The following general expression for output variance in terms of the C and D coefficients represents a combination of Eqs. (11), (14), (16), (17), and (18):

$$\begin{aligned} D^2(z) = {} & \frac{2I_1^2}{T}\left\{M^2 C_{oo}^{11} + 4M\sum_{s=1}^{M-1}(M-s)\,C_{os}^{11} + 2\sum_{r=1}^{M-1}\sum_{s=1}^{M-1}(M-r)(M-s)\left[C_{rs}^{11} + C_{-rs}^{11}\right]\right\} \\ & + \frac{2I_2^2}{T}\left\{M^2 C_{oo}^{22} + 4M\sum_{s=1}^{M-1}(M-s)\,C_{os}^{22} + 2\sum_{r=1}^{M-1}\sum_{s=1}^{M-1}(M-r)(M-s)\left[C_{rs}^{22} + C_{-rs}^{22}\right]\right\} \\ & + \frac{2N^2}{T}M^2\int_{-\infty}^{\infty}\rho_n^2(\tau)\,d\tau + \frac{4I_1I_2}{T}\left\{M^2 C_{oo}^{12} + 2M\sum_{q=1}^{M-1}(M-q)\left[C_{oq}^{12} + C_{qo}^{12}\right]\right. \\ & \left. + 2\sum_{r=1}^{M-1}\sum_{s=1}^{M-1}(M-r)(M-s)\left[C_{rs}^{12} + C_{-rs}^{12}\right]\right\} + \frac{4I_1N}{T}\left\{M^2D_o^1 + 2M\sum_{r=1}^{M-1}(M-r)\,D_r^1\right\} \\ & + \frac{4I_2N}{T}\left\{M^2D_o^2 + 2\sum_{r=1}^{M-1}(M-r)\,D_r^2\right\} \end{aligned} \tag{25}$$

For the assumed exponential autocorrelation functions, by Eqs. (19) and (22) through (25),

$$D^2(z) = \frac{2I_1^2}{T}\left\{\frac{M^2}{\omega_1} + 4M\sum_{s=1}^{M-1}\frac{(M-s)}{\omega_1}(1+s\omega_1\tau_1)e^{-s\omega_1\tau_1} + \right.$$

$$2\sum_{r=1}^{M-1}\sum_{s=1}^{M-1}(M-r)\frac{(M-s)}{\omega_1}\left[(|+|r-s|\omega_1\tau_1)e^{-|r-s|\omega_1\tau_1} + \right.$$

$$\left.\left.(1+|r+s|\omega_1\tau_1)e^{-(r+s)\omega_1\tau_1}\right]\right\}$$

$$+\frac{2I_2^2}{T}\{\text{terms like those for } I_1, \text{ with } \omega_1\tau_1 \text{ replaced by } \omega_2\tau_2\} +$$

$$\frac{2N^2}{T}\left\{\frac{M^2}{\omega_o}\right\}$$

$$+\frac{4I_1I_2}{T}\left\{\frac{2M^2}{\omega_1+\omega_2} + 2M\sum_{s=1}^{M-1}(M-s)\left[\frac{e^{-\omega_1 s\tau_2}+e^{-\omega_2 s\tau_2}}{\omega_1+\omega_2} + \frac{e^{-\omega_1 s\tau_2}-e^{-\omega_2 s\tau_2}}{\omega_2-\omega_1}\right]\right.$$

$$+2M\sum_{r=1}^{M-1}(M-r)\left[\frac{e^{-\omega_1 r\tau_1}+e^{-\omega_2 r\tau_1}}{\omega_1+\omega_2} + \frac{e^{-\omega_1 r\tau_1}-e^{-\omega_2 r\tau_1}}{\omega_2-\omega_1}\right]$$

$$+2\sum_{r=1}^{M-1}\sum_{s=1}^{M-1}(M-r)(M-s)\left[\frac{e^{-\omega_1\Delta}+e^{-\omega_2\Delta}}{\omega_1+\omega_2} + \frac{e^{-\omega_1\Delta}-e^{-\omega_2\Delta}}{\omega_2-\omega_1}\right.$$

$$\left.\left.+\frac{e^{-\omega_1\Sigma}+e^{-\omega_2\Sigma}}{\omega_1+\omega_2} + \frac{e^{-\omega_1\Sigma}-e^{-\omega_2\Sigma}}{\omega_2-\omega_1}\right]\right\}$$

$$+\frac{4I_1N}{T}\left\{\frac{2M^2}{\omega_1+\omega_o} + 2M\sum_{r=1}^{M-1}(M-r)\left[\frac{e^{-\omega_1 r\tau_1}+e^{-\omega_o r\tau_o}}{\omega_1+\omega_o} + \frac{e^{-\omega_1 r\tau_1}-e^{-\omega_o r\tau_o}}{\omega_o-\omega_1}\right]\right\}$$

$$+\frac{4I_2N}{T}\left\{\text{terms like those for } I_1, \text{ with } \omega_1\tau_1 \text{ replaced by } \omega_2\tau_2\right\} \quad (26)$$

In the above expression, Δ and Σ are defined as

$$\Delta = |r\tau_1 - s\tau_2| \qquad \Sigma = r\tau_1 + s\tau_2 \tag{27}$$

If neither interference is near the signal in bearing,[1] the products $\omega_1\tau_1$ and $\omega_2\tau_2$ are much greater than unity, and most of the terms in Eq. (26) may be neglected.

$$D^2(z) = \frac{2I_1^2}{T}\left[\frac{M^2}{\omega_1} + \frac{1}{\omega_1}\left(\frac{2}{3}M^3 - M^2 + \frac{1}{3}M\right)\right] + \frac{2I_2^2}{T}\left[\frac{M^2}{\omega_2} + \frac{1}{\omega_2}\left(\frac{2}{3}M^3 - M^2 + \frac{1}{3}M\right)\right]$$

$$+ \frac{2N^2}{T}\left[\frac{M^2}{\omega_o}\right] + \frac{4I_1I_2}{T(\omega_1+\omega_2)}\left[2M^2 + \left(\frac{2}{3}M^3 - M^2 + \frac{1}{3}M\right) X_{12}\right]$$

$$+ \frac{4I_1N}{T(\omega_1+\omega_o)}\left[2M^2\right] + \frac{4I_2N}{T(\omega_2+\omega_o)}\left[2M^2\right] \qquad (\omega_1\tau_1,\ \omega_2\tau_2 >> 1) \tag{28}$$

The "interaction factor" X_{12} measures the effect on output variance of the intermodulation of the two interference processes which results from the squaring operation in the standard detector. If both interferences are remote in bearing from the target, the factor X_{12} has a maximum value of 2 . This value is reached when both interferences have the same bearing. The factor is discussed in detail at the end of this section.

The effect of a signal having power S when the array is steered on target is demonstrated in Eq. (33) of Report No. 3. That effect is

$$\Delta \text{ (DC output)} = M^2S \tag{29}$$

From Eqs. (28) and (29), one may calculate the following figure of merit

---

[1] For the assumed values $\omega_1 = 2\pi \times 5000$ and hydrophone spacing d = 2 feet, calculations show that the term $e^{-\omega_1\tau_1}$ is less than .1 for bearings greater than about 10° relative to the target.

$$\frac{\Delta \text{ (DC output)}}{D \text{ (output)}} =$$

$$\sqrt{\frac{T}{2}}\,MS\left\{\left(\frac{I_1^2}{\omega_1}+\frac{I_2^2}{\omega_2}\right)\left[\frac{2}{3}M+\frac{1}{3M}\right]+\frac{N^2}{\omega_o}+\frac{I_1I_2}{\frac{1}{2}(\omega_1+\omega_2)}\left[2+\left(\frac{2}{3}M-1+\frac{1}{3M}\right)X_{12}\right]\right.$$

$$\left.+\left[\frac{I_1N}{\frac{1}{2}(\omega_1+\omega_o)}+\frac{I_2N}{\frac{1}{2}(\omega_2+\omega_o)}\right]\left[2\right]\right\}^{-\frac{1}{2}} \qquad (30)$$

The above equation may be rewritten as

$$\frac{\Delta \text{ (DC output)}}{D(\text{output})} =$$

$$\sqrt{\frac{T}{2}}\,MS\left\{\left[\frac{I_1^2}{\omega_1}+\frac{I_2^2}{\omega_2}\right]A+\left[\frac{I_1I_2}{\frac{1}{2}(\omega_1+\omega_2)}\right]B+\left[\frac{I_1N}{\frac{1}{2}(\omega_1+\omega_o)}+\frac{I_2N}{\frac{1}{2}(\omega_2+\omega_o)}\right]C+\frac{N^2}{\omega_o}\right\}^{-\frac{1}{2}} \qquad (31)$$

where the following definitions are implied:

$$A=\frac{2}{3}M+\frac{1}{3M} \qquad B=2+\left(\frac{2}{3}M-1+\frac{1}{3M}\right)X_{12} \qquad C=2 \qquad (32)$$

The factors A, B, and C measure the relative contributions of different intermodulation effects to the magnitude of the output variance $D^2(z)$. Specifically, A measures the importance of intermodulation of an interference process with itself; B pertains to the intermodulation of the two interferences, and C determines the contributions of interference-noise intermodulation. If it happens that τ_1 and τ_2 are roughly equal, then B is approximately 2A for large M; otherwise B is smaller.

Properties of X_{12}

From Eqs. (26) and (28), X_{12} is implicitly defined as follows:

$$2\sum_{r=1}^{M-1}\sum_{s=1}^{M-1}(M-r)(M-s)\left[\frac{e^{-\omega_1\Delta}+e^{-\omega_2\Delta}}{\omega_1+\omega_2}+\frac{e^{-\omega_1\Delta}-e^{-\omega_2\Delta}}{\omega_2-\omega_1}\right]=$$

$$\frac{1}{\omega_1+\omega_2}\left[\frac{2}{3}M^3-M^2+\frac{1}{3}M\right]X_{12}\text{ , where} \qquad (33)$$

$$\Delta=|r\tau_1-s\tau_2|\text{ .} \qquad (34)$$

For simplicity, assume $\omega_1 = \omega_2 = \omega_o$; then Eq. (21) indicates a simplification in the form of the terms involving Δ .

$$2 \sum_{r=1}^{M-1} \sum_{s=1}^{M-1} (M-r)(M-s) \frac{1}{\omega_o} (1+\omega_o \Delta) e^{-\omega_o \Delta} = \frac{1}{2\omega_o} \left[\frac{2}{3} M^3 - M^2 + \frac{1}{3} M \right] X_{12} \qquad (35)$$

Assume that $\tau_2 = k\tau_1$, where $k > 1$. The double summation may be written

$$2 \sum_{r=1}^{M-1} \sum_{s=1}^{M-1} (M-r)(M-s) \frac{1}{\omega_o} (1+\omega_o \tau_1 |r-ks|) e^{-\omega_o \tau_1 |r-ks|} \qquad (36)$$

Consistent with the assumption that $e^{-\omega_o \tau_1} \cong e^{-\omega_o \tau_2} \cong 0$, one may neglect terms in the summation except those for which $|r-ks| << |$. For concreteness, one may require $|r-ks| < 1/2$ as the condition for a term to be significant.[1] For a particular integer s' , suppose that the integer r' satisfies the relation $r'-ks' = 1/2$. Then $(r'-1) - ks' = -1/2$. In this case, for each s there are two values of r such that $|r-ks| \leq 1/2$. Except for a discrete set of values of k , no r will be found for which $r-ks = 1/2$ exactly. However, as long as $k < (M-1)$, some one value of r can be found for sufficiently small values of s such that $|r-ks| < 1/2$. Hence, in general, a reasonable assumption is that for each value of s , only one value of r need be considered.

Note that by definition $\tau = (d \sin \theta)/c$, where d is hydrophone spacing and c is sound velocity. Hence, $k = \tau_2 / \tau_1 = \sin \theta_2 / \sin \theta_1$. Since the basic assumption $e^{-\omega_o \tau_1} \cong 0$ is poor for angles less than about

---

[1] The assumption being made is that $\left[1+\omega_o \tau_1 (1/2)\right] e^{-\omega_o \tau_1 (1/2)}$ is $<< 1$, on the order of .01 , for instance. This condition is true for $\omega_o \tau_1 \geq 3.5$; for $\omega_o = 2\pi \times 5000$, $d = 2$ ft., the inequality holds for any relative bearing greater than about 15^o .

15°,[1] the minimum value of $\sin \theta_1$ for which the analysis is valid is about .25 . Hence, k is not more than $1/.25 = 4$.

In the expression (36), s values greater than $(M-1)/k$ find no corresponding r satisfying the requirement $|r-ks| < 1/2$. Hence, the maximum value of s which is significant is the integer nearest $(M-1)/k$ (or M/k for simplicity). The value of r corresponding to each s is the integer nearest ks . The expression (36) is then roughly

$$2 \sum_{s=1}^{\lfloor m/k \rfloor} (M-ks)\ (M-s)\ \frac{1}{\omega_o}\ (|+\omega_o \tau_1\ |r-ks|)\ e^{-\omega_o \tau_1 |r-ks|}\ , \qquad (37)$$

where $\lfloor M/k \rfloor$ denotes the largest integer smaller than M/k . Investigation reveals that for a given s , the value of $|r-ks|$ is the difference between sd and the nearest integer, where d is the fractional part of k . In general, the above expression cannot be significantly simplified. The expression has local maxima with respect to k when k is a multiple of $1/2$; local minima occur approximately where the fractional part of k is $1/4$ or $3/4$.

A rough estimate of the summation may be obtained for the cases where k is an integer. For all values of s yielding significant terms in the summation, $|r-ks| = 0$. Hence, by (37) the summation reduces to

$$2 \sum_{s=1}^{\lfloor m/k \rfloor} (M-ks)\ (M-s)\ \frac{1}{\omega_o} \approx \frac{2}{\omega_o} \int_1^{m/k} (M-ks)\ (M-s)\ ds =$$

$$\frac{2}{\omega_o} \int_1^{m/k} \left[M^2 - M(k+1)\ s + ks^2 \right] ds = \frac{2}{\omega_o} \left[M^2 s - \frac{M}{2}\ (k+1)\ s^2 + \frac{k}{3}\ s^3 \right]_1^{m/k}$$

---

[1] For the product $\omega_o d$ on the order of $4\pi \times 5000$.

$$= \frac{2}{\omega_o}\left[\frac{M^3}{k} - M^2 - \frac{M^3(k+1)}{2k^2} + \frac{M}{2}(k+1) + \frac{M^3 k}{3k^3} - \frac{k}{3}\right] =$$

$$\frac{2}{\omega_o}\left[M^3\left(\frac{1}{k} - \frac{k+1}{2k^2} + \frac{1}{3k^2}\right) - M^2\right] = \frac{2}{\omega_o}\left[\frac{M^3}{k^2}\left(k - \tfrac{1}{2}(k+1) + \frac{1}{3}\right)\right]$$

$$= \frac{2}{\omega_o}\frac{M^3}{k^2}\left(\frac{k}{2} - \frac{1}{6}\right) \qquad (38)$$

For large M, the above expression, where powers of M less than the third power are ignored, should be reasonably accurate. Referring to (B3), and assuming $M^2 << M^3$, one obtains an approximation for X_{12}.

$$X_{12} \cong 6\left(\frac{k/2 - 1/6}{k^2}\right) = \frac{3k-1}{k^2} \qquad \left(k = \frac{\tau_2}{\tau_1} = \text{integer}\right) \qquad (39)$$

It appears impossible to obtain a simple analytical expression for the factor X_{12} in terms of the bearings θ_1 and θ_2 and the parameters of the system. For this reason, extensive computer calculations have been performed. For the calculations, it is assumed that both processes have the same bandwidth. The precise form of the expression for X_{12}, derived from Eq. (35) is:

$$X_{12} = \frac{12}{2M^3-3M^2+M}\sum_{r=1}^{M-1}\sum_{s=1}^{M-1}(M-r)(M-2)\left(1+\omega_o|r\tau_1 - s\tau_2|\right)e^{-\omega_o|r\tau_1 - s\tau_2|}$$

$$= \frac{12}{2M^3-3M^2+M}\sum_{r=1}^{M-1}\sum_{s=1}^{M-1}(M-r)(M-s)\left(1+\frac{\omega_o d}{c}|r\sin\theta_1 - s\sin\theta_2|\right)\times$$

$$e^{-\frac{\omega_o d}{c}|r\sin\theta_1 - s\sin\theta_2|} \qquad (40)$$

where M is the number of hydrophones, d is hydrophone spacing, and c sound velocity. For calculation, ω_o was taken to be $2\pi \times 5000$, d two feet, c 5000 feet per second. Results were obtained for $M = 40$ and $M = 20$.

In Figure 2 curves of X_{12} versus θ, the arithmetic mean of the bearings of two point source interferences relative to the target, are plotted for different constant values of $\Delta\theta$, the difference in bearing between the interferences; for these curves M is taken to be 40 hydrophones. In Figure 3 curves of X_{12} versus breadth $\Delta\theta$, for fixed values of center angle θ, are plotted for both $M = 40$ and $M = 20$ to permit comparison of the results for different values of M.

In Figure 4 contours of constant delay-time ratios are plotted on the $\theta_1 - \theta_2$ plane.

A striking feature of the X_{12}-versus-θ curves (Figure 2) is that for a given value of θ in the range of about 25° to 65°, X_{12} is nearly independent of the breadth (angular separation) $\Delta\theta$ for values of $\Delta\theta$ between about 5° and 40° (.1 radian to .7 radian). Exceptions to this statement do occur in certain ranges where one or more curves have sharp relative minima or maxima with respect to θ. The limited calculations for $\Delta\theta$ on the order of one radian indicate that X_{12} does dip nearly to zero for at least one range of θ.

The curves may actually be somewhat more irregular than the plots indicate, since the points picked for calculation did not include all the combinations of angles yielding delay-time ratios which correspond to relative maxima or minima of X_{12}. It seems reasonable to conclude, however, that unless θ is fairly near 90° or $\Delta\theta$ is on the order of a radian or greater, detector performance is relatively insensitive to the value of $\Delta\theta$. It must be noted that for M set equal to 20, the curves separate appreciably at a smaller value of θ than for M equal to 40. Evidently a larger number of hydrophones increases the range of θ over which performance is insensitive to $\Delta\theta$.

The comparative flatness of the curves of X_{12} versus $\Delta\theta$ (Figure 3) illustrates the above remarks.

Form EE-12

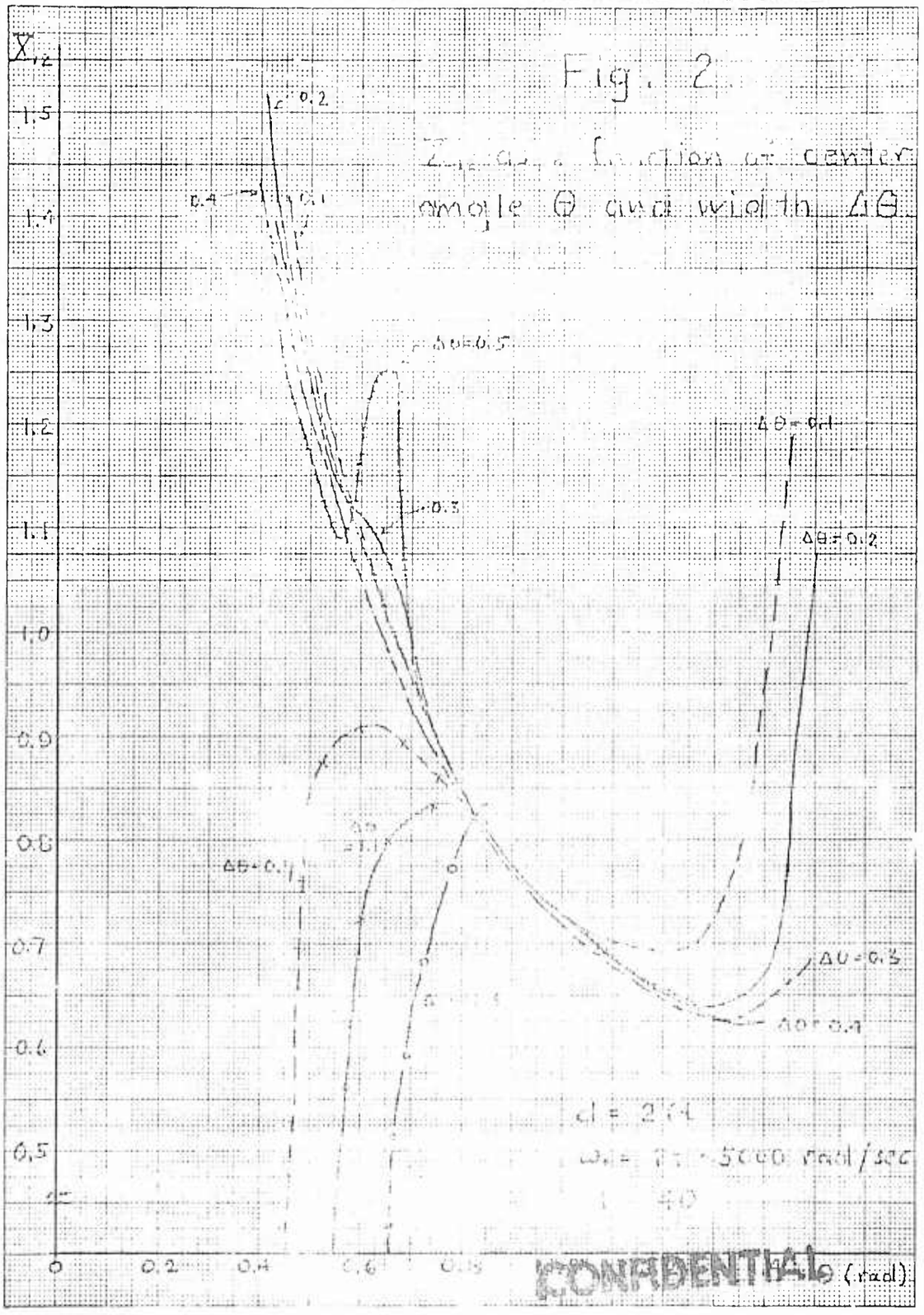

Fig. 2

Z as a function of center angle θ and width Δθ

Form EE-12 DUNHAM LABORATORY YALE UNIVERSITY

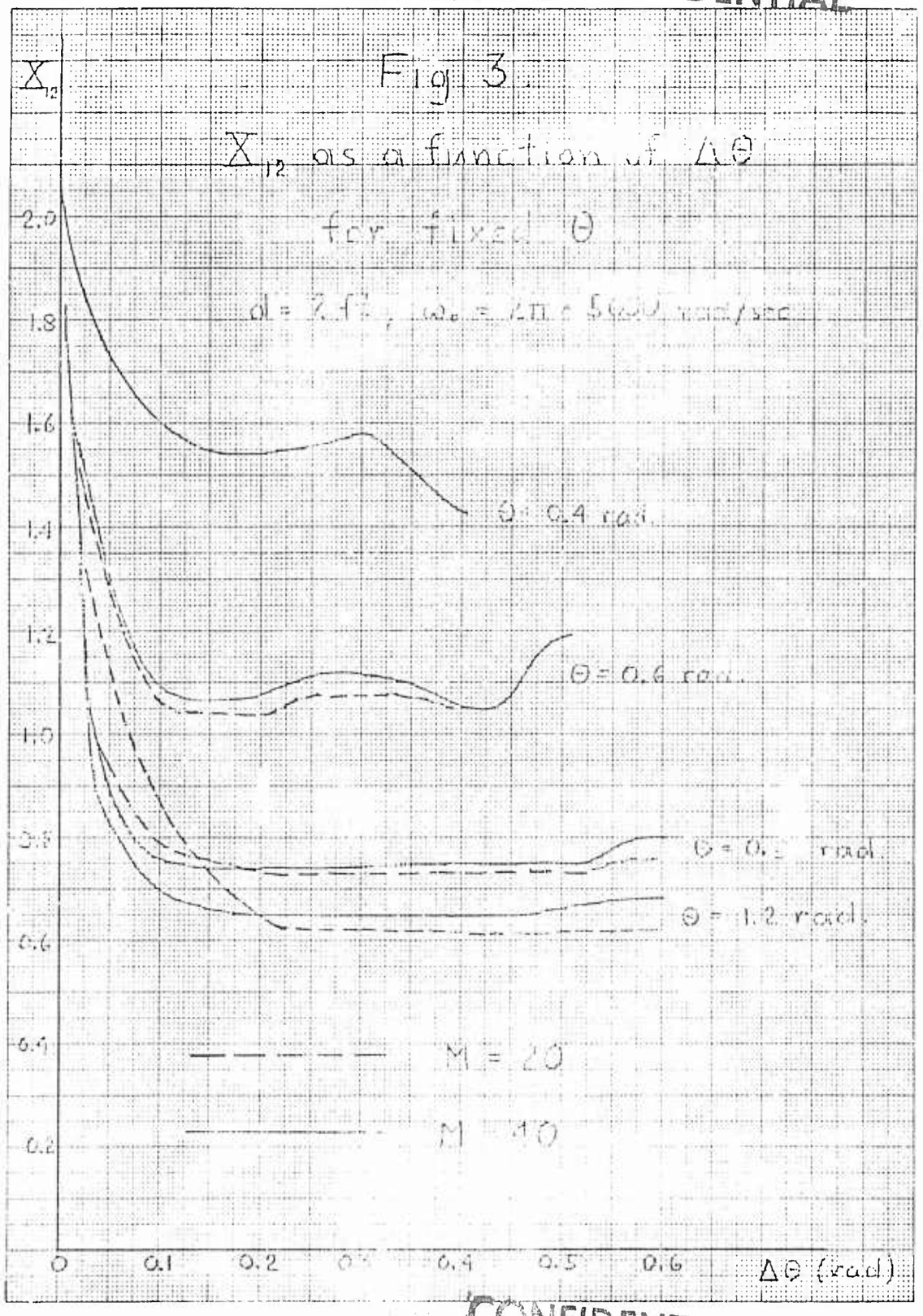

Form EE-12

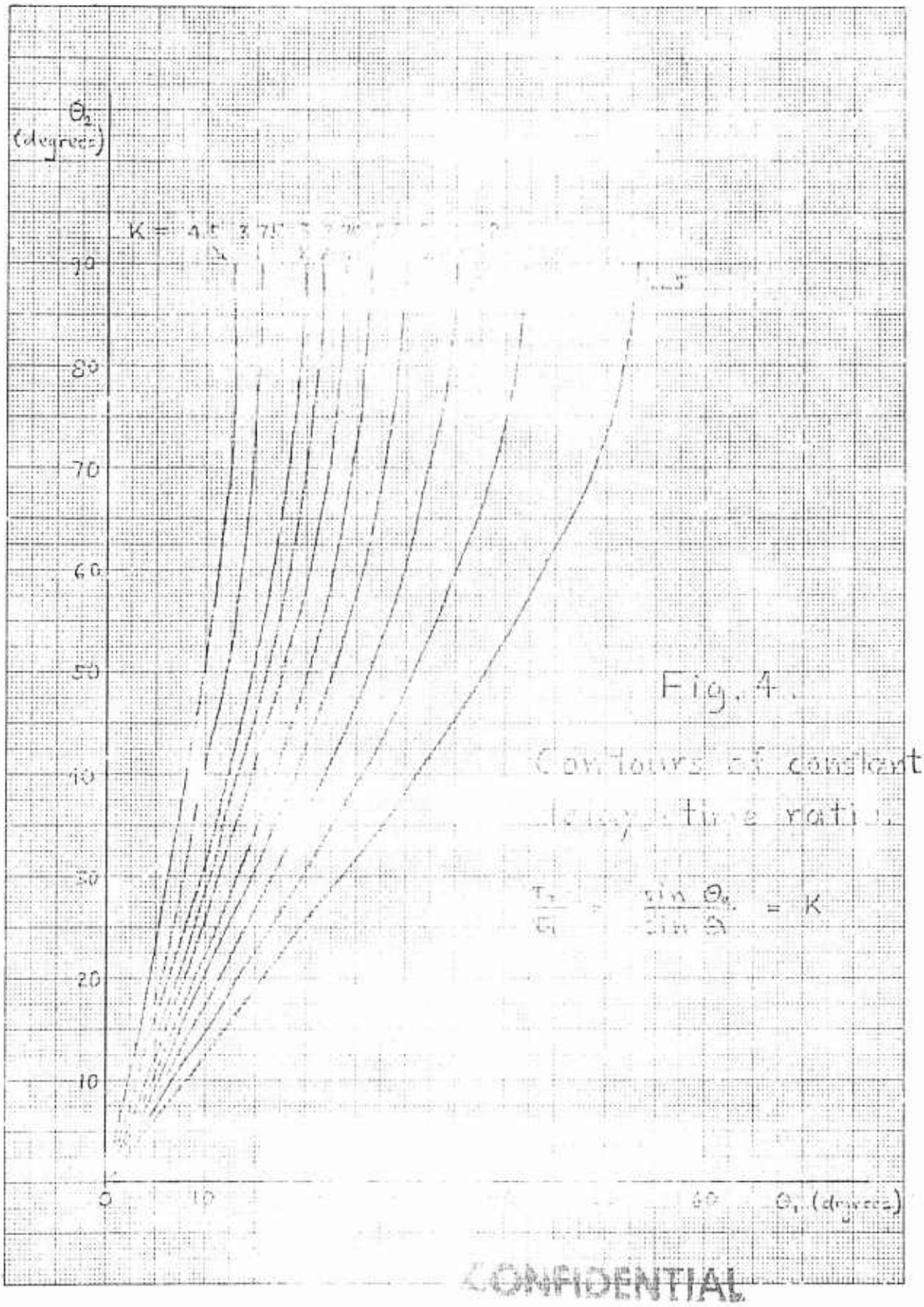

Fig. 4.

Contours of constant velocity ratio.

$$\frac{v_2}{v_1} = \frac{\sin \theta_2}{\sin \theta_1} = K$$

IV. Amendments to Report Number 17

On the basis of the derivations in the previous section, it will now be indicated where in Report No. 17 terms need to be added to expressions. For direct comparison with the results of the earlier report, it must be assumed that the interference "cutoff" frequency ω_1 is the same as ω_o. By Eqs. (11), (17), (18), (24), and (25), Eq. (16) of Report No. 17 is amended as follows:

$$\frac{\Delta(\text{DC output})}{D(\text{output})} =$$

$$\sqrt{\frac{T\omega_o}{2}}\;\frac{MS}{\left[N^2+I^2\left\{1+\frac{4}{M}\sum_{s=1}^{M-1}(M-s)\,(1+s\omega_o\tau_o)e^{-s\omega_o\tau_o}+\frac{2}{M^2}\sum_{s=1}^{M-1}(M-s)^2\left[1+(1+2s\omega_o\tau_o)e^{-2s\omega_o\tau_o}\right]\right.\right.}$$

$$\left.\left.+\frac{4}{M^2}\sum_{r=2}^{M-1}\sum_{s=1}^{r-1}(M-r)\,(M-s)\left(\left[1+(r-s)\omega_o\tau_o\right]e^{-(r-s)\omega_o\tau_o}+\left[1+(r+s)\omega_o\tau_o\right]e^{-(r+s)\omega_o\tau_o}\right)\right\}\right.$$

$$\left.+\,IN\left\{2+\frac{4}{M}\sum_{r=1}^{M-1}(M-r)\,(1+r\omega_o\tau_o)e^{-r\omega_o\tau_o}\right\}\right]^{\frac{1}{2}} \qquad (41)$$

Accordingly, Eq. (17) of Report No. 17 is amended to

$$\frac{\Delta(\text{DC output})}{D(\text{output})} = \sqrt{\frac{T\omega_o}{2}}\;\frac{MS}{\sqrt{N^2+I^2\left[1+\frac{2}{M^2}\sum_{s=1}^{M-1}(M-s)^2\right]+2IN}} \qquad (42)$$

Eq. (18) of Report No. 17 becomes

$$\frac{\Delta(\text{DC output})}{D(\text{output})} = \sqrt{\frac{T\omega_o}{2}}\;\frac{MS}{\sqrt{N^2+\frac{I^2}{3}\left(2M+\frac{1}{M}\right)+2IN}} \qquad (43)$$

In terms of the factors defined in Eq. (32), the above equation reads

$$\frac{\Delta(\text{DC output})}{D(\text{output})} = \sqrt{\frac{T\omega_o}{2}}\;\frac{MS}{\sqrt{N^2+AI^2+2IN}} \qquad (44)$$

Eq. (43) reveals that the term $2IN$ is relatively unimportant unless N and I are comparable and M is not large. To determine precisely the effect of this term, one may assume $I = N$ and, using Eq. (44), calculate a correction factor as a function of M which will convert Eq. (18) of Report 17 to agree with Eq. (43) above.

Table 1 (N = I)

M	Correction factor
10	.89
20	.94
30	.96
40	.97
50	.97

Since some of the curves in Report No. 17 take M as 40 and allow N/I to vary, a correction factor as a function of N/I may be useful.

Table 2 (M = 40)

N/I	Correction factor
.1	.99
1	.97
4	.92

V. Detector Performance with Ambient Noise and Several Interferences

Without further derivation, one can infer the expressions for output variance and figure of merit for k interferences from Eqs. (25), (28), and (30). Using the C and D coefficients defined in Eqs. (14) and (17), the general expression for output variance is

$$D^2(z) =$$

$$\frac{2}{T}\sum_{u=1}^{k} I_u^2\left\{M^2 C_{oo}^{uu} + 4M\sum_{s=1}^{M-1}(M-s)\,C_{os}^{uu} + 2\sum_{r=1}^{M-1}\sum_{s=1}^{M-1}(M-r)(M-s)\left[C_{rs}^{uu} + C_{-rs}^{uu}\right]\right\}$$

$$+\frac{4}{T}\sum_{u=1}^{k}\sum_{v=u+1}^{k} I_u I_v\left\{M^2 C_{oo}^{uv} + 2M\sum_{q=1}^{M-1}(M-q)\left[C_{oq}^{uv} + C_{qo}^{uv}\right] + 2\sum_{r=1}^{M-1}\sum_{s=1}^{M-1}(M-r)(M-s)\left[C_{rs}^{uv}+C_{-rs}^{uv}\right]\right\}$$

$$+\frac{4IN}{T}\sum_{u=1}^{k}\left\{M^2 D_o^u + 2M\sum_{r=1}^{M-1}(M-r)\,D_r^u\right\} + \frac{2}{T}N^2\left\{M^2\int_{-\infty}^{\infty}\rho_n^2(\tau)\,d\tau\right\} \qquad (45)$$

If autocorrelation functions are assumed to be exponential functions of the form $e^{-\omega_u|\tau|}$ and all products $\omega_u\tau_u$ are much greater than unity, the index of performance becomes

$$\frac{\Delta(\text{DC output})}{D(\text{output})} = \frac{\sqrt{\frac{T}{2}}\,MS}{\left\{\left(\frac{2}{3M}+\frac{1}{3M}\right)\sum_{u=1}^{k}\frac{I_u^2}{\omega_u} + \sum_{u=1}^{k}\sum_{v=u+1}^{k}\frac{I_u I_v}{\frac{1}{2}(\omega_u+\omega_v)}\left[2+\left(\frac{2}{3}M-1+\frac{1}{3M}\right)X_{uv}\right] + 2N\sum_{u=1}^{k}\frac{I_u}{\frac{1}{2}(\omega_o+\omega_u)} + \frac{N^2}{\omega_o}\right\}^{\frac{1}{2}}} \tag{46}$$

where X_{uv} is the same function as X_{12} of Section III, involving the uth and vth interferences.

It seems instructive to compare detector performance in the presence of several independent point source interferences with the performances in the presence of a single interference yielding the same average power as all the independent interferences together. If I represents the total average interference power in both situations,

$$I = \sum_{u=1}^{k} I_u \tag{47}$$

In Eq. (46) the coefficient of the I_u^2 terms is the factor A defined in Eq. (32), and the coefficients of the $I_u I_v$ terms are like B of Eq. (32). B ranges from 2 to 2A as X_{12} varies from 0 to 2.[1] In the limiting case where angular displacements between interferences are small (or bandwidths are narrow), the B factors in Eq. (46) approximately equal 2A. If all the ω_u's roughly equal ω_o, Eq. (46) then becomes

---

[1] Note that 2.0 is the maximum value of X_{12} for interferences remote in bearing from the target. For less remote interferences X_{12} exceeds 2. Wherever the assumption $e^{-\omega_o\tau_1} \cong 0$ is valid, $X_{12}(\theta_1, \theta_1) \cong 2.0$.

$$\frac{\Delta(\text{DC output})}{D(\text{output})} \approx \frac{\sqrt{\frac{T\omega_o}{2}}\,MS}{\sqrt{A\sum_{u=1}^{k} I_u^2 + 2A\sum_{u=1}^{k}\sum_{v=u+1}^{k} I_u I_v + 2N\sum_{u=1}^{k} I_u + N^2}} =$$

$$\sqrt{\frac{T\omega_o}{2}}\,\frac{MS}{\sqrt{A\left[\sum_{u=1}^{k} I_u\right]^2 + 2\left[\sum_{u=1}^{k} I_u\right]N + N^2}} = \sqrt{\frac{T\omega_o}{2}}\,\frac{MS}{\sqrt{AI^2 + 2IN + N^2}} \qquad (48)$$

This result is the same as that obtained in Eq. (44) for a single interference of power I. It seems reasonable that if multiple interferences span only a small arc, on the order of the beamwidth of two adjacent hydrophones, the effect on the detector is scarcely distinguishable from that of a single point source interference.

The opposite limiting case occurs in the very improbable event that the interferences are all located at critical bearings which make all the X_{uv} approximately zero. In this situation, the B factors roughly equal 2. Now Eq. (46) yields

$$\frac{\Delta(\text{DC output})}{D(\text{output})} \approx \frac{\sqrt{\frac{T\omega_o}{2}}\,MS}{\sqrt{A\sum_{u=1}^{k} I_u^2 + 2\sum_{u=1}^{k}\sum_{v=u+1}^{k} I_u I_v + 2N\sum_{u=1}^{k} I_u + N^2}} \qquad (49)$$

The best performance [smallest D(output)] occurs if all the I_u are equal to I/k.[1] In this event,

---

[1] This conclusion results from minimizing the denominator of Eq. (49) with the constraint $\Sigma I_u = I$.

$$\frac{\Delta(\text{DC output})}{D(\text{output})} = \frac{\sqrt{\frac{T\omega_o}{2}}\,MS}{\sqrt{Ak\left(\frac{I}{k}\right)^2 + 2\,\frac{k(k-1)}{2}\left(\frac{I}{k}\right)^2 + 2\,NI + N^2}} =$$

$$\sqrt{\frac{T\omega_o}{2}}\,\frac{MS}{\sqrt{I^2\left(\frac{A}{k} + 1 - \frac{1}{k}\right) + 2NI + N^2}} \cong \sqrt{\frac{T\omega_o}{2}}\,\frac{MS}{\sqrt{I^2\left(\frac{A}{k} + 1\right) + 2NI + N^2}} \qquad (50)$$

For a ratio $N/I \gg 1$, this result is, of course, about the same as that for a single interference. If $I \gg N$, however, the figure of merit in this case is greater than that for a single interference by a factor of about $\sqrt{\frac{Ak}{A+k}}$. If $k = 10$ and $M = 40$, for instance, this factor is roughly 3. In practice this performance would virtually never be achieved, since it depends on a freak distribution of the interferences in space.

A crude but hopefully more meaningful estimate of the best performance for a fixed total interference power is obtained by assuming that all the X_{uv} in Eq. (46) take on the minimum calculated values for X_{12} (page 17) with $\Delta\theta$ in the range of about 5^o to 40^o. This minimum value, for $M = 40$ or $M = 20$, is about .6. From Eq. (46),

$$\frac{\Delta(\text{DC output})}{D(\text{output})} = \frac{\sqrt{\frac{T\omega_o}{2}}\,MS}{\sqrt{Ak\left(\frac{I}{k}\right)^2 + \left[2+.6(A-1)\right]\frac{k(k-1)}{2}\left(\frac{I}{k}\right)^2 + 2NI + N^2}} \cong$$

$$\sqrt{\frac{T\omega_o}{2}}\,\frac{MS}{\sqrt{I^2\left(\frac{A}{k}+.3A\right) + 2NI + N^2}} \qquad (X_{uv} = .6, \text{ all } u, v) \qquad (51)$$

With large I/N, this figure of merit is greater than that for a single interference by a factor $\sqrt{\frac{k}{1+.3k}}$. For $k = 10$, this figure is about 1.6; for large k, it is about 1.8.

A crude estimate of average performance is obtained by letting all the X_{uv} in Eq. (46) take on the average calculated value of X_{12} for $\Delta\theta$ in the range of 5^{o} to 40^{o}. The average is close to 1.

$$\frac{\Delta(\text{DC output})}{D(\text{output})} \approx \frac{\sqrt{\frac{T\omega_o}{2}}\ MS}{\sqrt{I^2\left(\frac{A}{k}+\frac{A}{2}\right)+2NI+N^2}} \qquad (X_{uv} \approx 1.\text{, all u, v}) \qquad (52)$$

The improvement factor here is $\sqrt{\frac{k}{1+.5k}}$, which is about 1.2 for $k = 10$, and about $\sqrt{2}$ for large k.

VI. Detector Performance with Ambient Noise and a Distributed Interference

An interference distributed continuously over a finite arc may be treated as a limiting case of the multiple interference problem. The distributed interference is represented as an infinite number of elemental point source interferences spaced an infinitesimal angular distance apart throughout the arc. The derivation in the previous sections of this report have assumed the several interference processes to be statistically independent, and the results to be derived here will not reflect dependencies among different points along the arc of the distributed interference. These dependencies may be expected to degrade performance somewhat more than the subsequent results of this section will indicate. The assumption of exponential autocorrelation functions for interference and noise is inherent in these derivations, and the "cutoff" frequencies for interference and noise are assumed equal.

Angular power density functions may be defined as follows to correspond to the terms of Eq. (46):

$$I(\theta_u)\, d\theta_u = I_u \qquad I(\theta_v)\, d\theta_v = I_v \qquad (53)$$

The first two expressions in the denominator of Eq. (38) may be combined in one double sum. With all ω_u set equal to ω_o, by Eq. (46),

$$\frac{\Delta(\text{DC output})}{D(\text{output})} =$$

$$\sqrt{\frac{T\omega_o}{2}}\,MS\left\{\sum_{\theta_u=\theta_{min}}^{\theta_{max}}\sum_{\theta_v=\theta_u}^{\theta_{max}} I(\theta_u)\,d\theta_u\,I(\theta_v)\,d\theta_v\left[2+\left(\frac{2}{3}M-1+\frac{1}{3M}\right)X(\theta_u,\theta_v)\right]+2N\sum_{\theta_u=\theta_{min}}^{\theta_{max}} I(\theta_u)\,d\theta_u+N^2\right\}^{-\frac{1}{2}}. \quad (54)$$

θ_{min} and θ_{max} define the extent of the interference, and $X(\theta_u, \theta_v)$ is X_{12} of Section III with $\theta_1 = \theta_u$ and $\theta_2 = \theta_v$. (55)

In the limit as $d\theta_u$ and $d\theta_v$ approach zero, the equation reads

$$\frac{\Delta(\text{DC output})}{D(\text{output}} =$$

$$\sqrt{\frac{T\omega_o}{2}}\,MS\left\{\int_{\theta_{min}}^{\theta_{max}}d\theta_u\int_{\theta_u}^{\theta_{max}}d\theta_v\,I(\theta_u)\,I(\theta_v)\left[2+\left(\frac{2}{3}M-1+\frac{1}{3M}\right)X(\theta_u,\theta_v)\right]+2N\int_{\theta_{min}}^{\theta_{max}}I(\theta_u)\,d\theta_u+N^2\right\}^{-\frac{1}{2}} \quad (56)$$

If $I(\theta_u)$ is fairly constant over the arc of the interference, the following approximation is useful:

$$\int_{\theta_{min}}^{\theta_{max}}d\theta_u\int_{\theta_u}^{\theta_{max}}d\theta_v\,I(\theta_u)\,I(\theta_v)\left[2+\left(\frac{2}{3}M-1+\frac{1}{3M}\right)X(\theta_u,\theta_v)\right] \cong \frac{I^2}{2}\left[2+\left(\frac{2}{3}M-1+\frac{1}{3M}\right)\bar{X}\,(\theta_{min},\theta_{max})\right], \quad (57)$$

where $$I = \int_{\theta_{min}}^{\theta_{max}} I(\theta_u)\,d\theta_u \quad (58)$$

and

$$\bar{X}\,(\theta_{min},\,\theta_{max}) = \frac{2}{(\theta_{max}-\theta_{min})^2}\int_{\theta_{min}}^{\theta_{max}} d\theta_u \int_{\theta_u}^{\theta_{max}} d\theta_v\, X(\theta_u,\,\theta_v) \tag{59}$$

Now Eq. (46) is approximately

$$\frac{\Delta(\text{DC output})}{D(\text{output})} = \frac{\sqrt{\frac{T\omega_o}{2}}\,MS}{\sqrt{I^2\left[1+\left(\frac{2}{3}M-1+\frac{1}{3M}\right)\frac{\bar{X}(\theta_{min},\,\theta_{max})}{2}\right]+2NI+N^2}} \tag{60}$$

The factor $\bar{X}$ may be calculated numerically, but analytic approximation does not appear feasible. Computer calculations have been performed, using the parameter values $\omega_o = 2\pi \times 5000$, $d = 2$ ft., and both $M = 40$ and $M = 20$.[1] The results are shown graphically in Figures 5 and 6 in the same format used earlier for X_{12}. The curves of $\bar{X}$ resemble those of X_{12}, except that the $\bar{X}$ curves show no significant irregularities, and $\bar{X}$ does not approach 0 even for large values of the parameter $\Delta\theta$ (full angular spread of the interference). It must be emphasized that the factor $\bar{X}$ and the corresponding detector performance are quite insensitive to the breadth of the interference if the center of the interference is closer to the target than about 50°.

The results are not drastically different for the two values of M, the number of hydrophones. For a fixed center angle θ, the $\bar{X}$ curves for $M = 20$ lie above those for $M = 40$ at small values of $\Delta\theta$ and then approach the curves for $M = 40$ at larger values of $\Delta\theta$. The difference in results for the different values of M is seen to be more pronounced

---

[1] Details of the program in Appendix B.

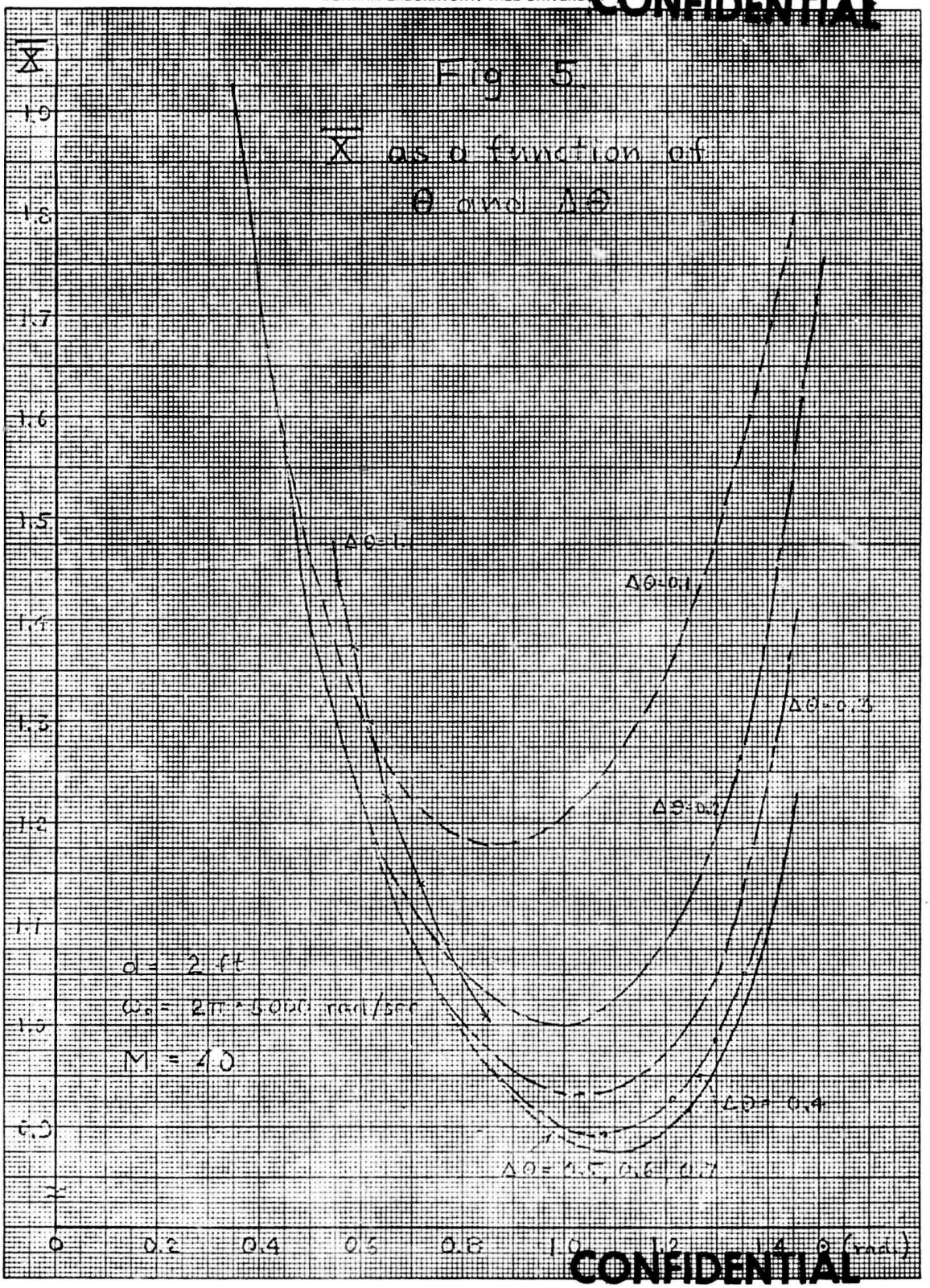

Form EE-12

DUNHAM LABORATORY, YALE UNIVERSITY

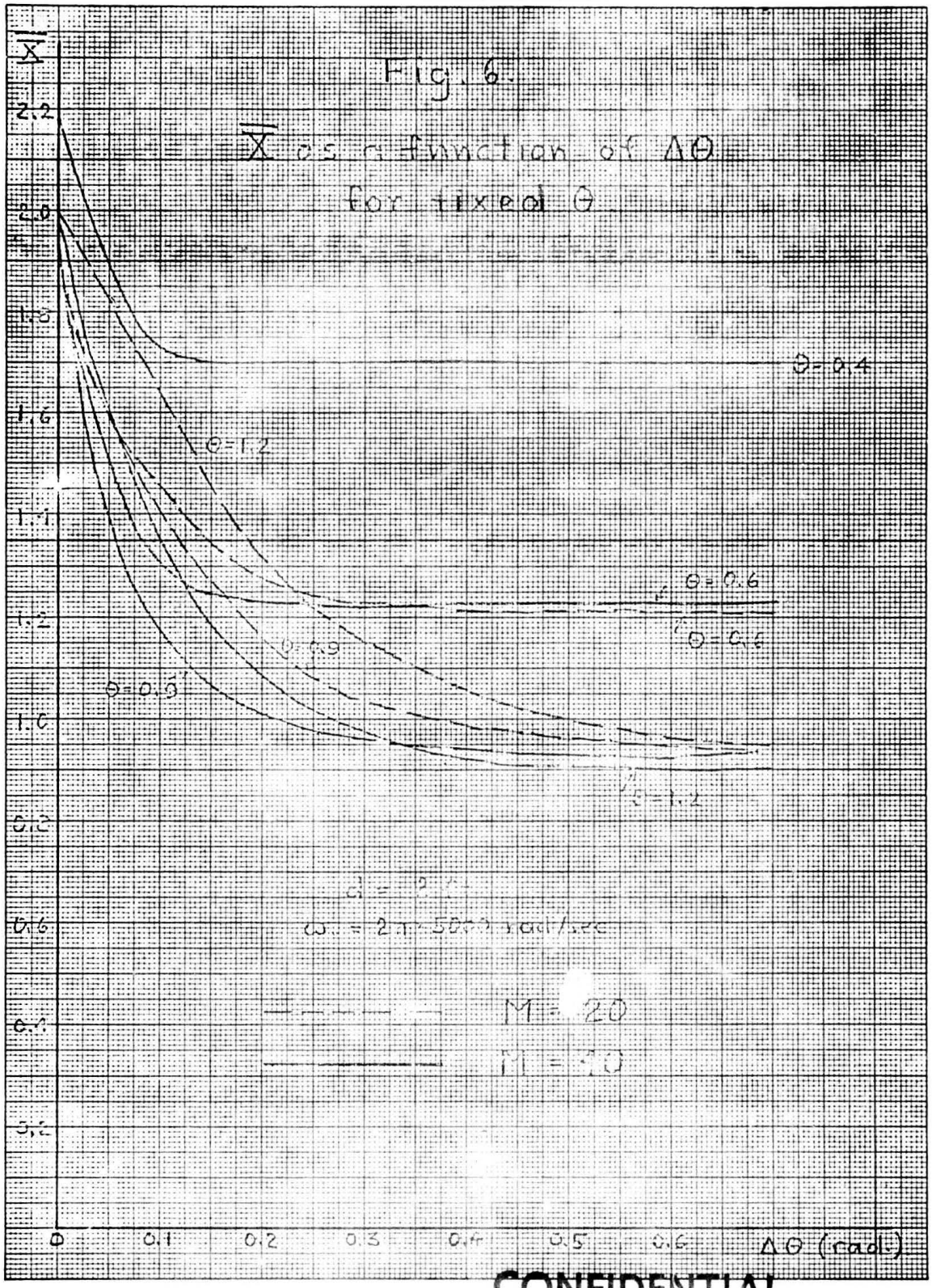

Fig. 6.

X as a function of ΔΘ for fixed Θ

for large values of breadth $\Delta\theta$. The implication of these results is that an increase in the number of hydrophones effects a small improvement in relative performance as measured by the figure of merit. For the smaller number of hydrophones, as compared with the larger number, performance is degraded more seriously by angularly narrow interferences than by broad interferences.

As in the previous section, one may compare performance in the presence of a distributed interference of total power I with that obtained for a point source interference of the same power. For the case where $I/N >> 1$, comparison of Eqs. (44) and (60) indicates that the "improvement factor" for a distributed interference is roughly $\sqrt{2A/\bar{B}}$, where, by analogy with Eq. (32),

$$A = \frac{2}{3} M + \frac{1}{3M} \qquad \bar{B} = 2 + \left(\frac{2}{3} M - 1 + \frac{1}{3M} \right) \bar{X} \tag{61}$$

Table 3 below displays sample results for 40 hydrophones.

Table 3 (distributed interference)

Center Angle θ (degrees)	Breadth $\Delta\theta$ (degrees)	$\bar{X}$	$\bar{B}/2$	A	Improvement Factor $\sqrt{2A/\bar{B}}$
25	5.7	1.60	22.4	26.7	1.09
	11.4	1.58	22.1		1.10
	22.9	1.58	22.1		1.10
	40.0	1.58	22.1		1.10
50	5.7	1.18	16.8		1.26
	11.4	1.02	14.6		1.35
	22.9	.95	13.7		1.40
	40.0	.95	13.7		1.40
75	5.7	1.51	21.2		1.13
	11.4	1.21	17.2		1.25
	22.9	1.00	14.4		1.36
	40.0	.97	14.0		1.38

The "improvement factors" indicated in Table 3 do not reflect a great difference in performance between the two cases of a point source interference and a distributed interference. Yet a factor of 1.3 or 1.4 is not entirely trivial, because of the fact that even if $\bar{X}$ approached zero, $\bar{B}$ could be no smaller than 2, and hence the improvement factor could be no larger than $\sqrt{A}$, which in this case is 5.2. The meaning of the hypothetical improvement factor $\sqrt{A}$ becomes clear when one considers Eq. (44) in the single interference case, which reads,

$$\frac{\Delta(\text{DC output})}{D(\text{output})} = \sqrt{\frac{T\omega_c}{2}} \quad \frac{MS}{\sqrt{N^2+AI^2+2IN}} \tag{62}$$

The improvement factor was defined by the fact that in the distributed interference case, the coefficient of I^2 in an equation of the above form is divided by the square of the improvement factor. As the improvement factor approacheds $\pm A$, therefore, the coefficient of I^2 approaches unity in the above equation. The denominator then becomes $\sqrt{N^2+I^2+2IN}$ $= \sqrt{(N+I)^2}$. The term I enters into the equation in the same manner as N, because the distributed interference is now so widely distributed that it has become simply ambient noise. The hypothetical maximum improvement factor for the case of multiple interferences is also $\sqrt{A}$, as indicated by the discussion following Eq. (50) The calculations reported here, however, indicate that even a very broad interference causes a degradation in performance far more severe than that caused by ambient noise independent from hydrophone to hydrophone. Note that the smallest calculated value of $\bar{X}$ is .87, for which the improvement factor is only about 1.5. The fact that all of the curves in Figure 5 approach their asymptotic values for relatively small $\bar{X}$ suggests that the equivalent of isotropic noise distribution has actually been reached. The

discrepancy between 1.5 and $\sqrt{A}$ would then have to be attributed to the phone to phone noise coherence which exists even in the isotropic case with the numerical parameters considered.

VII. Concluding Remarks

Although calculations of $\frac{\Delta(\text{DC output})}{D(\text{output})}$ for multiple or distributed interferences may become quite complicated, the upper and lower bounds may always be quickly determined if the total interference power I is known. The upper and lower bounds correspond respectively to treating I as isotropic ambient noise independent from hydrophone to hydrophone and as a point source. The following inequality must be satisfied.

$$\sqrt{\frac{T\omega_o}{2}}\ \frac{MS}{\sqrt{N^2 + \frac{I^2}{3}\left(2M+\frac{1}{M}\right) + 2IN}} < \frac{\Delta(\text{DC output})}{D(\text{output})} < \sqrt{\frac{T\omega_o}{2}}\ \frac{MS}{I+N} \qquad (63)$$

The numerical results of this report indicate that in most realistic situations the index of performance will be much closer to its lower bound than to its upper bound.

The major failing of the treatment given in this report is that the results are inaccurate for interferences near the target in bearing. Approximate computations and the results of Report No. 17 suggest that the error will be small if all interferences are separated from the target by appreciably more than the beamwidth of the array.

Appendix A: Calculation of C Coefficients

Initially one may assume $r\tau_u$ greater than $s\tau_v$, both r and s are positive. Now Eq. (19) may be expressed

$$C_{rs}^{uv} = \int_{-\infty}^{\infty} e^{-\omega_u|\tau+r\tau_u| - \omega_v|\tau+s\tau_v|} d\tau = \int_{-\infty}^{-r\tau_u} e^{\omega_u(\tau+r\tau_u) + \omega_v(\tau+s\tau_v)} d\tau$$

$$+ \int_{-r\tau_u}^{-s\tau_v} e^{-\omega_u(\tau+r\tau_u) + \omega_v(\tau+s\tau_v)} d\tau + \int_{-s\tau_v}^{\infty} e^{-\omega_u(\tau+r\tau_u) - \omega_v(\tau+s\tau_v)} d\tau =$$

$$e^{\omega_u r\tau_u + \omega_v s\tau_v} \int_{-\infty}^{-r\tau_u} e^{(\omega_u+\omega_v)\tau} d\tau + e^{-\omega_u r\tau_u + \omega_v s\tau_v} \int_{-r\tau_u}^{-s\tau_v} e^{(-\omega_u+\omega_v)\tau} d\tau$$

$$+ e^{-\omega_u r\tau_u - \omega_v s\tau_v} \int_{-s\tau_v}^{\infty} e^{-(\omega_u+\omega_v)\tau} d\tau =$$

$$\frac{e^{\omega_u r\tau_u + \omega_v s\tau_v}}{\omega_u+\omega_v} \left| e^{-(\omega_u+\omega_v)\tau} \right|_{-\infty}^{-r\tau_u} + \frac{e^{-\omega_u r\tau_u + \omega_v s\tau_v}}{-\omega_u+\omega_v} \left| e^{(\omega_u-\omega_v)s\tau_v} - e^{(\omega_u-\omega_v)r\tau_u} \right|$$

$$+ \frac{e^{-\omega_u r\tau_u - \omega_v s\tau_v}}{-\omega_u-\omega_v} \left| - e^{(\omega_u+\omega_v)s\tau_v} \right| =$$

$$\frac{e^{\omega_v(s\tau_v - r\tau_u)}}{\omega_u+\omega_v} + \frac{e^{\omega_u(-r\tau_u+s\tau_v)} - e^{\omega_v(s\tau_v-r\tau_u)}}{\omega_v-\omega_u} + \frac{e^{\omega_u(-r\tau_u+s\tau_v)}}{\omega_u+\omega_v} =$$

$$\frac{e^{-\omega_u(r\tau_u-s\tau_v)} + e^{-\omega_v(r\tau_u-s\tau_v)}}{\omega_u+\omega_v} + \frac{e^{-\omega_u(r\tau_u-s\tau_v)} - e^{-\omega_v(r\tau_u-s\tau_v)}}{\omega_v-\omega_u} \qquad (A1)$$

This result generalizes to

$$C_{rs}^{uv} = \frac{e^{-\omega_u|r\tau_u-s\tau_v|} + e^{-\omega_v|r\tau_u-s\tau_v|}}{\omega_u+\omega_v} + \frac{e^{-\omega_u|r\tau_u-s\tau_v|} - e^{-\omega_v|r\tau_u-s\tau_v|}}{\omega_v-\omega_u} \qquad (A2)$$

Appendix B: Computation of X_{12} and $\bar{X}$

The computer program employed to calculate X and $\bar{X}$ embodies a sub-routine which calculates X_{12} as a function of θ_1 and θ_2 according to Eq. (40), with the minor exception that the term M is neglected in the constant factor.

The factor $\bar{X}$ is a two-dimensional integral over a square in θ_a-θ_b space with θ_a and θ_b running from θ_1 to θ_2. The main program portions the square region into one hundred small squares of equal size. The value of X_{12} at the center of each small square, calculated by the sub-routine, is used as the value of X_{12} over the whole square. The approximation to $\bar{X}$ is then just a Riemann sum based on one hundred squares.

This method of approximation yields results which one expected to be slightly larger than the correct value of $\bar{X}$ because of the fact that at the center point of ten of the one hundred squares, $\theta_a = \theta_b$. When $\theta_a = \theta_b$, $X_{12}(\theta_a,\theta_b)$ has a value of at least 2.0. For small differences $(\theta_a - \theta_b)$ X_{12} falls fairly rapidly from its value of 2.0 or greater. Hence, the approximation to $\bar{X}$ is too large on these ten squares. In fact the result of the approximation to $\bar{X}$ cannot be less than .1 (2.0) = .2. All of the calculated results cited in this report are substantially greater than .2, and it is believed that the error in approximating $\bar{X}$ is at most a few percent. Spot checks were made using a higher precision method which partitioned the θ_a - θ_b space into squares .01 radian on a side. The results obtained in this way were lower by about five percent. Since the higher precision calculation required a long execution time, only a few calculations were made with it.

General Dynamics Corporation/Electric Boat division
PROCESSING OF DATA FROM SONAR SYSTEMS (U), VOL. V
Technical Report C417-68-078
1 July 1966 to 1 July 1967
John H. Chang, Verne H. McDonald, Peter M. Schultheiss, Franz B. Tuteur
117 Pages

Volume V, and its supplement, further pursues the general subject of passive sonars operating in an anisotropic noise environment, and has taken two new directions. Environments containing not one but several point sources of interference or a spatially distributed interference are studied. Conventional as well as optimal detectors were analyzed. The second direction was an examination of the effect of single plane wave interference on tracking accuracy. This volume also continues the study of active sonar systems initiated in Volume IV, and initiates an effort to deal with the signal detection and extraction problem in a noise environment whose statistical properties are largely or wholly unknown.

General Dynamics Corporation/Electric Boat division
PROCESSING OF DATA FROM SONAR SYSTEMS (U), VOL. V
Technical Report C417-68-078
1 July 1966 to 1 July 1967
John H. Chang, Verne H. McDonald, Peter M. Schultheiss, Franz B. Tuteur
117 Pages

Volume V, and its supplement, further pursues the general subject of passive sonars operating in an anisotropic noise environment, and has taken two new directions. Environments containing not one but several sources of interference or a spatially distributed interference are studied. Conventional as well as optimal detectors were analyzed. The second direction was an examination of the effect of single plane wave interference on tracking accuracy. This volume also continues the study of active sonar systems initiated in Volume IV, and initiates an effort to deal with the signal detection and extraction problem in a noise environment whose statistical properties are largely or wholly unknown.

General Dynamics Corporation/Electric Boat division
PROCESSING OF DATA FROM SONAR SYSTEMS (U), VOL. V
Technical Report C417-68-078
1 July 1966 to 1 July 1967
John H. Chang, Verne H. McDonald, Peter M. Schultheiss, Franz B. Tuteur
117 Pages

Volume V, and its supplement, further pursues the general subject of passive sonars operating in an anisotropic noise environment, and has taken two new directions. Environments containing not one but several point sources of interference or a spatially distributed interference are studied. Conventional as well as optimal detectors were analyzed. The second direction was an examination of the effect of single plane wave interference on tracking accuracy. This volume also continues the study of active sonar systems initiated in Volume IV, and initiates an effort to deal with the signal detection and extraction problem in a noise environment whose statistical properties are largely or wholly unknown.

General Dynamics Corporation/Electric Boat division
PROCESSING OF DATA FROM SONAR SYSTEMS (U), VOL. V
Technical Report C417-68-078
1 July 1966 to 1 July 1967
John H. Chang, Verne H. McDonald, Peter M. Schultheiss, Franz B. Tuteur
117 Pages

Volume V, and its supplement, further pursues the general subject of passive sonars operating in an anisotropic noise environment, and has taken two new directions. Environments containing not one but several point sources of interference or a spatially distributed interference are studied. Conventional as well as optimal detectors were analyzed. The second direction was an examination of the effect of single plane wave interference on tracking accuracy. This volume also continues the study of active sonar systems initiated in Volume IV, and initiates an effort to deal with the signal detection and extraction problem in a noise environment whose statistical properties are largely or wholly unknown.

Unclassified

Security Classification

DOCUMENT CONTROL DATA - R & D

(Security classification of title, body of abstract and indexing annotation must be entered when the overall report is classified)

1. ORIGINATING ACTIVITY *(Corporate author)*
General Dynamics Corporation
Electric Boat division
Groton, Connecticut

2a. REPORT SECURITY CLASSIFICATION
CONFIDENTIAL - DI

2b. GROUP
4

3. REPORT TITLE
PROCESSING OF DATA FROM SONAR SYSTEMS (U)
VOLUME V

4. DESCRIPTIVE NOTES *(Type of report and inclusive dates)*
Annual Report, 1 July 1966 to 1 July 1967

5. AUTHOR(S) *(First name, middle initial, last name)*
John H. Chang, Verne H. McDonald, Peter M. Schultheiss, and Franz B. Tuteur

6. REPORT DATE
July 31, 1968

7a. TOTAL NO. OF PAGES
117

7b. NO. OF REFS
—

8a. CONTRACT OR GRANT NO.
NOnr 2512(00)

b. PROJECT NO.

c.

d.

9a. ORIGINATOR'S REPORT NUMBER(S)
C417-68-078

9b. OTHER REPORT NO(S) *(Any other numbers that may be assigned this report)*

10. DISTRIBUTION STATEMENT
In addition to security requirements which apply to this document and must be met, each transmittal outside the agencies of the U.S. Government must have prior approval of the Office of Naval Research.

11. SUPPLEMENTARY NOTES

12. SPONSORING MILITARY ACTIVITY
Office of Naval Research
Washington, D.C.

13. ABSTRACT

Volume V, and its supplement, further pursues the general subject of passive sonars operating in an anisotropic noise environment, and has taken two new directions. Environments containing not one but several point sources of interference or a spatially distributed interference are studied. Conventional as well as optimal detectors were analyzed. The second direction was an examination of the effect of single plane wave interference on tracking accuracy. This volume also continues the study of active sonar systems initiated in Volume IV, and initiates an effort to deal with the signal detection and extraction problem in a noise environment whose statistical properties are largely or wholly unknown

DD FORM 1 NOV 65 1473 (PAGE 1)

S/N 0101-807-6801

Unclassified

Security Classification

14 KEY WORDS	LINK A		LINK B		LINK C	
	ROLE	WT	ROLE	WT	ROLE	WT

DD FORM 1 NOV 68 1473 (BACK)
(PAGE 2)